12-2017

The Effects of Dopamine on Frequency Dependent Short Term Synaptic Plasticity: A Comparison of Layer Contributions and Rhythmic Dynamics

Jonna Marie Jackson

UNIVERSITY OF NORTHERN COLORADO

Greeley, Colorado

The Graduate School

THE EFFECTS OF DOPAMINE ON FREQUENCY DEPENDENT SHORT TERM SYNAPTIC PLASTICITY: A COMPARISON OF LAYER CONTRIBUTIONS AND RHYTHMIC DYNAMICS

A Dissertation Submitted in Partial Fulfillment
of the Requirements for the Degree of
Doctor of Philosophy

Jonna Marie Jackson

College of Natural and Health Sciences
School of Biological Sciences
Biological Education

December 2017

This Dissertation by: Jonna Marie Jackson

Entitled: *The Effects of Dopamine on Frequency Dependent Short Term Synaptic Plasticity: A Comparison of Layer Contributions and Rhythmic Dynamics*

has been approved as meeting the requirement for the Degree of Doctor of Philosophy in College of Natural and Health Sciences, in School of Biological Sciences, Program of Biological Education

Accepted by the Doctoral Committee

_____
Mark P. Thomas, Ph.D., Research Advisor

_____
Patrick D. Burns, Ph.D., Committee Member

_____
Judith Leatherman, Ph.D., Committee Member

_____
Eric Peterson, Ph.D., Faculty Representative

Date of Dissertation Defense _____November 03, 2017_____

Accepted by the Graduate School

_____
Linda L. Black, Ed.D.
Associate Provost and Dean
Graduate School and International Admissions

ABSTRACT

Jackson, Jonna. *The Effects of Dopamine on Frequency Dependent Short Term Synaptic Plasticity: A Comparison of Layer Contributions and Rhythmic Dynamics.* Published Doctor of Philosophy dissertation, University of Northern Colorado, 2017.

Executive functions (e.g. working memory [WM]) are known to be mediated by prefrontal cortical areas of the human brain which share homology with mouse medial prefrontal cortex (mPFC). Furthermore, it is well established that optimal dopaminergic input is required for proper WM function in the PFC. While it is well established that the mPFC receives inputs from several different brain areas, impinging on different compartmental regions of cells, it remains unknown how layer V pyramidal cells, the major output cells of the mPFC, integrate this information. Additionally, it remains unknown how dopamine modulates this integration by way of separate afferents and compartments within the PFC. A subset of studies presented here focus attention on the excitatory synaptic responses of layer V cells in response to compartmentalized stimulation (i.e. within the somatic region [layer V] or within the apical tufts [layer I]). Overall, these data suggest that dopamine, through D1 receptor (R) activation promotes local connectivity (primarily layer V to layer V connections) in the somatic region, while simultaneously inhibiting synaptic plasticity within the apical tufts through the suppression of NMDAR-mediated responses. Additionally, D2R activation had no effect on local layer V connectivity, but may play a role in regulating the signal-to-noise ratio in the apical tufts, by inhibiting low-frequency inputs and promoting inputs firing at high

frequencies. Taken together, these results suggest that in the presence of normal dopamine levels local influences (i.e. environmental / "bottom-up") and plasticity will be promoted within layer V, while "top-down" or contextual information impinging on layer I is stabilized. Additional studies presented here focus attention on the excitatory synaptic responses, and modulation of dopamine, of layer V pyramids in response to inputs from the contralateral mPFC. These data suggest that D1R modulation enhances the ability of layer V cells to integrate information from the contralateral mPFC. In combination, these experiments provide insight into how normal dopaminergic receptor activation alters signal processing and integration properties of layer V cells within the mPFC and shed light on cellular mechanism disruptions in schizophrenia, a disorder characterized by dopaminergic dysregulation.

ACKNOWLEDGEMENTS

I would like to thank first my family for their overwhelming support throughout the years. Between you all, I have always had the support and push I needed to achieve my goals and aspirations. Without you all, I know I would not have made it through this process they call Graduate School. A childhood dream has come true because you provided me the opportunity to learn, and rarely said no whenever I had a crazy idea, like grad school. Thank you for everything you have done for me. A huge thank you to my amazing husband, Jason, who has supported me throughout my undergraduate and graduate degree and dealt with the late nights of research, days of grading and months of homework and reading. The overwhelming support you provided did not go unnoticed, and I am extremely grateful.

I thank my advisor, Mark Thomas, for listening to every research idea that has come out of my mouth over the last five years, whether they were sophisticated or less than par. Most importantly helping me come up with ways to test each of these ideas, and allowing me the freedom to develop new techniques. Thank you for your patience, guidance, and never-ending support. I truly could not have done this without having such a supportive advisor. Thank you to my committee members, Patrick Burns, Judy Leatherman, and Eric Peterson for always taking the time to sit down, hold me accountable, and push me to my full potential, in addition to helping me through the many difficulties associated with graduate school.

Thank you to all the faculty within the School of Biological Sciences for always taking the time to talk research, and pick my brain on numerous aspects of my projects. Anytime I had difficulties with absolutely anything, someone was always willing to help and provide their expertise, regardless of their personal schedules. Additionally, I would also like to thank Cindy Budde for all of the administrative help, and friendship that she has provided throughout the years.

Thank you to the incredible Thomas lab mates who have given me friendships that will last a lifetime as well as the support and help throughout the years. I would like to say a special thank you to Michael Spindle for all of the help with physiological techniques, and undergoing the learning process with me. An additional thank you to Vanessa Johnson and Ryan Pevey for the overwhelming support and help with imaging and various other things throughout the years.

Finally, thank you to my friends. I could not have done this without everyone. Thank you to everyone that has provided feedback on ideas and being there for moral support! Thank you for keeping me sane throughout this process and keeping me going on the days where frustration seemed to take over. Thank you for sticking with me through all of this, even when I seemed to go 'missing' for a while, and for making sure I still had a life, with people I will never forget!

TABLE OF CONTENTS

LIST OF TABLES

TABLE

LIST OF FIGURES

CHAPTER I

INTRODUCTION AND REVIEW OF LITERATURE

Goal-Directed Behavior

Humans demonstrate the ability to form simple and complex goals. However, the ability to form goals does not indicate that the person experiencing and developing this goal understands where it came from, how their mind represents it, or how they will eventually pursue it. A goal is defined as "an end state that the organism has not yet attained and that the organism is committed to approach or avoid it" (1).

Goals are maintained as mental representations within the brain. These representations shape behavior when goal-relevant information is presented. For example, one major sources of goals, are human needs. An individual's needs affects the end state (goal) and the behavior necessary to pursue that state (2). In other words, needs produce desires, which then specify incentives and behavioral direction. Another source of one's goals stems from an individual's implicit theories. These goals are often determined based on an individual's performance abilities. Individuals with such goals place heavy emotional responses towards negative outcomes. For example, a negative outcome results in lower persistence and discontinuation towards that goal (i.e. failed attempts to reach a goal results in changes/modifications to the end goal). Goals derived from implicit theories are often referred to as personal goals

that do not rely on external personal or external opinions, yet weigh heavily on that individual's personal thoughts. Goals are also known to arise due to an individual's desire to be approached or avoided. These goals are heavily reliant on other individuals based on ones desires.

Although there are multiple ways in which goals arise through conscious contemplation, there are also many ways goals can be triggered outside of conscious awareness. These goals are often triggered by contextual ques and outside representations and goals are known to share common features and representations; thus, goals can often prime and promote one another. Suggesting that goals can reside in associated networks and are interconnected through what is referred to as a 'goal system' (3). A 'goal-system' suggests there may be interconnectivity among all goals within the system/network, further suggesting that one goal does not exist in isolation from others. This idea implies that goals may aide each other in promoting a single 'end state' by facilitating one another. Thus, one goal may promote itself by inhibiting another, acting as faciliatory and inhibitor linkages.

Although people's goals vary widely from short term to long term, all goals have variables/aspects in common. Of most importance, goals must be translated into action to ensure future states. This ensures that an individual can translate abstract thoughts into intermediate goals that help facilitate action towards the end state (goal).

Unlike goals themselves, the behavior linking abstract thoughts and end states are known as goal-directed behaviors. Goal-directed behaviors, which are defined as behaviors oriented towards attaining a particular goal, are an essential part of animal nature. In fact, most animal behavior, especially prominent in humans, is driven by goals

and needs; which are often intertwined. Goal-directed behaviors can have a wide range of time courses; proximal goals, also defined as short-term goals, are generally made within a short period of time (4). Proximal goals are often associated with the present time or act as stepping stones before reaching a 'core goal'. For example, completing an assignment, aiding in classroom success, would be considered a proximal goal. A long-term goal, also known as a 'core goal', and is associated with long-term achievements and success (4). For example, completing the course with an 'A', or completing college.

Executive Functions

One of the most advanced stages of human evolution is the ability to execute goal-directed behaviors that require the performance of complex functions. Executive functions (EF), the least understood aspect of metacognition, include task flexibility, problem solving, reasoning, conflict resolution and working memory. Executive functions can be defined as any entity that plans, chooses, decides or engages in some way with higher cognitive processes. Although many people have attempted to define executive functions, most definitions are vague and do not conform to one conclusive definition. For this reason, executive functions have been difficult to study. The most widely used definition of executive functions classifies any EF as a function that includes responses or actions that leads to alteration in a future response of an individual. Thus, executive functions are not automatic or well-practiced, but are determinants of strategic approach to obtain a goal. Therefore, executive functions can also be defined as means of 'self-regulation' including the analysis, alteration and management of an individual's behavior. These regulations are human traits critical to proper attention, memory and

learning. While the study of executive functions is essential for studying memory and learning, the lack of proper definition has prevented extensive research within the field.

Metacomputational functioning, or the ability to define a problem and depict a strategy, plays an important role in defining executive functions. Executive functions consist of three metacomponents, including task analysis, strategy selection and strategy monitoring. Some researchers also consider an additional metacomponent, strategy revision, which shares similar traits to strategy selection. Each metacomponent is responsible for generating goals and establishing a route to achieve them. In fact, Denckla (5) describes that the unfolding of executive functions describes the differences between child and adult. The differences in independence, maturation of self-regulation and development of personal productivity gives rise to an adult. It is also interesting to note that varied levels of 'general giftedness' are thought to be due to varied levels of these metacomponents and abilities of executive functioning. For example, superior metacomponents and executive functioning abilities have been linked to exceptionally high-performance abilities and IQ, while inferior metacomponents and executive functioning has been correlated to retardation and low IQ.

Although executive functions escape a proper definition, it serves as an umbrella term for prefrontal function. The frontal lobes are consistently associated with executive functions, such to an extent that executive functions are often referred to as 'whatever function might involve the frontal lobe'. It is known that the prefrontal areas of the frontal lobe play an important role in the regulation of executive functions (6). In humans, prefrontal cortical (PFC) areas are known to support goal-directed behaviors by mediating a variety of functions that render behavior more flexible in the face of

changing environmental demands. It has been hypothesized that the function of medial regions of the human PFC is to learn associations between context, events, and their consequences, i.e. action-outcome associations (6). In mice, these functions are mediated by homologous regions in the medial prefrontal cortex (mPFC) (7, 8). When executive functions are disrupted, individuals often suffer losses in social capabilities, which is often associated with diseases such as bipolar disorder, schizoaffective disorder and schizophrenia (SZ). More subtle disturbances in these executive functions may cause attention deficit disorders (e.g. ADD) and anxiety disorders (e.g. post-traumatic stress disorder [PTSD]).

Working Memory

Working memory (WM) is a key executive function, and is essential for goal-directed behaviors. WM in the simplest form refers to the ability to keep events/information 'in-mind' for short periods of time. For example, WM allows an individual to hold information in mind long enough to perform a task, like holding a phone number long enough to dial and once that task is completed, the number is forgotten. Working memory has been captured by the analogy to a mental sketchpad (Baddeley, 1986) and can be defined as the process of retrieval and proper utilization of acquired knowledge (Goldman-Rakic, 1995). Working memory is reliant on short time frames and can be studied in non-human primates as well as rodents. Much evidence suggests that the prefrontal cortex plays a role in working memory processes; however, memory-guided behaviors are heavily dependent on the operation of a widely distributed system and interconnectivity of brain structures (Goldman-Rakic, 1995).

The prefrontal cortex is responsible for working memory functions through its ability to maintain/hold information for an extended period of time. Additionally, the PFC is crucial for connecting information over time by bridging time gaps and behaviors. Normal prefrontal cortical function is critically dependent on dopaminergic input and optimal levels of dopamine are necessary for proper working memory, which will be discussed in detail below. Understanding the neuronal circuitry behind working memory is essential to understanding how information is held within the PFC during working memory tasks and contributes to goal-directed behaviors.

Interestingly SZ, a debilitating mental disorder, is characterized by both emotional and cognitive dysfunctions. Patients with SZ often suffer from altered perceptions of reality and progressively withdrawal from reality (9). Individuals with SZ also are known to exhibit deficits in executive functions, specifically with working memory, problem solving, reasoning and goal-directed behaviors. As discussed above, cognitive and goal-directed functions are known to involve the prefrontal cortex (PFC), an area known to be highly dysfunctional in patients with SZ.

The Prefrontal Cortex

As discussed above, the PFC is essential for executive functioning, especially in tasks involving working memory. It is thought that the dorsal and ventral regions of the PFC share homologies between the monkey and the rodent. The dorsal region of the mPFC in rodents is thought to be homologous to the dorsomedial PFC of the monkey, while the ventral region of the mPFC in rodents may be homologous to the ventromedial PFC in monkey. The dorsal region of the mPFC is known to regulate skeletal movements, while the ventral region regulates visceral functions (e.g. smooth muscle and gut).

Further, it is of note that rodents only have a medial prefrontal cortex, while the monkey has evolved more lateral areas than the mPFC (e.g. dorsolateral and ventrolateral PFC), ultimately giving rise to higher-order cognitive abilities (10).

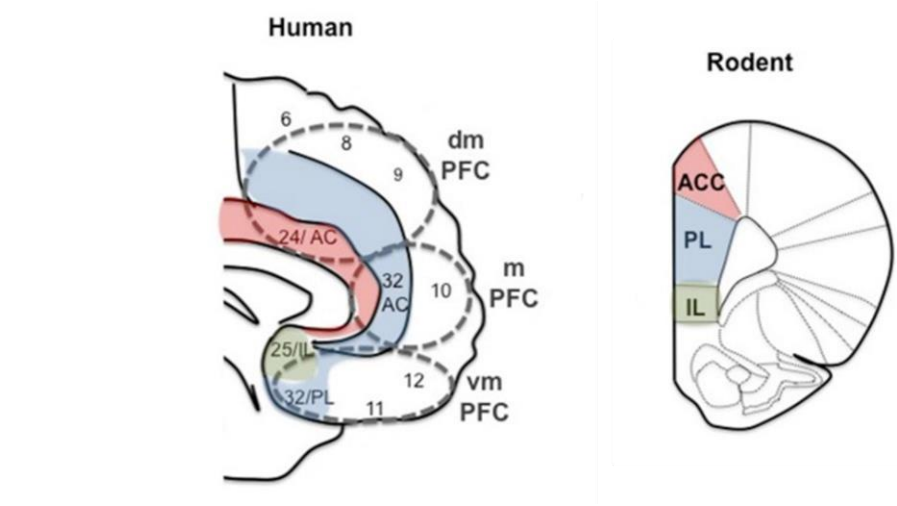

Figure 1: Homology between the human and rodent brain. Red implicates the homology locations between the anterior cingulate cortex between human and rodents. Blue represents homology between the prelimbic regions and green represents homology of the infralimbic cortices. (figure modified from Bicks et al. [10])

The ventral portion of the mPFC is known to be responsible for visceral conditioning (11). For example, object fear conditioning causes animals to associate an object (sound or light) with a foot shock (fearful). With this task, animals are first presented with either a noise or a light which is immediately followed by a foot shock. Animals then begin to pair the noise or the light with a fearful response. This type of task involves the amygdala, which associates objects (in this case the sound or light). To extinguish this fear, the noise or light activation is repeated without the foot shock. Eventually, the animal extinguishes the association between the noise/light and the foot shock. It is important to note that the mPFC, specifically the infralimbic region (12), is necessary to actively suppress this fear conditioning by inhibiting the amygdala. This

phenomenon is relatable to soldiers with post-traumatic stress disorder (PTSD), who have PFC dysfunction (13). These individuals have lost the ability to actively suppress their fear, for example, these individuals jump to loud noises in the everyday world (like a car horn), like they are still on the battlefield.

Similar to visceral object conditioning, context fear conditioning causes animals to associate a place/context with a foot shock. With context fear conditioning, animals are trained to associate a foot shock with a location/context. With this task, animals are placed in a cage and receive a foot shock every time they cross into one specific part of the cage. The animals eventually associate that area of the cage with the foot shock. While object fear conditioning is heavily reliant on amygdalar activation, contextual fear conditioning is heavily reliant on the hippocampal formation, an area known to make associations with contextual information. As with object fear conditioning, contextual fear conditioning can also be extinguished by repeated exposure to a location without foot shock pairing. As with object conditioning, contextual extinction is also reliant on the infralimbic mPFC (14, 15).

Fear extinction tasks suggested anatomical connectivity between the mPFC and the amygdala as well as the hippocampus. Recent studies support these anatomical connections and suggest that the reciprocal connectivity between the mPFC and the amygdala gives rise to object associations (16), while hippocampal connectivity gives rise to context associations (17). It is of note that dopaminergic neurons from the ventral tegmental area of the midbrain strongly innervate the mPFC, amygdala and the hippocampus, and may influence these associations.

Cortical Structure

The neocortex is a "sheet-like" piece of tissue that, in humans, has a surface area of roughly 2600cm^2 and has a thickness of roughly 3-4mm (18). The cells of the neocortex (cortical neurons) are heavily interconnected with each other and share reciprocal connections with other brain regions. In fact, the total number of all neocortical connections (synapses) can be of the order of 10^{12} (18). Like other cortical regions, the neocortex is organized into layers, which spans from layer I (apical/pial surface) to layer VI (deep). Of these layers, layer I contains dendritic tufts of pyramidal neurons located in layers II-V; layer II and III, which contain small pyramidal neurons; layer IV, which contains short-axoned stellate cells (which is absent in the rodent mPFC); layer V, which contains large pyramidal neurons that project subcortically; and layer VI, which contains some large pyramidal neurons and cells of varied morphology (see figure 2A on layered cortical structure). It has been verified in many studies that the layers of the cortex are connected in a highly organized fashion, with layer V pyramidal neurons being the final outputs to subcortical motor areas. Thus, layer V pyramidal neurons provide the major output of the cortex to ultimately control behavior. Due to this, layer V neurons are highly studied and have been extensively characterized in terms of their hodology (connectivity), morphology and their electrical properties (19-21). See figure 2B for the morphology of a layer V pyramidal neuron, where the soma is located within layer V and axon collaterals target all other cortical layers.

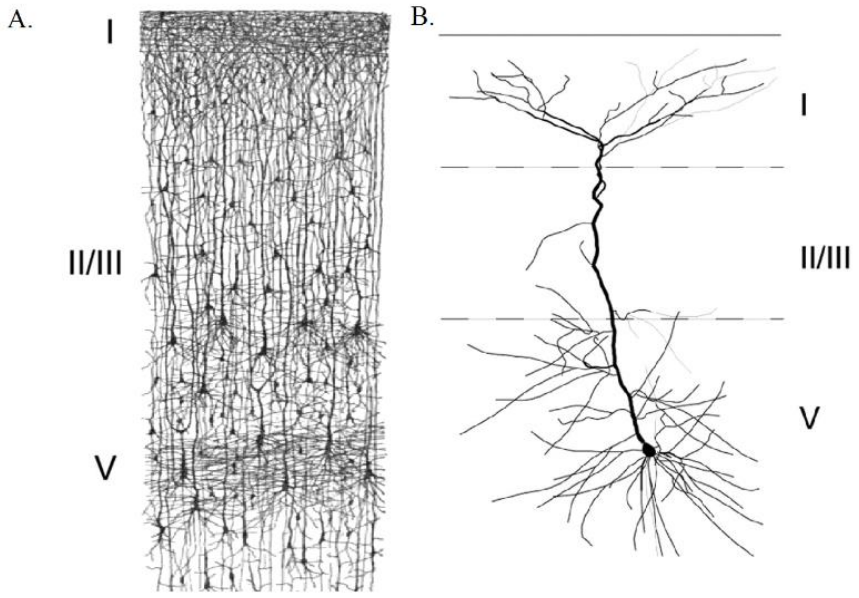

Figure 2: Cortical organization of the medial prefrontal cortex. A. Layer organization of the mPFC, where layer I is at the pial surface and layer V resides deep within the cortex and contains layer V pyramidal neurons. B. Morphological reconstruction of a layer V pyramidal cell where the soma is located within layer V and the apical dendrite extends to layer I. The axonal projections of these cells would extend from the soma to the contralateral mPFC (type II cells) or the pontine nuclei of the brainstem (type I cells). (Figure modified from: http://jn.physiology.org/content/jn/91/3/1 171/F8.large.jpg & https://blogs.scientificamerican.com/blogs/assets/sa-visual/Image/ Cajal_cortex_drawings.png)

In addition to this layered organization, it is well accepted that the neocortex is organized into 'functional units', which are made up of columns of vertically displaced neurons. The presence of an "elementary cortical unit of operation" was first proposed by Rafael Lorente de Nó in the mid-twentieth century, suggesting that the cortex was made up of vertical chains of neurons, forming small 'cylinders' necessary for cortical function (22). This hypothesis was further developed based on physiological and anatomical studies suggesting the presence of columnar organization within the neocortex (18, 23). Cortical columns are hypothesized to organize inputs targeting cortical areas. This organization is essential for integration of excitatory synaptic connections from these

inputs. Cortical columns are thought to play a role in processing excitatory inputs and connecting them to the proper downstream targets, ultimately leading to behavior. An example of cortical columns is shown in figure 3, showing that the cortex, regardless of location is made up of distinct units that each integrate distinct types of information.

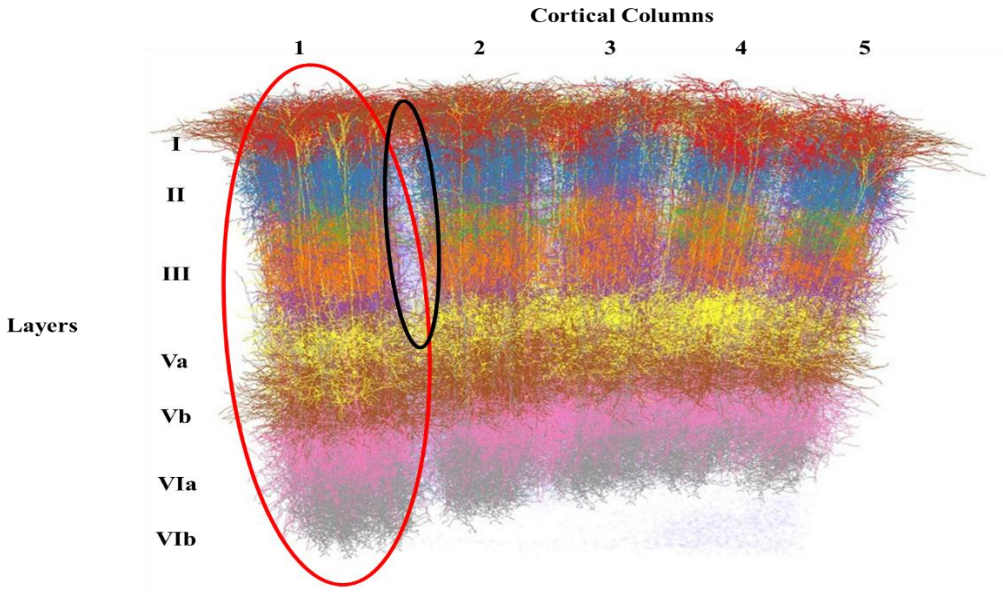

Figure 3: Cortical columnar organization. Reconstruction of cortical columns (5 in total, labelled 1-5) are shown. One cortical column is highlighted with a red outline. Additionally, these cortical columns span across all six cortical layers (labelled I-VIb). It is highlighted (with a black outline), that cortical columns can communicate with one another; however, these connections are sparser than intracolumnar connectivity. (Figure modified from http://www.kurzweilai.net/images/vibrissal-cortex-rat.jpg)

Although the idea of cortical columnar organization is widely accepted, it has proven difficult to assign specific 'parameters' or 'rules' to the term by which all columns are organized. For this reason, the most readily identified and characterized columns are located within barrel cortex of the rodent brain. This region is responsible for integrating information regarding whisker placement, where each individual whisker is mapped onto one single cortical barrel, located within the barrel cortex. As whisker movement occurs, this information is relayed to the corresponding cortical column where

it gets integrated and translated into whisker movement or action (for schematic see figure 4). For example, if a mouse is walking near a wall, and grazes its whiskers, this information is relayed to the appropriate cortical columns, where it is translated into action. In this case, the animals action would be to move its head away from the wall, to assure they do not run into it. Due to external access of inputs, these columns are more readily studied in rodents (compared to other cortical regions), more is known about these cortical columns than any other within cortical regions. However, it is suggested that the same general properties discovered in barrel cortex can be applied to cortical columns in all cortical regions.

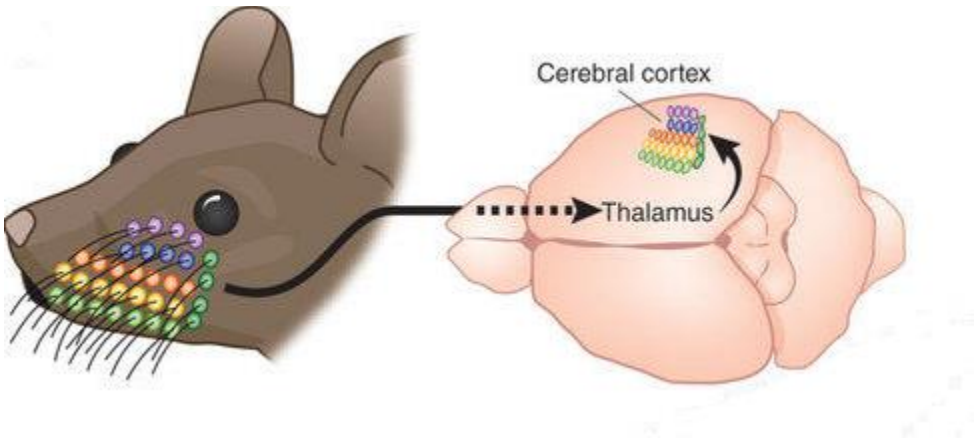

Figure 4: Cortical Columns of barrel cortex. Each whisker located on the mouse cheek, maps to a specific cortical column located with the 'barrel cortex', which is part of the cerebral cortex. As this diagram is relatively simplistic, it is of note that each cortical column within the barrel cortex can respond to individual changes in whisker vibration/movement. (Figure modified from https://images.nature.com/full/nature-assets/neuro/journal/v15/n9/images_article/nn.3191-F1.jpg)

Although primarily studied within the barrel cortex of the rodent, many studies have provided functional evidence that cortical columns exist and serve as the organizational unit of the cortex. Studies have shown that each cortical column receives

specific afferent innervation, which often target specific neuronal subtypes within the column. (24, 25). Additionally, others have provided evidence that neurons that share connections, generally share multiple synapses (26, 27), predicting that one single neuron within the circuit could have potentially powerful influence on the local network (24). Taken together, these data support the idea that circuits within the neocortex are connected in a highly organized fashion made up of functional 'cortical columns'.

Layer V Pyramidal Output Cells

Like pyramidal neurons identified in other brain areas, layer V of the mPFC consists of two subtypes of pyramidal neurons (19, 20). These two subtypes can be identified by characteristics including projection pattern, dendritic morphology and intrinsic properties. Although specific functions of these subtypes are unknown, it is postulated that they may play different roles in rhythm generation and behavior control (19). The two subpopulations have been identified as type I/corticopontine (CPn) neurons and type II/commissural (COM) neurons based on their projection patterns (19, 28). As their name implies, mPFC type I cells send long subcortical axonal projections to the pons of the brainstem, while type II cells project to the contralateral hemisphere of the mPFC, thus are termed commissural. Type I neurons maintain distinct morphological differences compared to type II neurons, including thick apical dendrites, broad tufts and large soma bodies, ranging from 18-19μm (29). Additionally, type I neurons can also be identified by intrinsic properties, including a prominent hyperpolarization activated cation current (I_h), increased temporal summation of excitatory post synaptic potentials (EPSPs), more hyperpolarized threshold as well as higher action potential amplitude (19). It is also important to note that type I neurons have the ability to selectively respond to

inputs at preferred frequency, also known as the ability to resonate. In this subset of neurons, resonance is suggested to occur within the theta frequency band (4-6Hz) (19). Further, it is also suggested that the somatic body of these cells reside primarily within deep layer V of the neocortex (29). Type II/COM layer V neurons have a morphology of thin apical dendrites, simple tuft branching and small soma bodies, compared to type I cells, between 12-13μm (29). Further, type II neurons, unlike type I neurons, do not have the ability to resonate, lack a prominent I_h current, decreased EPSP temporal summation, and maintain a more depolarized firing threshold (19). Unlike type I cells, type II cell somatic bodies primarily reside in superficial layer V (29). Due to their differences in projection patterns, morphology and intrinsic properties, it is suspected that these two subtypes may play a different role in rhythm generation, persistent activity and integration properties.

Although it has been well established that there are two major subtypes of layer V pyramidal cells, it remains unclear how these cells are interconnected within the mPFC, as well as how they integrate information from each other as well as other brain regions. Until recently, intrinsic and morphological differences were the only way to discern between these two layer V subtypes during electrical recordings. The development of retrograde and anterograde labelling techniques now allows labelling of these two subtypes based on their projection patterns. Retrograde labeling is defined as the tracing of a neuron from their point of termination (axonal synapse) to their origination (the soma). However, anterograde labeling embraces the opposite technique, labelling neuronal connections from the soma to the nerve terminals. Combined, these techniques

have been used to further identify how layer V subtypes are interconnected as well as how they are connected with other brain regions.

Initial studies identifying the connectivity between these two subtypes of layer V cells has revealed integration properties that may lend insight into their general functions. First, it has been reported that reciprocal connections are more likely to occur between like cells (i.e. type I-type I or type II-type II connections are more prevalent than type I-type II connections) (30). Additionally, although not layer V specific, it is of note that layer II/III cells selectively target layer V pyramidal cells based on their firing and intrinsic properties (30). Interestingly, this study also found that the probability that two layer V cells share contact with the same layer II/III cells is significantly higher if the pyramidal cells are of the same subtype. This probability is further increased if the two pyramidal cells are also connected with one another (30). Furthermore, type I cells are thought to receive more inputs from layer II/III cells than type II cells, yet another difference between the two subtypes suggesting differences in overall function and integration properties. Recent studies have now started identifying the characteristics and synaptic effects of differential afferents, originating in other brain regions onto layer V pyramidal cells which will be discussed later.

As discussed above, type I-type I cells exhibit greater reciprocal connectivity, and it has been shown that connections between these cells display stronger unitary synaptic transmission and more facilitation of paired pulse ratios (28, 30). In contrast, type II – type II connections display predominantly paired pulse depression of paired pulse responses (20, 28, 30). Interestingly, type II – type I connections more commonly display a depressing paired pulse response (30), especially when the presynaptic cell was type II;

however, a combination of both facilitating and depressing could be observed. Morishima and colleagues (2011) suggest that although type I and type II cells have similar connection probabilities, they show subtype-specific probabilities for synaptic reciprocity, synaptic strength as well as short-term plasticity characteristics. These connections provide evidence that type I cells may act as "driver" cells, that are more readily excitable by both intra- and extra-cortical targets (evident by facilitation properties) (31), whereas type II cells may act as temporal integrators and circuit regulators that depend on extracortical projection patterns of presynaptic cells (30, 32).

Persistent Firing

A ground breaking study in the research of working memory was conducted by Goldman Rakic (33). In this study, monkeys were trained to perform an oculomotor delayed task (see Figure 5 for pictorial representation). During these tasks, monkeys are trained to keep their eyes on a fixation point (a dot) in the middle of a screen. While maintaining their focus on the fixation point, a visual 'cue' is presented at a particular location around the fixation point, generally depicted at various degree points (i.e. 90º, 180º etc.) (Figure 5A). The monkeys were trained to not break contact with the fixation point when the 'cue' is delivered. The cue was then removed from the screen during delay period where the monkeys were to maintain visual fixation on the fixation point. Following the delay period, the monkeys were instructed to move their eyes to the visual 'cue' location; correct eye movement resulted in a juice reward (Figure 5A). To monitor cellular function during this task, single unit recordings were made from neurons within the prefrontal cortex. Single cells responded in one of three ways: to 'cue related activity', 'delay-related activity' or 'response-related activity' (Figure 5B). Further, the

study found that cells responding to the 'delay-related activity' were persistently active throughout the entire delay period, indicative of constitutively active cells during a working memory task (Figure 5B). This study was the first to report persistent activity, however the cellular mechanisms behind the phenomenon were not explored.

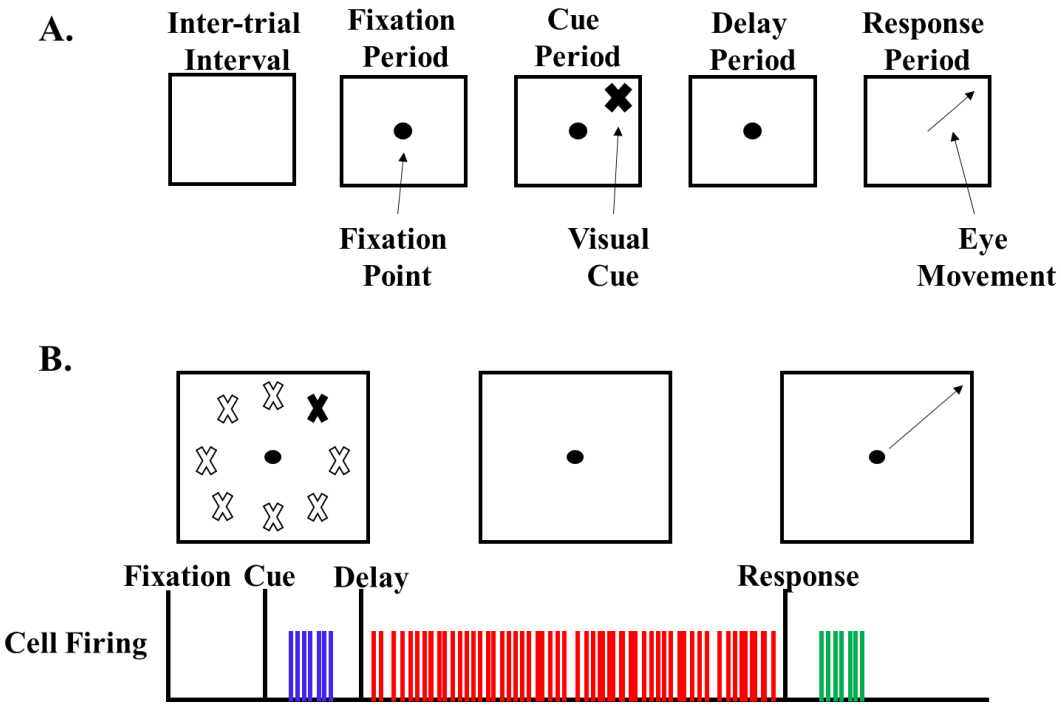

Figure 5: Schematic representation of an oculomotor delay task. A. oculomotor delayed-response task screen visual during the inter-trial interval, fixation period, cue period, delay period and response period. B. Neuronal activity during the 'cue'-period (top), the 'delay'-period (middle) and 'response'-period (bottom) can be observed in different subsets of neurons within the mPFC, represented by different colors (blue, red and green).

Currently, there have been three mechanisms hypothesized for how persistent activity occurs, which include cellular intrinsic properties, network synaptic properties, synchronized rhythmic activity, or a combination of the three (19, 34). First, it has been shown that single, synaptically isolated mPFC neurons are capable of persistent activity in the presence of neuromodulators (19), indicating that cells can fire persistently due to

intrinsic properties. In the presence of carbachol, a cholinergic receptor agonist, a subset of layer V mPFC pyramidal cells can fire persistently following a long depolarizing stimulus. It is thought that this persistent activity may be due to the presence of a calcium activated cation current, which is known to be present in the subset of layer V cells that elicit persistent activity in the presence of carbachol (19). Other studies have also shown persistent activity in the presence of the D2 agonist quinpirole (21), further indicating that pyramidal neurons are capable of firing persistently depending on their individual cellular properties.

Network synaptic properties have also been hypothesized to contribute to persistent firing. This hypothesis suggests that a network of cells can form 'recurrent loops', which allow the cells to maintain persistent activity by relaying excitation in a loop like fashion. For example, if one neuron (cell A) is connected to cell B, and cell B is connected to cell C, which is connected back to cell A, these cells can relay excitatory responses from one to another in a loop like fashion (see figure 6). Using these 'recurrent loops', cells can maintain an active state for a set period of time. It is important to note that in order for the activity to be maintained in the cell network, synaptic timing is critical. This timing is thought to be heavily dependent on the presence of the NMDA-receptor mediated synaptic component, which will be discussed in detail below (35).

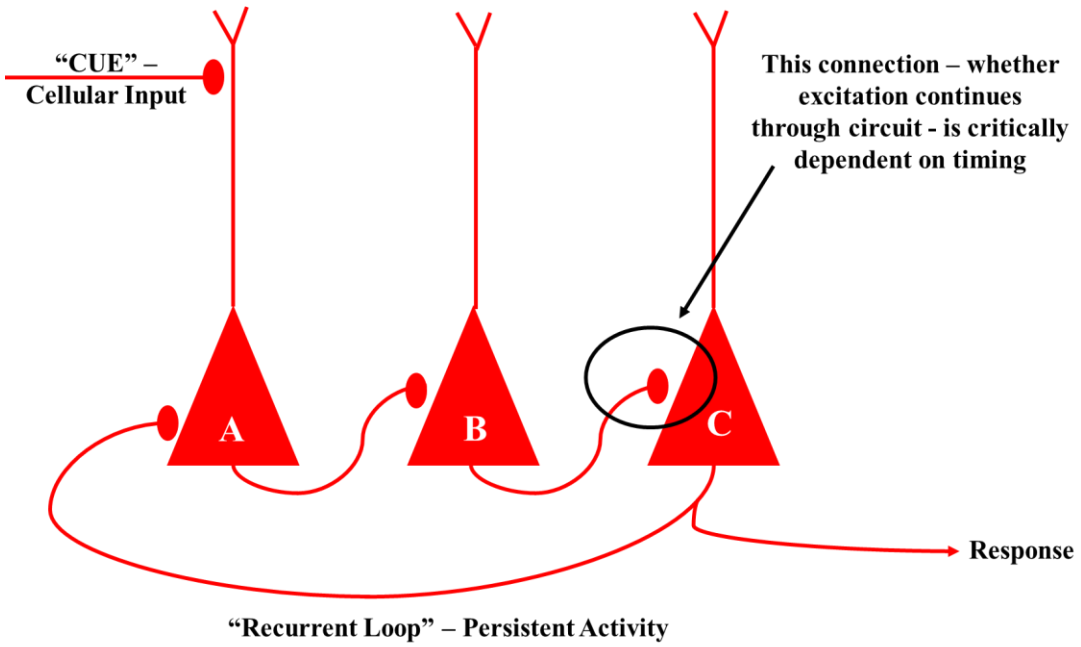

Figure 6: Schematic representation of a 'recurrent loop' present within a network of cells.

A modification of the network hypothesis suggests that persistent activity is maintained through synchronized rhythmic activity coordinated by GABAergic interneurons. Rhythmic activity is seen on a large scale during working memory tasks through electroencephalographs (EEG's). When electrodes are placed on the scalp of a human, rhythms are observed within the prefrontal cortex while the individual is conducting a working memory task (36). In addition, local field potentials (the summation of electric current flowing from multiple neurons in close proximity), measured using deep electrodes have also shown oscillations and rhythmic activity within the prefrontal cortex during working memory tasks (37). It is hypothesized that rhythms play a role in synchronizing local groups of neurons as well as different brain regions (38). Although evidence shows that rhythms can synchronize groups of neurons and brain

regions, our lab also entertains the idea that rhythms, at various frequencies, may promote persistent activity.

Cortical Column Processing: (Feedback vs Feedforward)

It has been proposed (39) that, in layer V neocortical pyramidal neurons, feed-back (top-down or contextual) information is received via apical tuft synapses (in layer I), while feed-forward (bottom-up or environmental) information is delivered to synapses on the apical trunk (via layer II or III cells) (See Figure 1&2 on cortical organization). Further, local processing occurs between layer V neurons via synapses located on the basal dendrites located predominantly in layer V. It is likely that this information, arriving in different layers, is coordinated by rhythms impinging on different compartments of the pyramidal neuron (40-42). It is noteworthy that, when synaptic inputs to the apical tufts are activated synchronously with postsynaptic action potentials, layer V pyramidal neurons act as coincidence detectors, capable of firing in a bursting pattern that may lead to synaptic plasticity in target neurons (39).

A hypothesis proposed by Matthew Larkum suggests that ‘coupling’ occurs when inputs targeting the apical tufts and postsynaptic action potentials occur simultaneously. This ‘coupling’ is thought to activate dendritic calcium channels, leading to cellular “bursting” (high frequency firing). Before the discovery of ‘coupling’, activation of the dendritic calcium ‘hotspot’ was originally termed “backpropagation-activated calcium spike firing” or BAC firing, which suggested that somatic bursting was due to the coincidence of a *single* backpropagating action potential and synaptic input targeting the distal dendrites (39). This concept has now been re-defined as “backpropagation activated coupling”, which suggests that dendritic calcium spiking, and cellular bursting, is due to

the synchronous activation of synaptic inputs targeting both the apical tufts and basal dendritic region. Furthermore, this idea implies that when a cell receives both internal/predictive information (also known as feedback information) and ongoing environmental information (also known as feedforward information) at the same time, dendritic calcium channels get activated, resulting in somatic bursting (39). This phenomenon, as outlined by Larkum (43), is shown in figure 7.

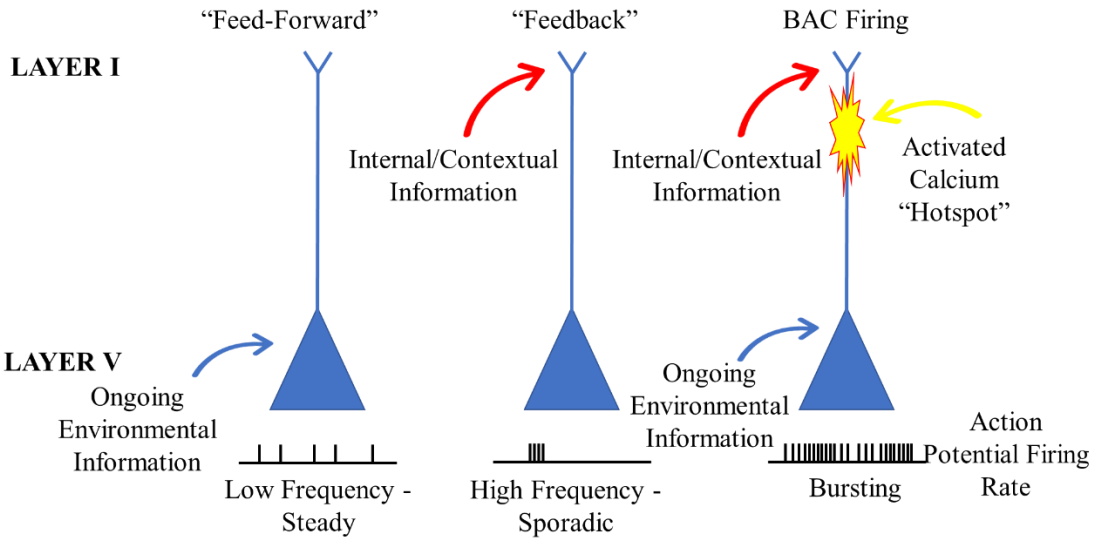

Figure 7: Backpropagating Activated Coupling (BAC). If inputs targeting layer V (the somatic region) are activated, the cell maintains a steady, low frequency firing rate (left). If inputs targeting layer I (apical tufts) are activated, the post-synaptic cell fires sporadically at high frequency (middle). If both inputs targeting layer V and layer I are activated simultaneously, the calcium hotspot is activated, leading to sustained bursting in the post-synaptic cell.

Interestingly, in-vivo BAC firing and cellular bursting has a direct relationship to perception of information, perhaps by integrating what is already known (feedback information) and what is currently occurring within the environment (feedforward information) (43). Recent techniques using opto-fiber technology have shown that BAC

firing occurs at an order of magnitude more in awake and moving animals compared to anesthetized animals, especially when the animal performed deliberate movements. This phenomenon was further shown in terms of whisker placement and movement. Constant 'feedback' information regarding whisker location arrives in the tufts to produce high frequency, spontaneous burst firing. However, inputs targeting the basal/somatic region are activated when the whisker undergoes movement (i.e. ongoing environmental information in regards to placement). When both are activated simultaneously, BAC firing can be observed in these cells in-vivo. Taken together, these in-vitro and in-vivo studies provide evidence for the proposed cellular mechanism for how cortical associations can lead to predictive behavior and perception of information.

It is likely that information arriving in different layers of the mPFC is coordinated by rhythmic properties. While our lab (44) and others (19) have established that layer V pyramidal cells resonate at theta frequency due to intrinsic ionic currents, it is known that neocortical circuits also generate local field potentials (LFPs) within the alpha, beta, and gamma ranges (38, 45, 46). In terms of feedback and feedforward information, it is possible that inputs targeting layer I and layer V (enabling BAC firing), are dependent on rhythmic dynamics of afferents targeting these regions.

Regional Inputs to the Prefrontal Cortex

As discussed above, the mPFC integrates synaptic inputs from several brain regions (47), including the contralateral mPFC (19, 20, 48), the mediodorsal thalamus (48-50), the basolateral amygdala (48, 51), the ventral hippocampus (47, 48), and orbital and agranular insular cortex (47). However, how pyramidal cells in different cortical layers integrate these various inputs remains poorly understood. Some studies have shown that the apical tufts in layer I are innervated by matrix (midline) thalamic neurons

that target the outermost portion of layer I (50) and by the nucleus reunions (52). Layer I has also been shown to be targeted by afferents from contralateral mPFC (48) which show preference for the innermost part of layer I (50). Utilizing optogenetic stimulation of synapses in recordings from superficial pyramidal neurons, Little and Carter (48) report that the ventral hippocampus projects throughout layer I, while the basolateral amygdala targets deep layer 1, as also demonstrated by Bacon et al. (53). However, Orozco-Cabal et al., (51) describe functional basolateral amygadalar inputs to layer V, targeting layer V pyramidal cells in rodent infralimbic and prelimbic cortex. Thus, characterization of the specific cellular and compartmental targets of mPFC afferents remains incomplete. A subset of studies within this dissertation focus on layer-specific inputs to layer V pyramidal neurons of the mPFC.

Some preliminary studies have been conducted to identify how layer V cells integrate information from afferents originating in other cortical and subcortical regions. Studies of commissural afferents targeting both subtypes of layer V cells have proven beneficial in determining how these cell subtypes may differentially integrate information from contralateral layer V pyramidal neurons. It has been found that commissural inputs (projecting from the contralateral hemisphere of the mPFC) target both type I and type II cells (20, 32). Lee and colleagues have demonstrated that the two layer V subtypes display distinct post-synaptic short term synaptic dynamics in response to commissural afferent activation. Interestingly, when activated via pre-synaptic commissural activation, type I cells display facilitating responses (meaning the second response is greater in amplitude than the first), while type II cells display depressing responses (the second response is less in amplitude than the first) during synaptic trains (20). Additionally, it

has been reported that commissural inputs, can evoke monosynaptic responses in both pyramidal subtypes, inferring that commissural inputs directly target layer V pyramids (32). In combination, these studies hypothesize different functions of type I and type II cells. As discussed above, these subtypes likely vary in computational functions, where type I cells likely act as coincidence detectors that respond to spatially distributed signals within a very short time-window, and type II cells likely act as temporal integrators that summate synaptic input across a broad temporal window (20, 32).

Aside from excitatory responses, it has also been reported that fast-spiking interneurons play a role in 'tuning' layer V cells in response to commissural inputs. Specifically, type I cells receive strong fast-spiking-interneuron (FSIN) innervation which may sharpen their responses to callosal inputs. Furthermore, di-synaptic inhibition and feedback inhibition is thought to occur more readily at type I cells than type II cells (20, 32). Combined, these studies suggest that callosal inputs elicit both excitation and inhibition differently between the two subtypes and may contribute to their distinct computational functions.

Although some aspects of commissural afferent fiber innervation of layer V cells have been studied, it is still not fully understood how the two subtypes differentially integrate this information, especially at varying frequencies or in the presence of dopamine. Thus, aspects of this dissertation are focused on identifying the differences in integration properties of layer V pyramidal cells in response to commissural/callosal inputs within the mPFC.

Channelrhodopsin-2

New optogenetic technology allows for anatomical and functional dissection of neuronal circuitry with high spatial and temporal resolution (54). This recently developed

technology uses genetically encoded light-sensitive proteins (originally isolated from microalgae Chlamydomonas) to manipulate neuronal activity both *in vitro* and *in vivo*. Channelrhodopsin-2 (ChR2) is a cation-selective ion channel that opens in response to light absorption of photons. Upon absorption of photons, this channel undergoes a conformational change, allowing for cations (primarily sodium) to flow through the channel. Interestingly, ChR2 desensitizes in response to continuous light. For this reason, ChR2 is better suited for rapid manipulation (55) and proved beneficial for studies conducted within this dissertation.

Channelrhodopsin-2 is one of the most widely used depolarizing opsins in neuroscience. When placed in neurons, blue light activation is known to induce depolarization of cells, leading to action potentials (56). It is well known that these action potentials are induced due rapid influx of sodium. A schematic representation of this is shown in figure 8. Through anterograde labelling, ChR2 can be inserted into neuronal populations based on cellular projection patterns. To express ChR2 into neuronal subpopulations, *in vivo* injections can be made into specific brain regions using a stereotaxic apparatus. Upon injection, ChR2 packaged in an adeno-associated virus (AAV), gets endocytosed into the somatic region of the neuron via a clathrin-mediated mechanism. Once endocytosed, the endosome containing the AAV-ChR2 is degraded and the viral DNA (ChR2) is released due to the acidic pH of the endosome. Once released it is thought that the viral DNA enters the nucleus where it is converted from a single strand to a double strand. The DNA is then transcribed into RNA, released from the nucleus and targeted by ribosomes and carried to the rough endoplasmic reticulum. Upon entry to the endoplasmic reticulum, translation of the channelrhodposin-2 protein occurs. Once the

protein is made, it is then transported to the golgi apparatus, where it is packaged for transport throughout the cell. Upon packaging and transport, the ChR2 channels can be placed throughout the axonal and dendritic projections of the neuron through an exocytosis mechanism. Through exocytosis, the protein is placed throughout the plasma membrane, where it spans from the intracellular to the extracellular side. Figure 9 provides details regarding this process.

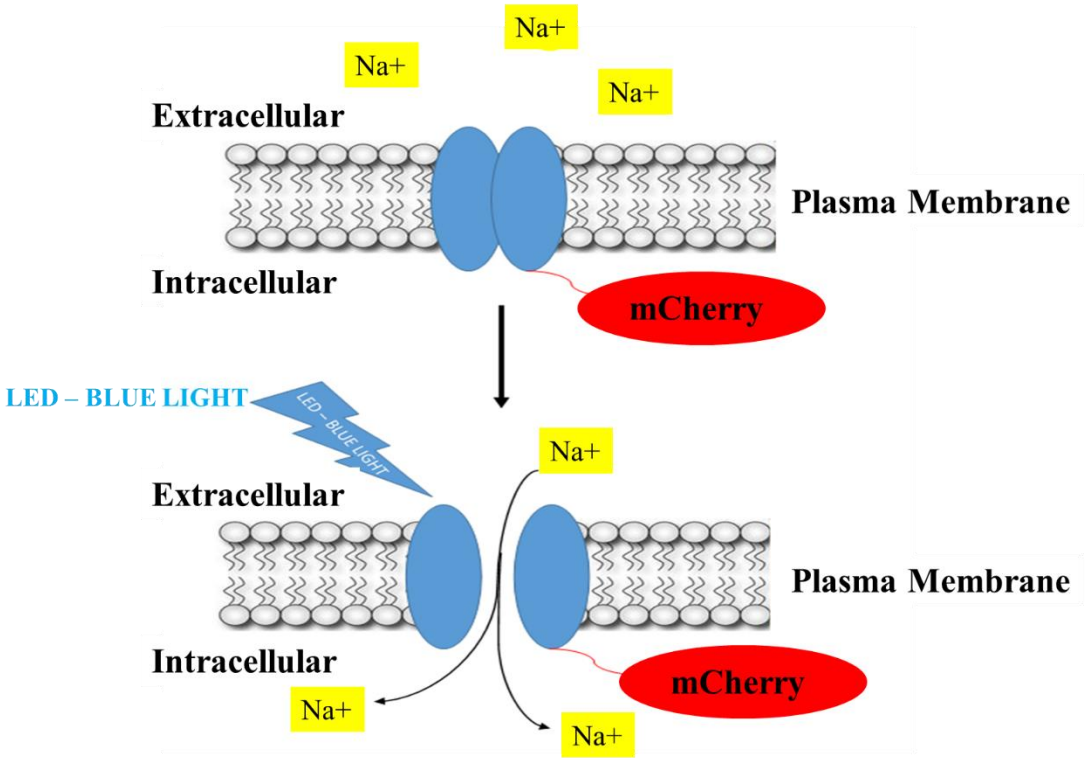

Figure 8: Schematic representation of channelrhodopsin-2 activation. In the resting state, channelrhodpsin-2 maintains a closed state (top). As these proteins absorb protons through blue light activation, the channel undergoes a conformational change, allowing sodium cations to flow across the plasma membrane and into the cell.

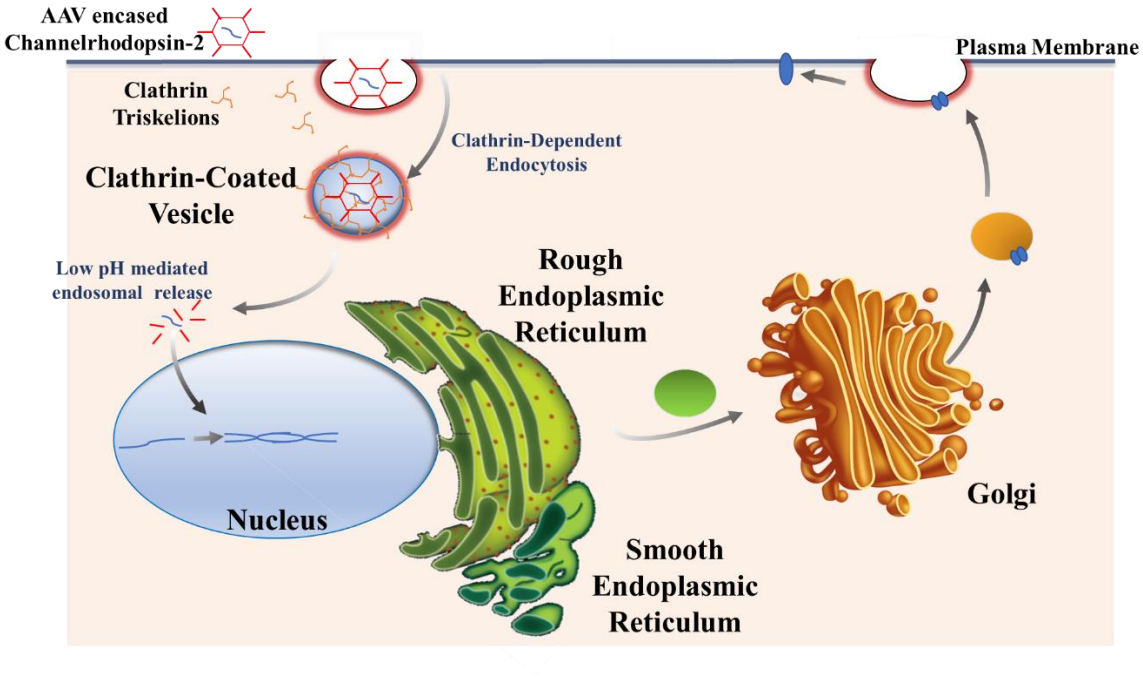

Figure 9: Simplistic representation of the process neurons undergo to express channelrhodopsin-2 after in-vivo viral injections.

Upon injections, fibers expressing ChR2 can be selectively activated using blue light from an LED light source. Specific activation of these fibers can allow for selective characterization of synaptic dynamics of specific cellular subtypes and connectivity. For this reason, ChR2 has become a novel tool for identifying synaptic connections and influences of specific neuronal subtype afferents on other brain regions. Specifically, experiments conducted in this dissertation use this novel technique to characterize synaptic dynamics of afferents impinging onto layer V pyramidal neurons of the mPFC.

Neuronal Activity/Synaptic Plasticity

Stable patterns of neuronal activity can be sensitive to frequency dependent changes in inhibitory and excitatory transmission. It is known that inhibitory and excitatory transmission varies across cortical layers of the mPFC (57), which likely contributes to rhythm generation and synchronization. Synaptic plasticity is partially

dependent on glutamatergic excitatory transmission, which can be measured by excitatory post synaptic potentials (EPSPs), a depolarization of the membrane potential due to activation of transmitter-gated channels. EPSPs are caused by the flow of sodium ions into the post synaptic cell due to the opening of glutamate-gated ion channels. The flow of sodium ions into a post synaptic cell causes a depolarization in membrane potential, bringing the cell closer to threshold, and therefore more likely to fire. An EPSP is made up of two components, a slow long lasting component, mediated by NMDA (N-methyl-D-aspartate) receptors, and a fast rising rapid component, which is mediated by AMPA (α-amino-3-hydroxyl-5-methyl-4-isoxazolepropionic) receptors. Together, NMDA and AMPA receptors are known to play a large role in synaptic plasticity, the strengthening or weakening of synapses in response to altered neuronal activity.

The fast component of an EPSP is mediated by the ionotropic AMPA receptor. The AMPA receptor is known to mediate the vast majority of communication between neurons within the central nervous system. It has been demonstrated that increasing or decreasing the amount of AMPA receptors on the post-synaptic spine is the basis for meditating long term potentiation (LTP) or long term depression (LTD), respectively. Immunocytochemical techniques have linked AMPA endocytosis and exocytosis to LTD and LTP respectively (58). The function of AMPA receptors indicates their important role in regulating the strength of synaptic transmission.

The calcium-permeable NMDA receptor is an ionotropic glutamate receptor predominantly responsible for controlling synaptic plasticity. Post synaptic depolarization leads to alleviation of a voltage-dependent blockade of the pore by magnesium ions, allowing the channel to act as a coincidence detector for presynaptic glutamate binding

and postsynaptic activity. The opening of NMDA channels has been shown to lead to a rise in post synaptic calcium in dendritic spines, activating downstream pathways which lead to synaptic plasticity. While strong activation of NMDA currents leads to LTP, moderate activation leads to LTD (59, 60). It is of note that the kinetics of NMDA channels renders a slower component to excitatory post synaptic potentials. As discussed above, this may promote persistent firing of recurrent networks by facilitating temporal summation of synaptic responses; thus, prolonged synaptic responses due to increased NMDA receptor activation may facilitate the "timing window" required for persistent firing. These same ideas may apply to the generation of rhythmic activity, given that oscillatory activity likely plays a role in synchronizing the timing of synaptic events, increasing the probability of inducing synaptic plasticity.

Dopamine

Dopamine (DA) functions as a neurotransmitter and plays an essential role in regulating goal-mediated behavior, motor control, arousal and cognition. Further, dopamine has been implicated in a wide variety of prefrontal functions, including updating working memory representations (61), context representations (62), and rewarding appetitive behaviors (63). The prefrontal cortex is highly innervated by dopaminergic neurons originating in the midbrain, which have been thought to play a role in encoding, updating and maintaining working memory processes (64). Although highly innervated, the PFC shares reciprocal connectivity with the ventral tegmental area, aiding in these functions. The midbrain maintains optimal dopaminergic activity within the prefrontal cortex, and has also been suggested to regulate rhythm generation. It is of note that normal prefrontal cortical function is critically dependent on dopaminergic input

from the ventral tegmental area of the midbrain (37). Interestingly, dopaminergic function in the mPFC is thought to be dysfunctional in patients with schizophrenia (65).

There are five known dopamine receptor types, including D1, D2, D3, D4 and D5. Of these types, D1/D5 are considered the "D1-like family" and D2/D3/D4 are considered the "D2-like family". These dopamine receptor families utilize different intracellular signaling pathways. The activation of D1-like receptors is linked to the G-protein G_s, which is known to activate adenylyl cyclase, leading to an increase in intracellular cAMP concentrations (66) and activation of protein kinase A, PKA. The D2-like receptors are known to activate the G-protein G_q pathway (67), inhibiting adenylyl cyclase and therefore decreasing cAMP levels, inhibiting PKA activation. Additionally, activation of the G-protein G_q pathway is known to activate phospholipase-C (PLC), leading to an increase in inositol 1,4,5-trisphosphate (IP_3) and DAG, and therefore, an increase in calcium release and protein kinase C (PKC) activation.

It has been proposed that type I and type II layer V pyramidal neurons of the mPFC exhibit differential surface expression of dopamine receptors. For example, Gee et. al. (21) has reported that type I (sub-cortically projecting) cells express both D1 and D2-type receptors, while type II (contralateral projecting) cells only express D1-type receptors. Further, it has been hypothesized by Gee et al. that D2-receptors, present only on type I cells, may play a critical role in enhancing outputs to subcortical brain regions. This differential expression pattern of dopaminergic receptors on layer V pyramidal subtypes suggests that dopamine may differentially regulate these cell subtypes. Further, it is likely that dopamine has differential effect on layer V pyramidal subtypes due to the different signaling pathways activated by D1 and D2 receptors.

In addition to layer V subtype expression patterns, dopamine receptors show differential cellular localization within the mPFC, with D1-like receptors being substantially greater than D2 receptors on pyramidal neurons (68, 69); additionally, both receptor types appear to be localized on inhibitory GABAergic interneurons as well as presynaptic excitatory glutamatergic terminals (70, 71). These differences in receptor expression suggests that dopamine may differentially regulate these cell types.

Studies within the mPFC have revealed that dopamine, acting through D1-type receptors, regulates cognition in a dose dependent manner. That is, insufficient activation of D1 receptors leads to distractibility, while excessive activation leads to perseverance (72-74). Despite many studies addressing the effects of dopaminergic D1-type receptor activation on synaptic responses in the PFC, it remains unclear how dopamine's actions at D1-type receptors leads to dose-dependent effects on PFC functions. One aspect that remains to be clarified regards the action of D1 receptor activation on glutamatergic synaptic responses evoked in different compartments of cortical pyramidal neurons.

Dopaminergic neurons are known to have two firing patterns: tonic and phasic. The 'tonic' dopamine state is defined as a spontaneous firing state of the population that regulates extra-synaptic dopamine levels in target regions. Some investigators have argued that tonic firing plays a role in constantly updating working memory (64). Dopaminergic high frequency firing, also known as burst firing, can lead to a transient or 'phasic' dopamine state, the response of a DA neuron to behaviorally relevant stimuli that results in a brief, large amplitude pulse of DA release. This brief and large pulse is proposed to activate post-synaptic DA receptors but is quickly removed by high capacity re-uptake systems. Although the exact mechanism by which dopamine exerts its effects

remains poorly understood, it is thought that proper balance between these two mechanisms is essential for proper executive function, and imbalances may give rise to phenotypes seen in patients with schizophrenia and other disorders.

Dopamine likely influences rhythm generation and persistent firing by modulating intrinsic and synaptic properties of layer V pyramidal neurons. Dopamine is known to influence excitatory synaptic transmission and plasticity in a frequency dependent manner in hippocampal CA1 pyramidal neurons (75). Furthermore, dopamine modifies short term plasticity in a frequency and layer dependent manner, through D1-like receptor activation in the prefrontal cortex of rats (76). Dopamine has also been shown to have effects on intrinsic currents such as I_h in entorhinal cortex (77) and the prefrontal cortex (78). In addition, dopamine, through D1/D5 receptor activation has also been shown to alter I_{Na} in the prefrontal cortex (78). It is also interesting to note that D1/D5 receptor activation enhances NMDA receptor-mediated currents in layer V pyramidal neurons of the mPFC (79, 80). Due to conflicting research reports and the complexity of dopamine's actions on intrinsic and synaptic properties, it is important to gain a better understanding of dopaminergic effects on frequency dependent synaptic dynamics, especially taking into consideration the location of the synapses on the extended dendritic tree of the layer V pyramidal cell.

Patients with schizophrenia are treated using antipsychotic medications, which exhibit therapeutic effects through blocking dopaminergic transmission. For this reason, it has been widely suggested that patients with schizophrenia exhibit abnormalities in dopaminergic regulation. Antipsychotics maintain their effectiveness by blocking dopaminergic D2-like receptors, with a general therapeutic dose occupying 60-80% of all

D2 receptors in treated patients (81). The long-term use of antipsychotics prevents psychotic symptoms in part by desensitizing dopamine receptors. Discontinued use of antipsychotics often results in the enhancement and over-sensitivity of dopamine receptors; thus, not only reintroducing psychotic symptoms but increasing the severity of symptoms. Currently, antipsychotics rely on the antagonism of dopaminergic D2-receptors to alleviate psychotic symptoms, and have been very effective in many cases; however, the drugs have serious side effects such as tardive dyskinesia (81), weight gain (82) and dystonia (83) while also having minimal effects on negative and cognitive symptoms. Due to these adverse side effects, the development of novel antipsychotics which lack harmful side effects remains of major interest. This will require a better understanding of the effects of endogenous dopamine on neuronal function in the prefrontal cortex.

Although some work characterizing dopaminergic modulation of excitatory transmission has focused on frequency-dependent synaptic properties, the proposed studies will be the first to characterize the synaptic properties of mPFC afferents on layer V pyramidal cells. In addition, the proposed studies would be the first to characterize the effects of dopaminergic modulation on the synaptic properties of specific dendritic compartments of layer V pyramidal cells.

Summary

In summary, executive functions are heavily reliant on both rhythm generation and dopaminergic modulation. Disruptions in either lead to symptoms observed in patients with schizophrenia and other cognitive disorders (e.g. ADD and PTSD). Currently, the only antipsychotic medications used for patients with schizophrenia target dopamine D2 receptors in an antagonistic manner. However, current antipsychotic

medications are only partly effective against positive symptoms and have serious side effects. Because alterations in dopaminergic modulation of rhythm generation give rise to detriments in working memory and other executive functions, it is important to understand the effects of dopamine on rhythm generation.

As discussed above, it has been well established that cortical rhythms are associated with working memory tasks and changes in rhythm generation are associated with deficits in cognitive functions, especially within the disorder of schizophrenia. In this dissertation, I aim to address the hypothesis that layer V pyramidal cells play a crucial role in integrating inputs from other brain regions. Therefore, synaptic inputs from different brain regions (e.g. amygdala, hippocampus and commissural mPFC) may be evoked at different frequencies, influencing synaptic integration and rhythm generation.

Further, it is known that proper working memory tasks are dependent on optimal levels of dopamine. Thus, these studies address how dopaminergic modulation may play a role in layer V cell integration of mPFC inputs. Activation of D1 and D2 receptors during frequency dependent synaptic activation may mimic how dopamine works *in vivo* to regulate layer V integration mechanisms and therefore working memory tasks. The results presented here may lend insight into how dopamine may play a role in regulating working memory, and may provide insight into how dopaminergic dysregulation can lead to working memory dysfunction, similar to that seen in schizophrenia. These results may not only lend insight into how dopamine may regulate layer V integration of mPFC inputs, but may also lend insight into specific treatment options in disorders involving working memory dysfunction. Additionally, the studies of dopaminergic effects on synaptic integration of layer V pyramidal neurons could lend further insight into the

investigation of additional therapeutics, which can target specific aspects of layer V pyramidal neurons to improve working memory functions in patients with schizophrenia and attentional disorders.

The work presented herein addresses all of the topics reviewed above with the overarching theme of characterizing the effects of dopamine on frequency dependent synaptic properties of layer V pyramidal neurons of the prefrontal cortex. This work addresses the following: (1) frequency has differential effects on the two components of excitatory transmission, non-NMDA (primarily AMPA) and NMDA receptor-mediated EPSPs (2) location of the excitatory synapses on the layer V pyramidal cells effect their response to altered frequencies (3) Dopamine D1 receptor activation versus D2 receptor activation has differential effects on synaptic components (4) EPSP dynamics differ between the two major subtypes of layer V pyramidal neurons, and finally, (5) EPSP dynamics differ as a function of specific inputs to layer V pyramidal neurons. The primary aims of my doctoral research are as follows:

Aim I. Identify the effects of dopamine D2 receptor activation on frequency dependent EPSP components (AMPA and NMDA receptor mediated) of layer V pyramidal neurons in the mouse mPFC with varying layer stimulation. Determining the effects of D2 receptor activation on frequency dependent EPSP components will allow me to make inferences on how dopamine regulates synaptic plasticity. Using layer I and layer V stimulation, it will be determined how dopamine, through D2 receptor activation affects cortical layers differently, in retrogradely labeled layer V pyramidal cells.

Aim II. Identify the effects of dopamine D1 receptor activation on frequency dependent EPSP components (AMPA and NMDA receptor mediated) of layer V pyramidal neurons in the mouse mPFC with varying layer stimulation. Determining the effects of D1 receptor activation on frequency dependent EPSP components will allow me to make inferences on how dopamine regulates synaptic plasticity. Using layer I and layer V stimulation, it will be determined how dopamine, through D2 receptor activation affects cortical layers differently, in retrogradely labeled layer V pyramidal cells.

Aim III. Determine the frequency dependent EPSP dynamics of layer V pyramidal neurons due to activation of specific inputs from the contralateral mPFC. Determining the frequency dependence of EPSP dynamics will allow inferences to be made on how layer V pyramidal neurons integrate information coming from other brain regions including the amygdala (what information), hippocampus (where/contextual information) and the contralateral mPFC. Channelrhodopsin-2 containing fibers (coming from the contralateral mPFC) will be activated using blue light to study frequency dependent EPSP dynamics on retrogradely labelled layer V pyramidal cells.

CHAPTER II

OVERVIEW OF RESEARCH DESIGN AND METHODS

All procedures used throughout this research project were conducted in accordance with the University of Northern Colorado Institutional Care and Use Committee (IACUC) protocols. Specific protocol numbers are listed in Appendix A. Furthermore, all animals used in this study were housed 1-4 animals per cage with a 12:12 light/dark cycle, on-site at the university animal facility and were given ad libitum access to food and water.

Each specific aim outlined above incorporates different methodology to address the research question. For this reason, an overview of each method is presented below. Additionally, if deemed necessary, background information regarding methodology is provided within individual sections. Within the subsequent chapters, a more detailed methodology regarding each specific aim is provided. Furthermore, because aim I has additional protocols, including stereotaxic surgery, compared to aim II, the methodology for the two aims are summarized below in reverse order. Here, aim II is presented first followed by aim I, for simplicity and clarity.

Methods for Aim II

Tissue Slice Preparation

Tissue slices of the mPFC were prepared from 25-42 day old male and female mice (C57 BL/6 strain, UNC breeding colony). Animals were anesthetized with carbon dioxide and rapidly decapitated following procedures outlined in an Institutional Animal Care and Use Committee approved protocol in accordance with NIH guidelines. The brain was then rapidly removed and immersed in ice-cold carbogen (95% O2 / 5% CO2)-saturated sucrose-enriched cutting solution containing (in mM): sucrose, 206; $NaHCO_3$, 25; KCl, 3.3; NaH_2PO_4, 1.23; $CaCl_2$, 1.0; $MgSO_4$, 4.0; dextrose, 10, osmolarity adjusted to 295±5 mOsm and pH adjusted to 7.40±0.03. The brain was then transferred to the cutting chamber of a vibrating tissue slicer and coronal slices of the prefrontal cortex (PFC) were prepared. Slices containing the mPFC were cut 300µm thick and taken from approximately 200µm to 1400µm caudal to the frontal pole. Slices were then placed in a holding chamber filled with recording solution containing (in mM): NaCl, 145; $NaHCO_3$, 25; KCl, 3.3; NaH_2PO_4, 1.2; $CaCl_2$, 0.9; $MgSO_4$, 2.0; dextrose, 10 (pH 7.40±0.03 and osmolarity 295±5), and were continuously bubbled with carbogen and incubated at 34°C for 45 minutes before allowing to cool at room temperature before use. Slices were then transferred to a recording chamber where they were perfused continuously at a flow rate of 1-2 mls/min with filtered, carbogen-saturated recording solution. Throughout recordings, the recording chamber was held between 32±1°C with a temperature controller.

Electrophysiology

Electrophysiological recordings of layer V pyramidal cells were obtained via whole-cell patch-clamp techniques (See figure 10 for schematic representation). Giga-seal whole-cell visualized patch recordings were made from the soma of mPFC Layer V pyramidal neurons located within the anterior cingulate, prelimbic or infralimbic cortices. Recording pipettes (4-6MΩ tip resistance) were filled with an intracellular solution consisting of (in mM): $KMeSO_3$, 135; NaCl, 8; EGTA, 0.5; HEPES, 10; $MgCl_2$, 2; TrisATP, 2; TrisGTP, 0.3 (280 mOsm, pH 7.2). An additional glass micropipette (filled with 3M NaCl) was placed in either layer V or layer I of the mPFC to activate primarily fibers located within that layer. EPSP's were evoked in current clamp mode using an 8-pulse stimulus train, at varying frequencies (10-50Hz). This protocol was repeated 5 times with a 10 second inter-train interval, and the 5 responses were averaged. In experiments isolating AMPA-mediated excitatory post synaptic potentials, the recording solution contained 50μM APV (2R-amino-5-phosphonovaleric acid; an NMDA antagonist). In experiments isolating NMDA-mediated excitatory post synaptic potentials, the recording solution contained 10μM DNQX (6,7-dinitroquinoxaline-2,3-dione; an AMPA antagonist) and low magnesium recording solution containing (in mM): NaCl, 145; $NaHCO_3$, 25; KCl, 3.3; NaH_2PO_4, 1.2; $CaCl_2$, 0.9; $MgSO_4$, 0.5; dextrose, 10 (pH 7.40±0.03 and osmolarity 295±5). AMPA (non-NMDA) and NMDAR-mediated EPSPs were isolated for all experiments within aim I and II. For non-NMDAR-mediated EPSP isolating experiments, cells were manually held at -80mV. Pulse trains were applied in control (APV-containing) aCSF, and again following a 5 minute application of the D1 agonist, SKF-38393. NMDA EPSP's were evoked using the same current clamp

mode protocol, while cells are held manually at -65mV throughout the experiment. Additionally, NMDAR-mediated EPSP isolating experiments were performed in a solution containing DNQX and low magnesium aCSF (0.5mM replaced 2mM $MgSO_4$). Pulse trains were applied in control (DNQX-containing) aCSF, and again following a 5-minute application of SKF-38393. The averaged responses were digitized at 10KHz, and saved on disk using a Digidata 1322A interface (Axon instruments) and Pclamp version 8.1 software (Clampex program, Axon Instruments). Data was then analyzed in Clampfit (Axon Instruments Inc.). Responses were compared between control and D1 agonist containing solutions at the various frequencies, and between cell types.

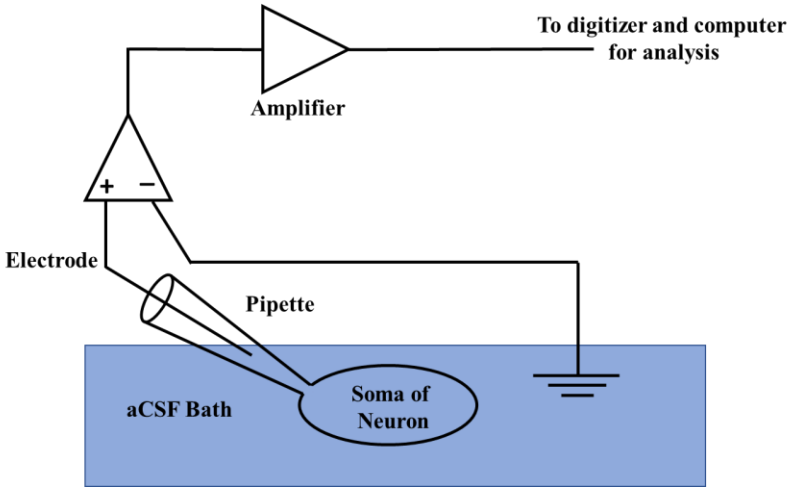

Figure 10: Schematic diagram of whole-cell patch-clamp electrophysiology. Illustration of a basic whole-cell patch-clamp circuitry. The recording pipette was filled with intracellular solution, and is used to seal onto and rupture the plasma membrane of soma of the neuron, to allow electrical access. Within the glass pipette is a silver-silver chloride electrode that transmits neuronal electrical activity to an amplifier from which the signal is digitized for computer processing.

Methods for Aim I

Retrobead labeling (background)

For this aim, fluorescent microbeads were utilized to label layer V neurons based on their axonal projections. When microbeads are injected into a brain region, they are picked up by projections that target that area. Once picked up, they are transported backwards in the axonal process (retrogradely) towards the soma of the neuron. Once in the soma, they can be visually identified through the use of fluorescent light. Either green or red beads were used for these experiments, which were excited by blue and green light, respectively. In figure 11, a visual representation for bead injections is provided in part A. Fluorescent somatic bodies are shown in part B, displaying a typical pyramidal shaped soma, upon high magnification.

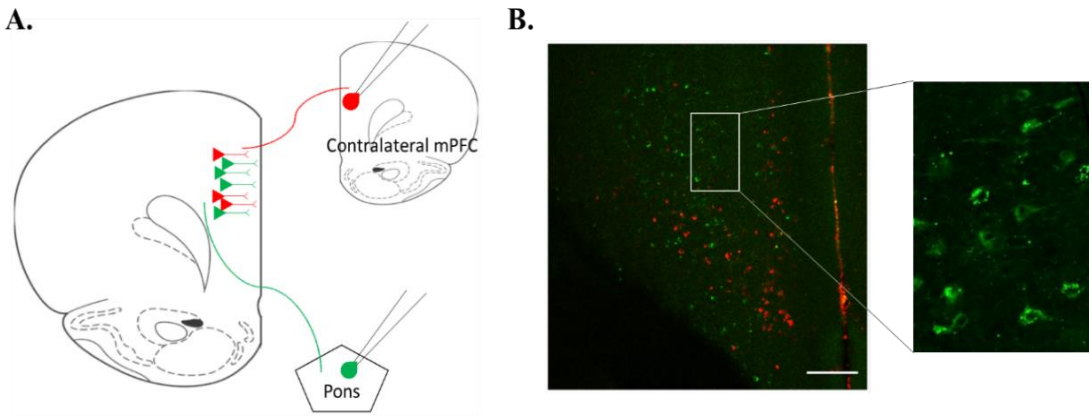

Figure 11: Retrogradely labeled layer V pyramidal neurons. A. Schematic representation of microbead injections into either the commissural mPFC or the pontine of the brainstem to label type II and type I layer V cells, respectively, with fluorescent retrobeads. **B.** Retrograde labelled layer V pyramidal neurons, containing microbeads within their soma (green: type I; red: type II).

Stereotaxic Injections

Mice were anesthetized with a combination of isoflurane and oxygen. Once under full anesthesia, the head of the mouse was shaved, and the mouse was transferred

to a stereotaxic apparatus, where it was properly position with ear bars and a nose cone. While in the stereotaxic apparatus, the mouse was placed on a heating pad to ensure proper body temperature. An iodine clean wash was then applied to the skin around the injection sight. This was then followed by an alcohol wash, and both were repeated three times in total. Following washes, a single incision was made directly on the top of the head above the skull, using a scalpel blade. The connective tissue was then pushed aside using a q-tip, to insure no further damage to the skin.

Using the stereotaxic apparatus, a specific location on the contralateral side of the mPFC as well as in the pontine of the brainstem, was found using the dimensions of the stereotaxic. Coordinates for the contralateral mPFC and the pontine injections, from bregma (in mm): medial-lateral, +0.3; dorsoventral, -2.3 to -1.3; rostrocaudal, +1.7; and medial-lateral +1.1; dorsoventral, -5.2; rostrocaudal, -3.5, respectively. Once these coordinates were obtained, a single burr-hole was made in the skull using a micro-drill. Once the small hole was made, a neuro-specific injection needle was placed into the brain and positioned to the proper coordinates, where the fluorescent microbeads were injected at the proper location. Injections lasted approximately 10 minutes to insure proper release of the microbeads from the syringe. The injection pipette was then retracted slowly over the course of five minutes.

Once the needle was fully extracted, the skin on top of the skull, as well as the open wound, was sterilized with a betadine and saline solutions. The skin was then pulled together and sutured with 3-5 stitches. Once completed, the mouse received a subcutaneous injection of carprofen (animal ibuprofen), and was then transferred to a ‘recovery’ cage. Throughout recovery, animals were monitored for pain (i.e. abnormal

movements/behavior, excessive itching at or around suture site; lethargy etc.). If pain was observed, additional carprofen was administered. Recovery of the animal was observed for a minimum of 24 hours before the mouse was sacrificed and slices were made. Slices were made according to the methods listed under aim II (slice preparation). For these experiments, an LED was used to identify retrogradely labelled pyramidal neurons. Cells that contain prominent fluorescence in their soma were used for recording (see aim II methods – electrophysiology). Experimental protocols regarding AMPA and NMDAR-mediated responses were followed according to those outlined under aim II above.

Methods for Aim III

As discussed in chapter I, ChR2 is a well-established molecular tool for activating specific populations of nerve axons. For this study, an adeno-associated virus (AAV) containing the ChR2 gene sequence was injected into the commissural mPFC, resulting in expression of the ChR2 protein in callosal/commissural afferents. Additionally, a fluorescent marker protein was also expressed by the construct, resulting in an mCherry tag following translation. The construct was injected into the commissural mPFC, which is known to send axons to the contralateral side of the mouse prefrontal cortex, utilizing a stereotactic apparatus. Stereotaxic injections were followed according to the protocol outlined in aim I above. Following several days recovery, slices of prefrontal cortex were prepared from the injected animals, and the nerve fibers expressing ChR2 were then activated using short light pulses (1ms) delivered by a blue LED located on the electrophysiology microscope.

As stated above, these injections were followed per the surgical procedures outlined under ‘aim II methods – stereotaxic injections’. However, there were differences between the two methods. Aim III incorporated a dual injection technique, where

fluorescent retrograde microbeads (as described in aim II) were used to label the two subpopulations of layer V pyramidal cells, and ChR2, packaged within the AAV, was used at the second injection site to anterogradely label afferents coming from the commissural mPFC and impinging onto layer V cells. Packaged ChR2 were purchased from PennVectors and was injected at the volumes of 600-900nL. Using this dual injection technique, type I and type II pyramidal cells were distinguished based on somatic fluorescent labelling (green), and fibers containing ChR2 were labelled with red fluorescence and could be selectively activated using blue light.

CHAPTER III

FREQUENCY DEPENDENT EFFECTS OF DOPAMINERGIC D2 RECEPTOR ACTIVATION ON SYNAPTIC RESPONSES IN A SUBSET OF LAYER V PYRAMIDAL NEURONS IN THE MOUSE PREFRONTAL CORTEX

Contribution of Authors and Co-Authors

Manuscript in Chapter III

Author: Jonna M. Jackson

Contributions: Developed and implemented the study design. Generated and analyzed data. Wrote first draft of the manuscript.

Co-Author: Dr. Mark P. Thomas

Contributions: Helped conceive the study topic. Provided guidance on study design. Provided feedback data interpretation and manuscript preparation.

Abstract

In humans, prefrontal cortical areas are known to support executive functions. In mice, these functions are mediated by homologous regions in the medial prefrontal cortex (mPFC). Executive processes are critically dependent on optimal levels of dopamine (DA), but the cellular mechanisms of DA modulation are incompletely understood. Stable patterns of neuronal activity may be sensitive to frequency dependent changes in synaptic transmission. We characterized the effects of D2 receptor (D2R) activation on short-term excitatory postsynaptic potential (EPSP) dynamics evoked at varying frequencies in the two subtypes of layer V pyramidal neurons in mouse mPFC. We isolated NMDA receptor and non-NMDA receptor mediated components of EPSP trains evoked by stimulating fibers within layer V or layer I. All significant effects of D2 receptor activation were confined to type I (corticopontine) cells. First, we found that with layer I stimulation, D2R activation reduces the amplitude of NMDAR-mediated EPSP's, with no effect on facilitation or depression of these responses at lower frequencies, but leading to facilitation with high frequency stimulation. Further, the non-NMDA component also underwent synaptic depression at low frequencies. Second, with layer V stimulation, D2R activation had no effect on NMDA or non-NMDA receptor mediated EPSP components. Overall, our results suggest that D2R activation may modulate memory functions by inhibiting 'top-down' influences from apical tuft inputs activated at low frequencies, while promoting 'top-down' influences from inputs activated at higher frequencies. These data provide further insight into mechanisms of dopamine's modulation of executive functions.

Introduction

In humans, prefrontal cortical (PFC) areas are known to support goal-directed behaviors, mediating a variety of functions that render behavior more flexible in the face of changing environmental demands. It has been hypothesized that the function of medial regions of the PFC is to learn associations between contextual events, and corresponding emotional responses, ie. action-outcome associations (6). In mice, these functions are mediated by homologous regions in the medial prefrontal cortex (mPFC) (7, 8). When executive functions are disrupted, individuals suffer losses in social capabilities, which is often associated with diseases such as bipolar disorder, schizoaffective disorder and schizophrenia. More subtle disturbances in these executive functions may cause attention deficit disorders and anxiety disorders (e.g. post-traumatic stress disorder).

Normal prefrontal cortical function is critically dependent on dopaminergic input from the ventral tegmental area of the midbrain (37). Dopamine, acting on D1-like and D2-like receptors in the PFC, has been implicated in a wide variety of prefrontal functions, including updating working memory (61) and context representations (62), as well as rewarding appetitive behaviors (63). The major neocortical output cells located in layer V comprise two subtypes: subcortically-projecting (type I) and contralaterally-projecting or commissural (type II) (84). It has been proposed that type I and type II layer V pyramidal neurons of the mPFC exhibit different surface expression of dopamine receptors. For example, Gee et al. (21) have suggested that type I cells express both D1 and D2-type receptors, while type II cells only express D1-type receptors. Further, they hypothesize that D2-receptors, located only on type I cells, may play a critical role in enhancing outputs to subcortical brain regions. This differential expression pattern of

dopaminergic receptors on layer V pyramidal subtypes suggests that dopamine has the ability to differentially regulate these pyramidal cell subtypes. However, it is of note that both receptor types localize on GABAergic interneurons and on presynaptic excitatory glutamatergic terminals (70, 71).

In layer V neocortical pyramidal neurons, feed-back (top-down or contextual) information is received via apical tuft synapses (in layer I), while feed-forward (bottom-up or environmental) information is delivered to synapses on the apical trunk (39). Further, local processing occurs between layer V neurons via synapses on basal dendrites located predominantly in layer V. When synaptic inputs to the apical tufts are activated synchronously with postsynaptic action potentials (i.e. when feedback and feedforward signals coincide), layer V pyramidal neurons act as coincidence detectors, firing in a high frequency bursting pattern, which may lead to synaptic plasticity locally and in target neurons (39). It is conceivable that this high frequency bursting also serves as an attentional component, indicating relevant environmental information. Considered in the context of a circuit with recurrent connections (especially prominent in the mPFC), here we explore phenomena relevant to the hypothesis that layer-specific, frequency-dependent short-term synaptic dynamics and their modulation by dopamine play a significant role in generating persistent activity observed in prefrontal cortical networks during memory-related tasks.

Excitatory post synaptic potentials (EPSPs) are characterized by two components, a non-NMDA receptor (primarily AMPA receptor) mediated component that confers fast synaptic transmission, and an NMDA receptor (NMDAR) mediated component necessary for synaptic plasticity. Previous work characterizing dopaminergic modulation of

excitatory transmission has focused on synaptic responses evoked at low frequencies. In this study, we studied the effects of D2 receptor activation on isolated NMDAR and non-NMDAR mediated components of EPSPs evoked over a range of frequencies that mimic high frequency bursting, in layer V pyramidal cell subtypes. We also examined D2 receptor effects on EPSP trains evoked by stimulation of synapses in layer I (reflecting feed-back activity) versus EPSP trains evoked by layer V stimulation (reflecting local connections between layer V output neurons). The intent of this study was to describe the overall effects of quinpirole on non-NMDA and NMDA receptor mediated, frequency-dependent synaptic dynamics in the two major dendritic compartments of mPFC layer V pyramids, without addressing subcellular mechanisms of D2 receptor modulation. Some of these results have been presented previously in abstract form (85).

Materials and Methods

Stereotaxic Surgery

Young (28-42 day old) mice, of both sex, were anesthetized with a combination of isoflurane and oxygen. Once under full anesthesia, the mouse was transferred to a stereotaxic frame (Stoelting 51500U, Ultra-Precise, Wood Dale, IL, USA), and a nose cone was placed for continuous administration of anesthesia during the surgery. A burr hole was made at coordinates ML: +0.35mm, DV: -2.3 to -1.3mm and +1.8mm (for contralateral injections) and ML: -1.1, DV: -5.2mm and RC: -3.5mm (for pontine injections) from bregma. Coordinates were determined based on previous literature (20, 21) as well as the Paxinos Brain Atlas. Lumafluor (Naples, FL) 1X green or 1X red retrobeads were injected with either a 1µL or 5µL neuros syringe (Hamilton Company, Reno, NV, USA) at the coordinates above at volumes of 600-800nL. Following injection,

the incision site was sutured with 4-6 stitches (Roboz RS-7985-12 needles; Roboz SUT-15-2 sutures). Mice were then subcutaneously injected with Rimadyl (Carprofen; Pfizer Pharmaceuticals, Brooklyn, NY, USA) for pain and individually housed for 2-7 days before tissue slices were made.

Tissue Preparation

Tissue slices were prepared from 30-52-day old bead-injected mice (C57 BL/6 strain, UNC breeding colony). Animals were anesthetized with carbon dioxide and rapidly decapitated following procedures outlined in a UNC Institutional Animal Care and Use Committee approved protocol in accordance with NIH guidelines. Brains were rapidly removed and immersed in ice-cold carbogen (95% O_2 / 5% CO_2) saturated sucrose-enriched artificial cerebrospinal fluid (cutting aCSF) containing (in mmol/L): sucrose, 206; $NaHCO_3$, 25; dextrose, 10; KCl, 3.3; NaH_2PO_4, 1.23; $CaCl_2$, 1.0; $MgCl_2$, 4.0, osmolarity adjusted to 295±5 mOsm and pH adjusted to 7.40±0.03. The brains were then transferred to the cutting chamber of a vibrating tissue slicer (OTS500, Electron Microscopy Sciences, Hatfield, PA) and coronal slices of the prefrontal cortex (PFC) were prepared in ice-cold cutting aCSF. Slices were cut 300µm thick and were taken from approximately 200µm to 1400µm caudal to the frontal pole. Slices were then placed in a holding chamber filled with recording aCSF solution containing (in mmol/L): NaCl, 120; $NaHCO_3$, 25; KCl, 3.3; NaH_2PO_4, 1.23; $CaCl_2$, 0.9; $MgCl_2$, 2.0; dextrose, 10, osmolarity adjusted to 295±5 mOsm and pH adjusted to 7.40±0.03. The holding chamber aCSF was continuously bubbled with carbogen and incubated at 34°C for 45 minutes and then allowed to cool to room temperature before slice recording. Prior to experiments,

slices were transferred to a recording chamber where they were perfused continuously at a flow rate of 1-2 mls/min with filtered, carbogen-saturated recording aCSF solution.

Throughout recordings, the recording chamber was held at 32±1°C with a temperature controller equipped with a chamber heater and an in-line heater (TC-344B, Warner Instruments, Hamden CT). In experiments isolating non-NMDAR-mediated EPSPs, the recording aCSF contained 50μM aminophosphonovalerate (D-APV; an NMDA receptor antagonist). In experiments isolating NMDAR mediated EPSPs, the recording aCSF contained 20μM 6,7dinitroquinoxaline-2,3-dione (DNQX; a non-NMDA [AMPA] receptor antagonist) and recording buffer $MgCl_2$ concentration was reduced to 0.25 mM to facilitate NMDAR activation at -65mV.

Electrophysiology

Layer V pyramidal neurons of the infralimbic, prelimbic and anterior cingulate cortices were visually identified using infrared DIC microscopy at 400x magnification with an Olympus BX51WI microscope (Tokyo, Japan). Fluorescence was visualized using light emitted from an X-Cite LED (Excelitas, Waltham, MA, USA). Whole cell recordings were made from the soma of fluorescent layer V pyramidal neurons after establishing a Giga-ohm seal (resistance range: 1-10 Gohm). Only cells that exhibited a thin (i.e. amplitude at half-width less than 2ms), overshooting action potential, as well as continuous spiking throughout a depolarizing current injection were used in this study. Access resistance (R_A) was compensated throughout experiments, and cells were excluded from analysis if uncompensated R_A exceeded 20MΩ. Liquid junction potentials (estimated at approximately -6mV for K^+ gluconate internal solution) were not compensated in adjusting Vm for synaptic recordings. Amplifier bridge balance was

utilized and monitored throughout current injections. Recording pipettes (4-6MΩ tip resistance), produced from thin-wall glass capillary tubes (1.5µm OD, 1.12µm ID, World Precision Instruments, Sarasota, FL), were filled with an intracellular solution containing (in mM): potassium gluconate, 135; KCl, 10; EGTA, 1.0; HEPES, 10; MgATP, 2; TrisGTP, 0.38, osmolarity adjusted to 285±5 mOsm and pH adjusted to 7.30±0.01. Additional glass micropipettes, filled with 3M NaCl, were placed within either layer V or layer I of mPFC and used as stimulating pipets to activate fibers located within that layer.

In addition to retrograde labeling, type I and II layer V pyramidal cells were also identified based on the presence of a prominent "sag" in response to a 150 pA hyperpolarizing current (type I: minimal 12% depolarization from peak of hyperpolarization, indicating the strong presence of the hyperpolarization activated cation current), and by initial firing of doublets (only observed in type I cells); both of these criteria have been used in previous studies (19-21, 86). For all analyses, type I and type II subtypes were categorized and compared between experimental groups. The responses were digitized at 10kHz and saved on disk using a Digidata 1322A interface (Axon instruments) and pCLAMP version 8.1 software (Clampex program, Axon Instruments). Data were analyzed off-line in Clampfit (Axon Instruments).

Statistical Analyses

All values are presented as mean ± SEM (standard error of the mean). All cells received every stimulus frequency (10Hz-50Hz) and the D2R agonist. An ANOVA was performed on all experimental data except for comparisons between Rm and resting membrane potential (where a Student's t-test was utilized). A two-way repeated measures

ANOVA was used to analyze the effects of drug and frequency of stimulation. The statistical model also included mouse and slice as random variables.

Experimental Protocols

We began each experiment by establishing a "stimulus current / evoked response" curve where stimulus intensity was increased while measuring the evoked EPSP amplitude. The stimulus current was adjusted to establish an unsaturated response near the midrange of this curve. The position of the stimulating pipette was located at a distance from the recorded cell to establish a baseline response ranging from 7-10 mV and 2-5 mV (for non-NMDAR and NMDAR EPSPs respectively). These amplitudes were chosen to avoid cell spiking during the pulse trains, where summation was often observed at higher stimulus train frequencies. EPSP's were evoked in current clamp mode using an 8-pulse stimulus train, at varying frequencies (10-50Hz). This protocol was repeated 5 times with a 10 second inter-train interval, and the 5 responses were averaged. All experiments were conducted in the presence of the $GABA_A$ antagonist, gabazine (10μM), to isolate glutamatergic responses. For non-NMDAR-mediated EPSP experiments, cells were manually held at -80mV throughout the experiment. Pulse trains were applied in control (APV-containing) aCSF, and again immediately following a 5 minute application of the D2 agonist, Quinpirole (20 μM). NMDAR-mediated EPSPs were evoked using the same current clamp protocol as for non-NMDAR-mediated EPSP experiments. During NMDAR EPSP experiments, cells were manually held at -65mV throughout the experiment. Pulse trains were applied in control (low magnesium and DNQX-containing) aCSF, and again immediately following a 5 minute application of the D2 agonist quinpirole (20 μM) (low magnesium, DNQX and Quinpirole-containing). For

antagonist experiments, sulpiride (10µM) was included in the bath during control recordings.

EPSP amplitudes were measured in millivolts (mV), from the membrane potential directly before the stimulus was applied. The initial EPSP amplitude was measured from resting baseline, whereas subsequent EPSP amplitudes were measured from the minimal amplitude directly before the EPSP was evoked (figure 12A). Maximal peak amplitude was measured from baseline (before the train was delivered) to the peak amplitude reached during the train of EPSPs; the time to reach this peak amplitude within the train (time-to-peak) was also measured (figure 12B).

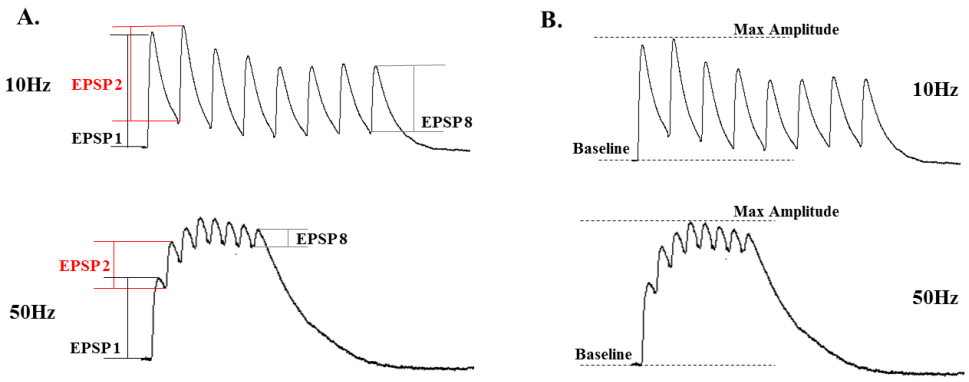

Figure 12: Analysis of EPSP characteristics. (A) Example traces of 10Hz (top) and 50Hz (bottom), depicting how amplitude of EPSP's were measured throughout the train. Although all EPSPs within the train were measured, for simplicity, only EPSP1, EPSP2 and EPSP8 are shown here. **(B)** Example traces for 10Hz (top) and 50Hz (bottom), are shown to display how maximal/peak amplitude was measured throughout the train.

Drugs

The NMDA antagonist, D-APV, the dopamine D2-like receptor agonist, quinpirole, the $GABA_a$ antagonist, gabazine, and the dopamine D2-like antagonist,

sulpiride, were purchased from Tocris Biosciences (Bristol, UK). The non-NMDA antagonist, DNQX, was purchased from Alomone Labs (Jerusalem, Israel). D-APV, quinpirole, gabazine, sulpiride and DNQX were diluted into aliquots of 50mmol/L, 20mmol/L, 10mmol/L, 10mmol/L and 20mmol/L stocks, respectively. All drugs were stored at -80ºC and diluted to working concentrations of 50µmol/L D-APV, 20µmol/L quinpirole, 10µmol/L gabazine, 10µmol/L sulpiride and 20 µmol/L DNQX; any drugs not used within 3 days of thawing were discarded.

Results

Type I and Type II Cells Can Be Distinguished Based on Axonal Projections and Electrophysiological Properties

Using a retrograde labeling technique, two subtypes of layer V pyramidal neurons were identified based on their axonal projection patterns. We identified two distinct subtypes of pyramidal cells that projected to either the brainstem (cortico-pontine/type I cells) or the commissural mPFC (commissural/type II cells), with no overlap in populations (fig. 13B). As demonstrated in previous studies (19, 21, 86) these two populations also showed differences in electrophysiological properties, where type I neurons often displayed an initial spiking doublet in response to a 150pA depolarizing current (fig. 13C, left, green trace) and type II neurons displayed a relatively constant spiking pattern in response to the same current (fig. 13C, right, red trace). Additionally, Type I neurons displayed a prominent depolarizing sag due to a hyperpolarization-activated cation current in response to a 150pA hyperpolarizing current, compared to Type II neurons (fig. 13D; type I, green; type II, red). Type I and type II neurons did not

differ significantly in regards to membrane resistance (R_M) or resting membrane potential (V_{REST}) (fig. 13E&F).

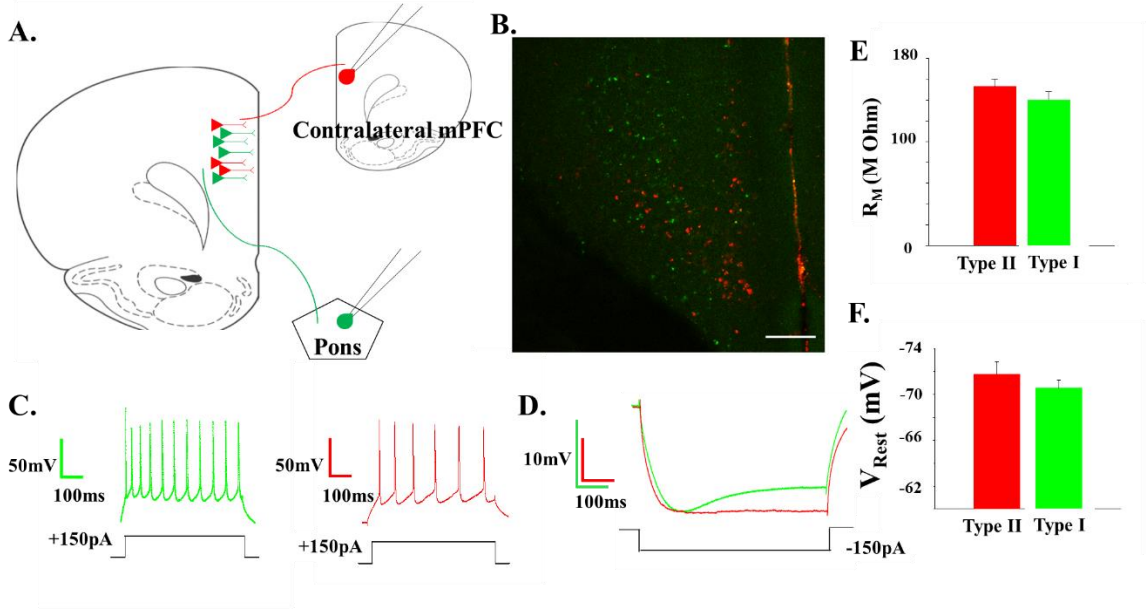

Figure 13: Layer V pyramidal cells of the prefrontal cortex are defined by axonal projections and intrinsic properties. (A) Schematic representation of retrograde labeling; type I cells were labeled with green retrobeads injected into the pontine of the brainstem; type II cells were labeled with red retrobeads injected into the contralateral mPFC. **(B)** Image showing accurately labeled type I and type II layer V pyramidal cells, with no overlap of red and green retrobeads, definitively labeling two distinct cellular populations. (scale bar = 200µm) **(C)** Type I cell spiking pattern showing a distinct initial spiking doublet with a 150pA current injection (green; left); Type II cell spiking pattern lacking initial spike doublet with 150pA current injection (red; right). **(D)** Type I cells display a large depolarizing 'sag' in response to a 150pA hyperpolarizing current (type I: green trace; type II: red trace). **(E)** Type I cells display a lower, yet non-significant, average R_M (140±8.0mΩ) than type II cells (153±7.4mΩ). **(F)** Type I cells display a more depolarized, yet non-significant, average membrane potential (-70.6±0.7mV) than type II cells (-71.8±1.1mV). (Student's t-test)

Non-N-Methyl-D-Aspartate Receptor Mediated Excitatory Post-Synaptic Potentials

Non-NMDA receptor (non-NMDAR) mediated EPSP trains were measured from layer V pyramidal neurons by blocking NMDA receptor activation with 50 µM APV.

Representative traces, for all frequencies (10-50Hz), recorded following layer V stimulation are shown in figure 14A. At a frequency of 10Hz, non-NMDAR EPSPs show two distinct amplitude profiles, which we define simply as facilitating (the second EPSP is larger than the first EPSP; EPSP2>EPSP1; fig. 14C, top; black trace) or depressing (the second and subsequent EPSPs are smaller than the first EPSP; EPSP2<EPSP1; fig. 14C, bottom; blue trace). In 23 out of 27 layer V cells (15 type I; 8 type II), layer V-evoked non-NMDAR EPSPs showed a depressing pattern in control solution. In the remaining 4 of 27 cells (2 type I, 2 type II), layer V-evoked non-NMDAR EPSPs were facilitating. Further, in 21 out of 22 cells (15 type I, 6 type II), layer I-evoked non-NMDAR EPSPs were depressing, while one cell (type II) showed a facilitating pattern. Notably, we did not see a significant difference between type I and type II cells with regard to their short term synaptic dynamics (layer V evoked non-NMDAR EPSPs [EPSP2/EPSP1 $p>0.05$; $n=27$]; layer I evoked non-NMDAR EPSPs [EPSP2/EPSP1; $p>0.05$; $n=22$]).

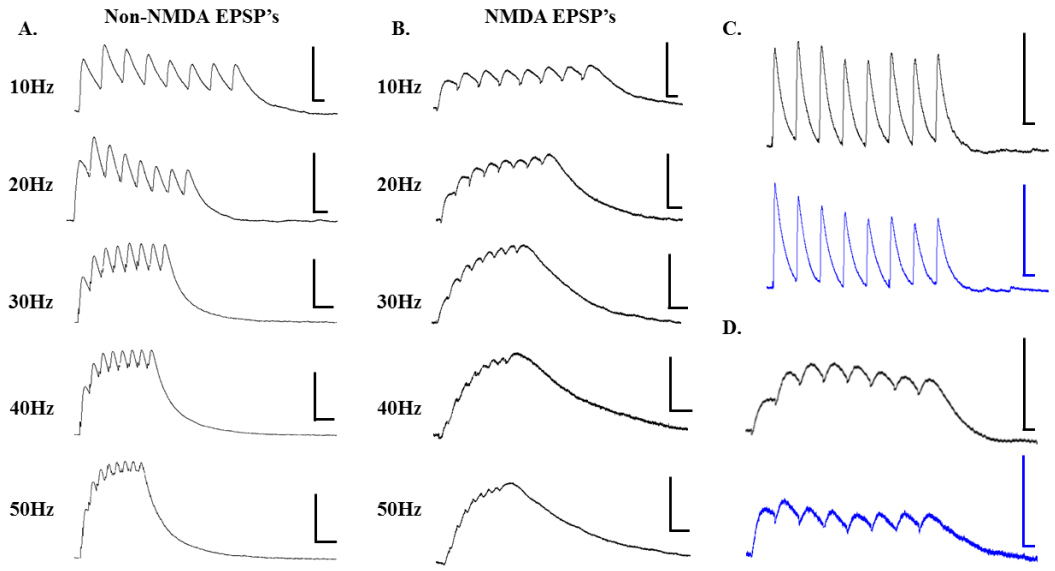

Figure 14: EPSP trains evoked by layer V stimulation. (A) Representative traces showing non-NMDAR-mediated EPSP trains evoked by layer V stimulation. Traces are shown for each stimulation frequency (10-50 Hz from top to bottom). **(B)** Representative traces showing NMDAR-mediated EPSP trains evoked by layer V stimulation. Traces are shown for each stimulation frequency (10-50 Hz from top to bottom). **(C)** non-NMDAR-mediated EPSP trains show two types of short-term dynamics, facilitating (EPSP2> EPSP1; black trace, top) and depressing (EPSP2<EPSP1; blue trace, bottom). **(D)** NMDAR-mediated EPSP trains show facilitating (EPSP2> EPSP1; black trace, top) and depressing (EPSP2<EPSP1; blue trace, bottom) short-term dynamics. All scale bars, x=10mV and y=50ms.

N-Methyl-D-Aspartate-Receptor Mediated Excitatory Post-Synaptic Potentials

NMDA receptor (NMDAR) mediated EPSP trains were measured from layer V pyramidal neurons by blocking non-NMDA receptors with 20µM DNQX. Representative traces, for all frequencies (10-50Hz), recorded following layer V stimulation are shown in figure 14B. Like non-NMDAR EPSPs, NMDAR EPSPs also showed two distinct amplitude profiles, which we have defined as facilitating and depressing. A representative trace of an NMDAR EPSP facilitating and depressing response is shown

(fig. 14D; top [black trace] and bottom [blue trace], respectively). In 29 out of 34 layer V cells (15 type I, 14 type II), layer V-evoked NMDAR EPSPs showed a depressing pattern in control solution. In the remaining 5 cells (4 type I, 1 type II), layer V-evoked NMDAR EPSPs were facilitating. Moreover, in 19 out of 22 cells (7 type I, 12 type II), layer I-evoked NMDAR EPSPs showed a depressing pattern, while the remaining 3 cells (1 type I, 2 type II) showed a facilitating pattern. Again, we did not see a significant difference between type I and type II cells with regard to their short term synaptic dynamics (layer V evoked NMDAR EPSPs [EPSP2/EPSP1; $p>0.05$; $n=34$]; layer I evoked NMDAR EPSPs [EPSP2/EPSP1; $p>0.05$; $n=22$]).

Frequency Dependent Properties of Excitatory Post Synaptic Potential Trains

We examined the frequency dependent properties of both non-NMDAR and NMDAR-mediated EPSP's by stimulating at various frequencies between 10Hz and 50Hz. Non-NMDAR-mediated EPSP's showed similar trends in frequency dependent properties with layer V and layer I stimulation. For both layer I and layer V stimulation, the ratio of EPSP2/EPSP1 was not different between 10Hz and 50Hz (fig. 15A&B). However, with both layer V and layer I stimulation, the maximal amplitude is higher, and the latency to peak is shorter, at 50Hz compared to 10Hz (fig. 15A&B, tables). Thus, temporal summation of non-NMDAR EPSP's is more robust at higher frequencies. However, with layer I stimulation, the latency to peak amplitude remains unchanged from 10 to 50Hz although there is a trend for the latency to be shorter at 50Hz ($p=0.06$).

NMDAR-mediated EPSP's showed similar trends in frequency dependent properties with layer V and layer I stimulation. For both layer I and layer V stimulation,

the ratio of EPSP2/EPSP1 was not different between 10Hz and 50Hz (fig. 15C&D). However, with both layer V and layer I stimulation, the maximal amplitude is higher, and the latency to peak is shorter, at 50Hz compared to 10Hz (fig. 15C&D, tables). These results indicate that, regardless of layer stimulation, temporal summation of NMDAR-mediated EPSP's is more robust at higher frequencies.

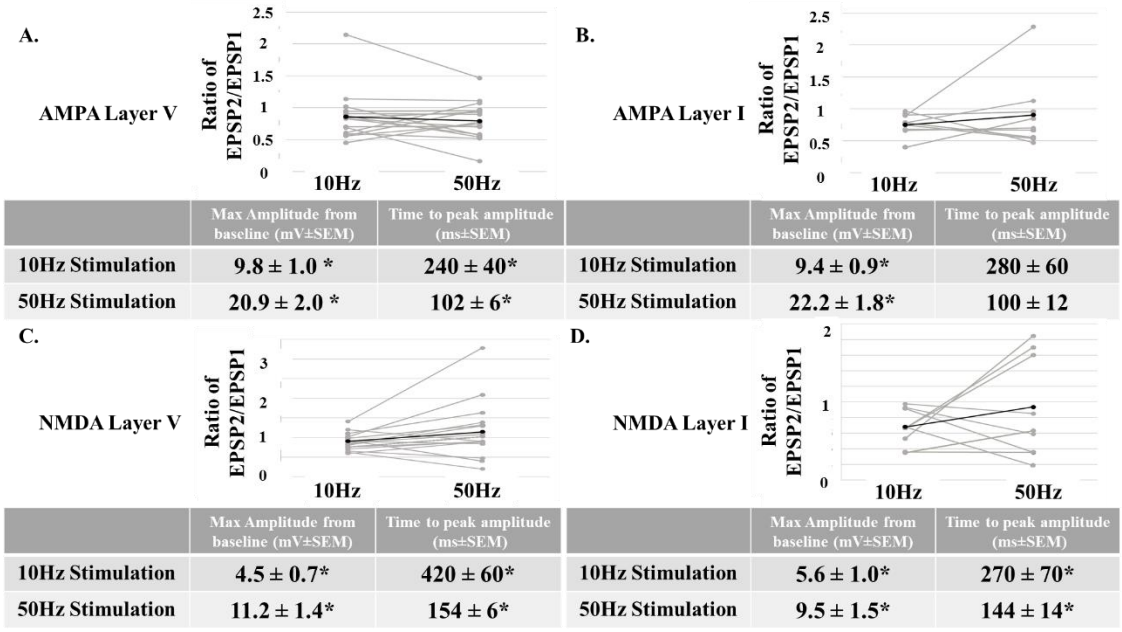

	Max Amplitude from baseline (mV±SEM)	Time to peak amplitude (ms±SEM)
10Hz Stimulation	9.8 ± 1.0 *	240 ± 40*
50Hz Stimulation	20.9 ± 2.0 *	102 ± 6*

	Max Amplitude from baseline (mV±SEM)	Time to peak amplitude (ms±SEM)
10Hz Stimulation	9.4 ± 0.9*	280 ± 60
50Hz Stimulation	22.2 ± 1.8*	100 ± 12

	Max Amplitude from baseline (mV±SEM)	Time to peak amplitude (ms±SEM)
10Hz Stimulation	4.5 ± 0.7*	420 ± 60*
50Hz Stimulation	11.2 ± 1.4*	154 ± 6*

	Max Amplitude from baseline (mV±SEM)	Time to peak amplitude (ms±SEM)
10Hz Stimulation	5.6 ± 1.0*	270 ± 70*
50Hz Stimulation	9.5 ± 1.5*	144 ± 14*

Figure 15: Frequency dependent properties of non-NMDA and NMDA EPSP's evoked by either layer V or layer I stimulation. With layer V **(A)** and layer I **(B)** stimulation, for non-NMDA EPSP's, the ratio of EPSP2/EPSP1 is unchanged from 10Hz to 50Hz (top). Addition characteristics are tabled (bottom). With layer V **(C)** and layer I **(D)** stimulation, for NMDA EPSP's, the ratio of EPSP2/EPSP1 is unchanged from 10Hz to 50Hz (top). Addition characteristics are tabled (bottom). For each graph, gray lines represent each individual cell and black lines represent the average of all cells. Asterisks in tables depict a significant difference ($p<0.05$; RM ANOVA) between 10Hz and 50Hz.

D2 Receptor Effects on Excitatory Post Synaptic Potential Trains

Layer I evoked non-N-methyl-D-Aspartate-Receptor mediated excitatory post synaptic potentials. The D2 agonist, quinpirole, had no effect on the initial EPSP amplitude in either cell type (type I cells, from 7.7±0.8V to 8.8±1.7mV at 10Hz [$p>0.05$;

n=9]; type II cells, from 9.9±2.4mV to 9.1±2.2mV [p>0.05; n=3]). The effects of quinpirole on synaptic trains were frequency-dependent. At lower frequencies, quinpirole decreased the ratio of EPSP2/EPSP1 in type I (trending towards significance at 10Hz, and highly significant at 20Hz and 30Hz), but not type II cells compared to controls (fig. 16A). Thus, D2 receptor activation increases synaptic depression at low train frequencies only in type I cells. These effects on type I cells were blocked by the D2 antagonist, sulpiride (fig. 16E). However, quinpirole had no effect on peak amplitude from baseline or the latency to peak amplitude at any frequency, compared with controls (data shown for 10 and 50Hz; fig. 16F).

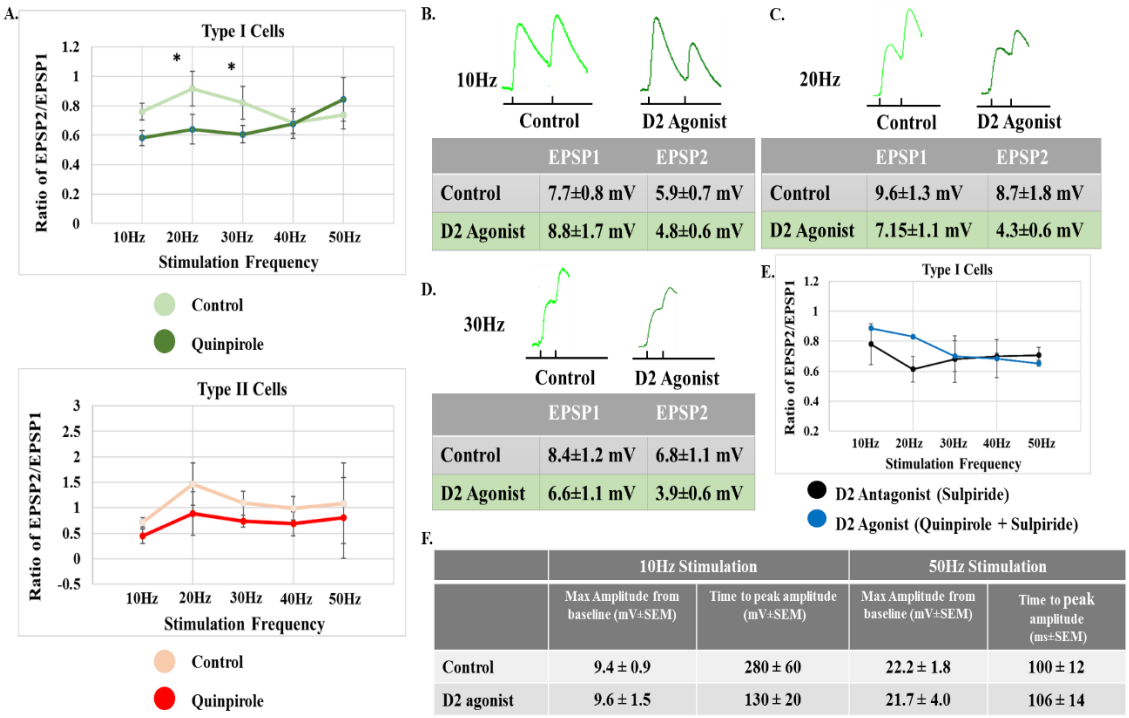

	EPSP1	EPSP2
Control	7.7±0.8 mV	5.9±0.7 mV
D2 Agonist	8.8±1.7 mV	4.8±0.6 mV

	EPSP1	EPSP2
Control	9.6±1.3 mV	8.7±1.8 mV
D2 Agonist	7.15±1.1 mV	4.3±0.6 mV

	EPSP1	EPSP2
Control	8.4±1.2 mV	6.8±1.1 mV
D2 Agonist	6.6±1.1 mV	3.9±0.6 mV

F.

	10Hz Stimulation		50Hz Stimulation	
	Max Amplitude from baseline (mV±SEM)	Time to peak amplitude (mV±SEM)	Max Amplitude from baseline (mV±SEM)	Time to peak amplitude (ms±SEM)
Control	9.4 ± 0.9	280 ± 60	22.2 ± 1.8	100 ± 12
D2 agonist	9.6 ± 1.5	130 ± 20	21.7 ± 4.0	106 ± 14

Figure 16: D2 receptor modulation of non-NMDA EPSP's evoked by layer I stimulation. (A) D2 receptor activation decreases the ratio of EPSP2/EPSP1 compared to the controls significantly at 10Hz, 20Hz and nearly significant at 30Hz (p=0.08) in type I (top) but not type II cells (bottom). **(B-D)** Representative traces highlighting EPSP1 and EPSP2 are shown for type I cells in control solution and in the presence of the D2 agonist for 10-30Hz. Black dashes represent stimulation time points. Amplitude of EPSP 1 and EPSP 2 are shown (tables) for stimulation frequencies of 10-30Hz. **(E)** The effects of quinpirole on the ratio of EPSP2/EPSP1, in type I cells, are blocked with the D2 antagonist, sulpiride. **(F)** The effects of the D2 agonist on maximum amplitude and time to peak amplitude at 10 and 50Hz. Asterisks (*) indicate $p<0.05$; RM ANOVA.

Layer V evoked non-N-methyl-D-Aspartate-receptor mediated excitatory post-synaptic potentials. Quinpirole had no significant effects on non-NMDAR EPSP trains evoked by layer V stimulation. In both type I and type II cells, quinpirole did not alter the initial EPSP amplitude (type I cells, from 7.9±1.2V to 9.6±1.2mV at 10Hz [$p>0.05$; $n=10$]; type II cells, from 8.3±1.4mV to 9.4±0.9mV at 10Hz [$p>0.05$; $n=7$]) or the ratio of EPSP2/EPSP1 at any frequency (data not shown). Further, quinpirole had no

effect on peak amplitude from baseline, or latency to peak at any frequency compared with controls (data shown for 10 and 50Hz; table 1).

Table 1: D2 receptor activation has no significant effect on frequency dependent properties of layer V evoked non-NMDA EPSP's.

	10Hz Stimulation		50Hz Stimulation	
	Max Amplitude from baseline (mV±SEM)	Time to peak amplitude (ms±SEM)	Max Amplitude from baseline (mV±SEM)	Time to peak amplitude (ms±SEM)
Control	9.8 ± 1.0	240 ± 40	20.9 ± 2.0	102 ± 6
D2 agonist	10.9 ± 0.8	160 ± 10	25.5 ± 2.0	104 ± 8

Layer I evoked N-methyl-D-Aspartate-receptor mediated excitatory post-synaptic potentials. Quinpirole significantly decreased the amplitude of the first EPSP in type I cells, but not type II cells (type I cells, from 4.3±1.7V to 1.4±0.3mV at 10Hz [$p<0.05$; n=6]; type II cells, 3.9±1.1V to 2.0±0.6mV at 10Hz [$p>0.05$; n=6]). Representative NMDAR EPSP traces recorded from type I and type II cells, evoked by layer I stimulation are shown in control solution (low magnesium, GZ and DNQX containing; fig 3.6A, type I: green; fig. 3.6B, type II: red) and in the presence of the D2 agonist (low magnesium, GZ, DNQX and Quinpirole; fig.17A; type I: dark green traces; fig. 17B, type II: dark red traces). However, quinpirole significantly increased the ratio of EPSP2/EPSP1 in type I but not type II cells, at 40Hz and 50Hz (fig. 17C). Thus, quinpirole leads to facilitation of NMDAR EPSP's in type I cells at higher frequencies. The effects of quinpirole on the initial EPSP amplitude and the ratio of EPSP2/EPSP1 in type I cells was blocked by the D2 receptor antagonist, sulpiride (data not shown and fig.

17D, respectively). D2 receptor activation had no effect on peak amplitude from baseline or latency to peak at any frequency (data shown for 10 and 50Hz; fig. 17E).

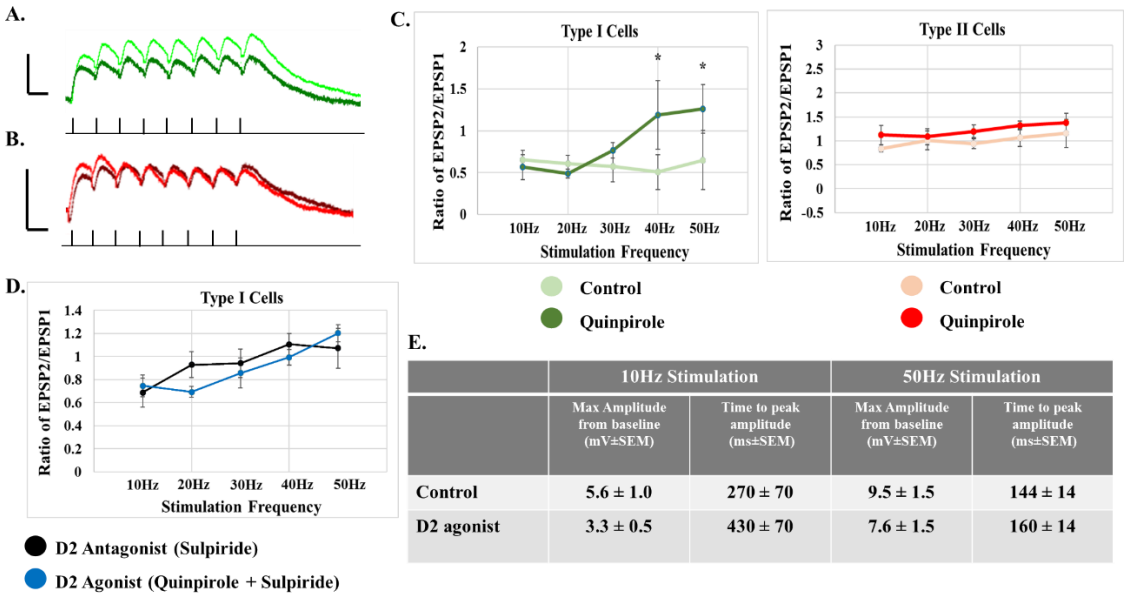

E.

	10Hz Stimulation		50Hz Stimulation	
	Max Amplitude from baseline (mV±SEM)	Time to peak amplitude (ms±SEM)	Max Amplitude from baseline (mV±SEM)	Time to peak amplitude (ms±SEM)
Control	5.6 ± 1.0	270 ± 70	9.5 ± 1.5	144 ± 14
D2 agonist	3.3 ± 0.5	430 ± 70	7.6 ± 1.5	160 ± 14

Figure 17: D2 receptor activation on NMDA EPSP's evoked by layer I stimulation. **(A)** D2 receptor activation with quinpirole significantly decreases the amplitude of NMDA EPSP's in type I pyramidal neurons. Representative traces of type I cells, evoked at 10Hz, are shown (control: green trace; quinpirole: dark green trace). **(B)** D2 receptor activation with quinpirole has no effect on the amplitude of NMDA EPSP's in type II pyramidal neurons. Representative traces of type II cells, evoked at 10Hz, are shown (control: red trace; quinpirole: dark red trace). Black dashes represent stimulation time points; scale bars: x=100ms; y=5mV. **(C)** The EPSP amplitude ratio of EPSP2/EPSP1 was significantly increased at 50Hz in type I (left) but not type II cells (right). **(D)** The effects of quinpirole on the ratio of EPSP2/EPSP1, in type I cells, are blocked with the D2 antagonist, sulpiride. **(E)** The effects of the D2 agonist on maximum amplitude and time to peak amplitude at 10 and 50Hz. Asterisks (*) indicate $p<0.05$; RM ANOVA.

Layer V evoked N-methyl-D-Aspartate-receptor mediated excitatory post-synaptic potentials. D2 receptor activation had no effect in either cell type on initial EPSP amplitude evoked by layer V stimulation (type I cells, from 3.1±0.6mV to 2.7±0.4mV at 10Hz [$p>0.05$; n=10]; type II cells, 4.1±1.4mV to 1.0±0.2mV at 10Hz [$p>0.05$; n=10]), or on the ratio of EPSP2/EPSP1 at any frequency (data not shown).

Furthermore, D2 receptor activation also had no effect on peak amplitude from baseline or the latency to peak, at any frequency (data for 10 and 50Hz shown; table 2).

Table 2: D2 receptor activation has no significant effect on frequency dependent properties of layer V evoked NMDA EPSP's.

	10Hz Stimulation		50Hz Stimulation	
	Max Amplitude from baseline (mV±SEM)	Time to peak amplitude (ms±SEM)	Max Amplitude from baseline (mV±SEM)	Time to peak amplitude (ms±SEM)
Control	4.5 ± 0.7	420 ± 60	11.2 ± 1.4	154 ± 6
D2 agonist	4.2 ± 0.7	510 ± 60	9.3 ± 1.6	156 ± 4

Discussion

Summary

In the present study, type I (corticopontine) and type II (commissural) layer V pyramidal cells were identified using fluorescent retrobeads, and the effects of D2 receptor activation on high frequency synaptic trains evoked by apical tuft (layer I) or basal dendritic (layer V) stimulation were characterized. The main results were as follows: (1) Isolated non-NMDAR and NMDAR-mediated EPSP's display some differences in frequency dependent properties, but display predominantly depressing EPSP trains. (2) D2 receptor activation modulates type I, but not type II, layer V pyramidal neurons. In type I cells, D2 receptor activation (3) increases synaptic depression of layer I evoked non-NMDAR-mediated EPSP's at lower frequencies, (4) had no effect on layer V evoked non-NMDAR-mediated EPSP's at any frequency, (5) decreases the initial EPSP amplitude and leads to facilitation at higher frequencies in

layer I evoked NMDAR-mediated EPSP's, and lastly (6) had no effect on layer V evoked NMDAR-mediated EPSP's at any frequency.

Comparisons with Previous Studies

As other labs have demonstrated, we have shown that layer V pyramidal cell subtypes are unambiguously distinguished based on their axonal projection patterns (19-21) using retrograde transport of fluorescent beads, since type I and type II cells are known to send axonal projections to the pons of the brainstem and the commissural mPFC, respectively. As observed in previous studies (19, 86), we found that these subtypes differ in their intrinsic properties, where type I cells often display an initial spiking doublet and a large 'sag' due to a hyperpolarization activated inward current, and type II cells do not. The results of this study show that dopaminergic D2 receptor activation only affects type I pyramidal cells, supporting the idea that type I, but not type II, pyramidal cells express D2 receptors, which had been previously proposed by Gee et al. (21).

To our knowledge, this is the first study to identify the effects of D2 receptor activation on frequency dependent synaptic properties in layer V pyramidal cells. However, frequency-dependent synaptic properties have been studied in various cell populations. Within the nucleus accumbens and the ventral tegmental area, Chuhma et al. (87) reported that summation (i.e. a higher peak amplitude is reached within the train) occurs much more readily when cells are stimulated at high frequencies. The same phenomenon has been shown in the ventrobasal thalamus (88, 89), as well as within CA1 pyramidal cells of the hippocampus (90). Lastly, this phenomenon has also been demonstrated in layer V pyramidal cells, evoked with dendritic current injections varying

in frequency (32). These studies, in addition to ours, demonstrate that temporal summation is enhanced at higher frequencies, and suggest that high frequency synaptic activation may facilitate persistent firing.

There is strong evidence that dopaminergic D2 receptor activation is crucial for cognitive PFC-related functions (91, 92) and has been shown to improve memory performance in primates (91); however, the physiology behind the phenomenon remains unclear and controversial. Similar to our results of D2 receptor activation on layer I evoked NMDAR-mediated EPSP's, others have reported that D2 receptor activation decreases the amplitude of layer II/III evoked EPSP's (93) and layer V evoked IPSC's (94, 95) in layer V pyramidal neurons of the mouse mPFC. D2 receptor activation has also been reported to suppress NMDAR-mediated responses in CA1 pyramidal neurons of the hippocampus, evoked by stimulation of Schaffer collaterals, (96), in the neostriatum (97) and in rat mPFC layer V pyramidal neurons, evoked by layer I and VI stimulation (98) or bath applied NMDA (99). Further, D2 receptor activation decreases excitatory response amplitude within the nucleus accumbens of adolescent rats (100, 101). In combination, these studies suggest that D2 receptor activation may attenuate synaptic plasticity by depressing the amplitude of both non-isolated EPSP's as well as NMDAR-mediated EPSP's, similar to that observed in layer I evoked NMDAR-mediated EPSP's in the current study.

While modulation of single, low frequency EPSP properties by D2 receptor activation has been previously studied, to our knowledge minimal research has been conducted to identify changes in high-frequency synaptic trains elicited by D2 receptor activation, including facilitation (EPSP2>EPSP1) and depression (EPSP2<EPSP1) at

different frequencies. One study that has explored this phenomenon in non-isolated EPSC's, report similar results to those seen in layer I evoked NMDAR-mediated EPSP's in the current study. Studying synaptic connections within the nucleus of the solitary tract, Kline et al. report that non-isolated EPSC's display paired-pulse depression in control solution. With D2 receptor activation the ratio of EPSP2/EPSP1 was enhanced from control responses (102). This study also reported that D2 receptor activation decreased the amplitude of the initial EPSC, but had minimal effect on the second evoked EPSC, similar to our results. Because D2 receptor activation decreases the initial EPSC1 amplitude, with a lesser effect on EPSC2, it has been hypothesized that D2 receptor activation may promote a decrease in presynaptic quantal release rather than a decrease in postsynaptic glutamate sensitivity (102). It is difficult to compare isolated NMDAR-mediated EPSP's evoked in the PFC with non-isolated EPSC's of the nucleus of the solitary tract; however, we it is possible that a similar mechanism may be responsible for the results observed in the current study.

While many studies quantifying NMDAR-mediated synaptic responses use low magnesium containing extracellular aCSF solutions, as in the current study, we acknowledge that these conditions could conceivably alter the short-term synaptic dynamics of NMDAR-mediated responses, or their modulation by quinpirole. To our knowledge, the effects of alterations in extracellular [Mg^{2+}] on short-term synaptic dynamics of NMDAR-mediated responses have not been studied. Thus, it remains to be determined whether the frequency-dependent effects of quinpirole would be altered under conditions of normal magnesium concentrations.

Although our study focused primarily on short-term synaptic dynamics, many others have identified the effects of D2 receptor activation on long-term synaptic plasticity. Specifically, many studies have demonstrated that D2 receptor activation facilitates long-term depression in various brain regions, including layer V pyramidal neurons of the rat mPFC, induced with tetanic stimulation to layer II/III (103), as well as CA1 pyramidal neurons of the hippocampus, evoked by Schaffer collateral stimulation (104). Although these studies identify the effects of D2 receptor activation on long-term synaptic changes, the depression of layer V evoked NMDAR-mediated and layer I evoked non-NMDAR-mediated EPSPs by D2 receptor activation observed in our study may lend some insight into the long term depression observed in these studies.

Implications for Prefrontal Cortical Function

The mPFC is highly interconnected with other cortical regions, where afferents target both apical and somatic regions. The current study suggests that dopamine, through D2 receptor activation, has compartmentalized effects on non-NMDAR and NMDAR-mediated EPSP's on layer V pyramids. First, we found that D2 receptor activation reduces the amplitude of layer I evoked NMDAR-mediated EPSP's, yet had no effect on facilitation or depression of these responses at lower frequencies. For this reason, we hypothesize that dopamine, acting via D2 receptors, may play a role in limiting excessive influences of "top-down" signals by decreasing EPSP amplitude and stabilizing low frequency evoked NMDAR-mediated responses at apical tuft synapses on type I cells. However, with high frequency stimulation, D2R activation leads to facilitation of NMDAR-mediated EPSP's, which may promote the influence of high frequency inputs targeting the apical tuft region. Thus, D2R activation may promote synaptic plasticity in

the tufts, but only when inputs are activated at higher frequencies. Although synaptic plasticity may be enhanced at higher frequencies, the non-NMDA component was depressed at lower frequencies with D2R activation, indicating that fast synaptic transmission is blunted at layer I synapses of type I cells. Combined, these results would amount to an effective increase in the signal-to-noise ratio, assuming that synapses activated at high frequency are carrying more pertinent information. In contrast, with layer V stimulation, D2R activation had no effect on non-NMDAR-mediated or NMDAR-mediated EPSP's. This implies that D2R activation stabilizes fast synaptic transmission and plasticity at basal dendritic synapses of type I cells.

Overall, our results suggest that one role of D2R activation in modulating memory functions may thus be to inhibit influences from tuft inputs activated at low frequencies while promoting influences from tuft inputs activated at higher frequencies. Our demonstration of differential regulation of synaptic dynamics within distinct compartments of PFC layer V output neurons by D2 receptor activation may provide further insight into the mechanisms by which dopamine modulates mPFC function.

Implications for Schizophrenia

The dopaminergic system is highly dysregulated in patients with schizophrenia, contributing in part to the schizophrenic phenotype. Antipsychotics, in part, are effective by blocking dopaminergic D2-like receptors, with a general therapeutic dose occupying 60-80% of all D2 receptors in treated patients (81). However, the cellular mechanisms responsible for the antipsychotic effects of D2 receptor antagonism are poorly understood. We hypothesize that during times of elevated dopamine in schizophrenic patients, abnormally enhanced D2 receptor activation leads to excessive synaptic

plasticity when tuft inputs are firing at high frequencies and thus inappropriate contextual associations are made by the patient. We further hypothesize that antipsychotic drugs may in part elicit their therapeutic effects by preventing this excessive plasticity and thus preventing the false attributions regarding contextual information. However, for a more complete understanding of how dopamine regulates PFC function in the normal and pathological brain, it will be important to integrate the effects of D2 receptor activation with the effects of D1 receptor activation.

CHAPTER IV

LAYER-SPECIFIC EFFECTS OF DOPAMINERGIC D1 RECEPTOR ACTIVATION ON EXCITATORY SYNAPTIC RESPONSES IN LAYER V MOUSE MEDIAL PREFRONTAL CORTICAL CELLS

Contribution of Authors and Co-Authors

Manuscript in Chapter IV

Author: Jonna M. Jackson

Contributions: Conceived the study topic, developed and implemented the study design. Generated and analyzed data. Wrote first draft of the manuscript.

Co-Author: Dr. Mark P. Thomas

Contributions: Helped conceive the study topic. Aided in development of study design. Provided feedback data interpretation and manuscript preparation.

Abstract

In humans, prefrontal cortical areas are known to support working memory (WM) processes, mediated by homologous regions within the medial prefrontal cortex (mPFC), in mice. While it is well established that WM tasks are critically dependent on optimal levels of dopamine (DA) in the PFC, the cellular mechanisms of DA actions regulating WM are incompletely understood. WM processes depend on stable patterns of neuronal activity, which may be frequency dependent. We aimed to determine the effects of D1 receptor (D1R) activation on short-term excitatory postsynaptic potential (EPSP) dynamics evoked at varying frequencies (10-50Hz) in layer V pyramidal neurons in mouse mPFC. We isolated NMDA receptor (NMDAR) and non-NMDA receptor (non-NMDAR) mediated components of EPSP trains evoked by stimulating fibers in layer V or layer I. We found that D1R activation had layer-specific effects on non-NMDAR and NMDAR mediated EPSP trains. We found that D1R activation increased the amplitude of both components with layer V stimulation, yet with layer I stimulation D1R activation had no effect on non-NMDAR mediated EPSP trains but decreased the amplitude of NMDAR mediated EPSP trains. Our results suggest that DA, acting through D1 receptors, increases the influence of local inputs from other layer V pyramidal cells, while restricting the influence of layer I (tuft) inputs. Our demonstration of differential regulation of synaptic dynamics on distinct compartments of PFC layer V output neurons by dopamine may provide an important step to linking cellular level phenomena with normal PFC functioning and dopaminergic effects on working memory.

Introduction

In humans, goal-directed behaviors and hierarchical functioning is mediated by prefrontal cortical (PFC) areas. Together, functions mediated by this region allow for flexible behavior in the face of constantly changing environmental demands. Furthermore, the medial regions of the PFC mediate action-outcome associations (i.e. learning associations between behaviors and emotional responses) (6). These functions are mediated by homologous regions within the medial prefrontal cortex (mPFC) in mice (7, 8). It is known that optimal levels of dopamine, released from dopaminergic afferents originating in the ventral tegmental area, within the PFC are essential for normal executive tasks (37). Acting on D1-like and D2-like receptors, dopamine is suggested to play a role in prefrontal functions such as updating working memory (61), rewarding appetitive behaviors (61) as well as updating contextual representations (62). Dysregulation of dopaminergic inputs to the PFC often results in deficits in working memory and social withdrawal, symptoms commonly observed in patients with bipolar disorder, schizoaffective disorder and schizophrenia.

Layer V pyramidal cells are known to be the major neocortical output cells of the prefrontal cortex, and are comprised of two major subtypes: subcortically-projecting (type I) and contralaterally projecting (type II) (19, 20, 84). These cells are known to differ in hodology, morphology and intrinsic properties. Furthermore, it has been proposed that type I and type II cells differ in their expression patterns of dopamine receptors, where type I cells express both D1-like and D2-like receptors, and type II cells only display D1-like receptors (21). Due to the difference in expression pattern, it is feasible that dopamine may differentially regulate these pyramidal cell subtypes.

Layer V neocortical pyramidal neurons receive compartmentalized inputs from various brain regions, which provide feed-back (top-down or contextual) information to the apical tuft region (within layer I), and feed-forward (bottom-up or ongoing environmental) information to the basal dendrites, a compartment where local processing between layer V cells is also prominent (39). When these signals coincide (i.e. synaptic inputs to the apical tufts are activated synchronously with post-synaptic action potentials), pyramidal cells act as coincidence detectors, firing in a high frequency (bursting) pattern. It has been hypothesized that this burst firing may lead to synaptic plasticity locally and in target neurons (39). When considered in the context of the mPFC, we aim to explore phenomena relevant to the hypothesis that frequency-dependent, layer-specific, short-term synaptic dynamics and their modulation by dopamine play a significant role in generating the persistent activity observed in prefrontal cortical networks during memory-related tasks.

Excitatory post synaptic potentials (EPSPs) are characterized by two components, a non-NMDA receptor (non-NMDAR) mediated (primarily AMPA receptor) and an NMDA receptor (NMDAR) mediated component that confers fast synaptic transmission and synaptic plasticity, respectively. Studies characterizing dopaminergic D1 receptor modulation of excitatory transmission have primarily focused on synaptic responses evoked at low frequencies and have yielded inconsistent results (76, 105, 106). Thus, we aimed to determine the effects of D1 receptor activation on isolated non-NMDAR- and NMDAR-mediated responses over a range of frequencies that mimic high frequency bursting, in both layer V pyramidal cell subtypes. We also examined the effects of D1 receptor activation on layer I and layer V evoked EPSP trains, reflecting feed-back and

feed-forward/local activity, respectively. The intent of this study was to describe the overall effects of the D1 receptor agonist, SKF38393, on non-NMDA and NMDA receptor mediated synaptic dynamics in the two major dendritic compartments of mPFC layer V pyramids, without addressing subcellular mechanisms of D2 receptor modulation. Some of these results have been presented previously in abstract form (107).

Materials and Methods

Tissue Preparation

Tissue slices were prepared from 25-42 day old male and female mice (C57 BL/6 strain, UNC breeding colony). Animals were anesthetized with carbon dioxide and rapidly decapitated following procedures outlined in a UNC Institutional Animal Care and Use Committee approved protocol in accordance with NIH guidelines. Brains were rapidly removed and immersed in ice-cold carbogen (95% O_2 / 5% CO_2) saturated sucrose-enriched artificial cerebrospinal fluid (cutting aCSF) containing (in mmol/L): sucrose, 206; $NaHCO_3$, 25; dextrose, 10; KCl, 3.3; NaH_2PO_4, 1.23; $CaCl_2$, 1.0; $MgCl_2$, 4.0, osmolarity adjusted to 295±5 mOsm and pH adjusted to 7.40±0.03. The brains were then transferred to the cutting chamber of a vibrating tissue slicer (OTS500, Electron Microscopy Sciences, Hatfield, PA) and coronal slices of the prefrontal cortex (PFC) were prepared in ice-cold cutting aCSF. Slices were cut 300µm thick and were taken from approximately 200µm to 1400µm caudal to the frontal pole. Slices were then placed in a holding chamber filled with recording aCSF solution containing (in mmol/L): NaCl, 120; $NaHCO_3$, 25; KCl, 3.3; NaH_2PO_4, 1.23; $CaCl_2$, 0.9; $MgCl_2$, 2.0; dextrose, 10, osmolarity adjusted to 295±5 mOsm and pH adjusted to 7.40±0.03. The holding chamber aCSF was continuously bubbled with carbogen and incubated at 34°C for 45 minutes and

then allowed to cool to room temperature before slice recording. Prior to experiments, slices were transferred to a recording chamber where they were perfused continuously at a flow rate of 1-2 mls/min with filtered, carbogen-saturated recording aCSF solution.

Throughout recordings, the recording chamber was held at 32±1°C with a temperature controller equipped with a chamber heater and an in-line heater (TC-344B, Warner Instruments, Hamden CT). In experiments isolating non-NMDAR-mediated EPSPs, the recording aCSF contained 50µM aminophosphonovalerate (D-APV;an NMDA receptor antagonist). In experiments isolating NMDAR mediated EPSPs, the recording aCSF contained 20µM 6,7dinitroquinoxaline-2,3-dione (DNQX; a non-NMDA receptor antagonist) and $MgCl_2$ concentration was reduced to 0.25 mM to facilitate NMDAR activation at -65mV.

Electrophysiology

Layer V pyramidal neurons of the infralimbic, prelimbic and anterior cingulate cortices were visually identified using infrared DIC microscopy at 400x magnification with an Olympus BX51WI microscope (Tokyo, Japan). Whole cell recordings were made from the soma of layer V pyramidal neurons after establishing a Giga-ohm seal (resistance range: 1-10 Gohm). Only cells that exhibited a thin (i.e. action potential half-width was less than 2ms), overshooting action potential, as well as continuous spiking throughout a depolarizing current injection were used in this study. Access resistance (R_A) was compensated throughout experiments, and cells were excluded from analysis if uncompensated R_A exceeded 20MΩ. Liquid junction potentials (estimated at approximately -6mV for K^+ gluconate internal solution) were not compensated in adjusting Vm for synaptic recordings. Amplifier bridge balance was utilized and

monitored throughout current injections. Recording pipettes (4-6MΩ tip resistance), produced from thin-wall glass capillary tubes (1.5µm OD, 1.12µm ID, World Precision Instruments, Sarasota, FL), were filled with (in mM) potassium gluconate, 135; KCl, 10; EGTA, 1.0; HEPES, 10; MgATP, 2; TrisGTP, 0.38, osmolarity adjusted to 285±5 mOsm and pH adjusted to 7.30±0.01. Glass micropipettes, used as stimulating electrodes, were filled with 3M NaCl were placed within either layer V or layer I of mPFC to activate fibers located within that layer (fig. 18).

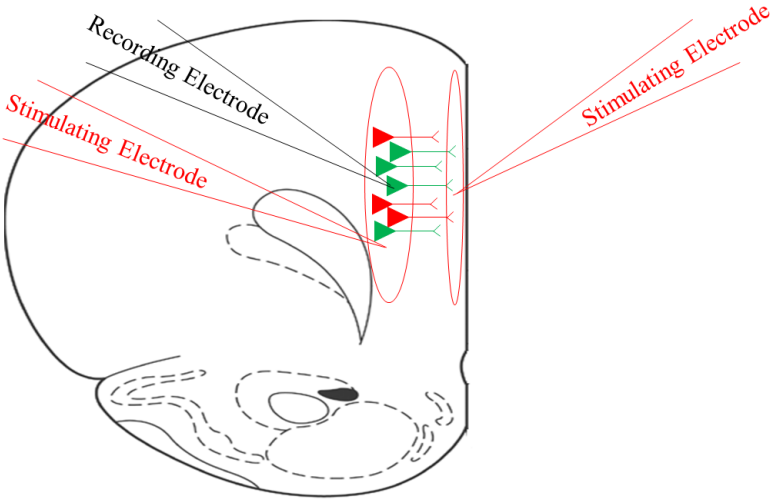

Figure 18: Recording and stimulating electrode placement. Recordings were made from the soma of both type I and type II layer V pyramidal neurons. The stimulating electrode was placed within layer V or layer I, within 100µm from the soma of the recorded cell, within the medial prefrontal cortex as indicated by the red circles.

Type I and II layer V pyramidal cells were identified based on the presence of a prominent "sag" in response to a 150 pA hyperpolarizing current (type I: minimal 12% depolarization from peak of hyperpolarization, indicating the strong presence of the hyperpolarization activated cation current), and by initial firing of doublets (type I cells only); both criteria have been used in previous studies (19, 86). For all analyses, type I

and type II subtypes were categorized and compared between experimental groups. The responses were digitized at 10kHz and saved on disk using a Digidata 1322A interface (Axon instruments) and pCLAMP version 8.1 software (Clampex program, Axon Instruments). Data were analyzed off-line in Clampfit (Axon Instruments).

Statistical Analyses

All values are presented as mean ± SEM (standard error of the mean). All cells received every stimulus frequency (10Hz-50Hz) and the D1R agonist. We performed an ANOVA on all experimental data except for comparisons between cellular properties of type I and type II cells (i.e. resting membrane potential, membrane capacitance, 'sag' amplitude etc.), where a Student's t-test was utilized. A two-way repeated measures ANOVA was used to analyze the effects of drug and frequency of stimulation. The statistical model also included mouse and slice as random variables.

Experimental Protocols

We began each experiment by establishing a "stimulus current / evoked response" curve where stimulus intensity was increased while measuring the evoked EPSP amplitude. The stimulus current was adjusted to establish an unsaturated response near the midrange of this curve. The position of the stimulating pipette was located at a distance from the recorded cell to establish a baseline response of approximately 7-13 mV and 2-7 mV (for non-NMDAR and NMDAR-mediated EPSP's, respectively). These amplitudes were chosen to avoid cell spiking during the pulse trains, where summation was often observed at higher stimulus train frequencies. EPSP's were evoked in current clamp mode using an 8-pulse stimulus train, at varying frequencies (10-50Hz). This protocol was repeated 5 times with a 10 second inter-train interval, and the 5 responses

were averaged. For non-NMDAR-mediated EPSP experiments, cells were manually held at -80mV throughout the experiment. Pulse trains were applied in control (APV-containing) aCSF, and again immediately following a 5 minute application of the D1 agonist, SKF-38393 (10µM). NMDAR-mediated EPSPs were evoked using the same current clamp protocol as for non-NMDAR-mediated EPSP experiments. During NMDAR EPSP experiments, cells were manually held at -65mV throughout the experiment. Pulse trains were applied in control (DNQX-containing) aCSF, and again immediately following a 5 minute application of the D1 agonist SKF38393 (10µM). For antagonist experiments, SCH23390 (10µM) was included in the bath during control recordings.

For analysis, the EPSP amplitude was measure in millivolts (mV), from the membrane potential directly before the stimulus was applied. For the first EPSP within the train, the EPSP size was measured from resting baseline, where simultaneous EPSPs were measured from the baseline directly before the EPSP was evoked. Additionally, maximal peak amplitude was measured from baseline (before the train was delivered), to the peak amplitude reached throughout the train of 8-EPSPs. The time it took to reach the maximal amplitude within the train was also recorded. See figure 12 for representation (chapter 3).

Drugs

The NMDA antagonist, D-APV, the dopamine D1/D5 receptor agonist, SKF38393, and the dopamine D1/D5 antagonist, SCH23390, were purchased from Tocris Biosciences (Bristol, UK). The non-NMDA antagonist, DNQX, was purchased from Alomone Labs (Jerusalem, Israel). D-APV, SKF38393, SCH23390, and DNQX were

diluted into aliquots of 50mmol/L, 10mmol/L, 10mmol/L and 20mmol/L stocks, respectively. All drugs were stored at -80ºC and diluted to working concentrations of 50µmol/L D-APV, 10µmol/L SKF38393, 10µmol/L SCH23390 and 20 µmol/L DNQX; any drugs not used within 3 days of thawing were discarded.

Results

Electrophysiological Properties Differ Between Type I and Type II Layer V Pyramidal Cells

As demonstrated in previous studies (19, 21, 86), we have also identified two subtypes of layer V pyramidal cells that differ in electrophysiological properties. These subtypes have been shown by others to differ based on their axonal projection patterns, where type I cells and type II cells send their axonal projections to the pontine of the brainstem and the commissural mPFC, respectively (19, 21). We have demonstrated that the two cell types differ in spiking characteristics, where type I cells generally display an initial spiking doublet and type II cells do not (fig. 19A). Additionally, type I cells display a significantly greater ‘sag’ amplitude during a hyperpolarizing stimulus of 150pA, compared to type II cells (type I: 15.6±1.0%; type II: 5.2±1.0%; $p<0.05$; fig. 19B). Although the two cell types differed in some characteristics, they did not differ in membrane capacitance (pF), membrane resistance (mΩ) or resting membrane potential (mV) (fig. 19C,D &E, respectively).

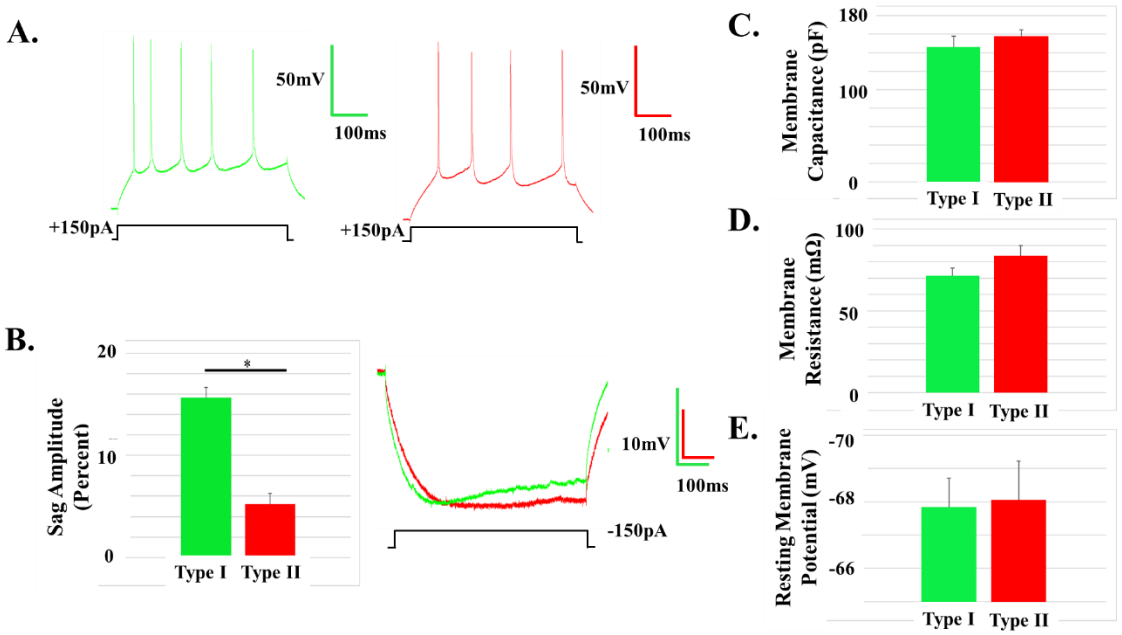

Figure 19: Characteristics of type I and type II pyramidal cells. (A) Type I cell spiking pattern showing a distinct initial spiking doublet and an adapting response to a 150pA current injection (green; top); Type II cell spiking pattern, lacking an initial spiking doublet with 150pA current injection (red; bottom). **(B)** Type I and type II cells display significantly different 'sag' amplitude in response to a 150pA hyperpolarizing current (type I: green; type II: red; $p<0.05$). Representative "sag" traces of type I (green trace) and type II (red trace) cells are shown. Type I cells display a lower, yet non-significant, average membrane capacitance (type I:146.4±11.4pF; type II: 157.3±7.5pF) **(C)** and average membrane resistance (mΩ) (type I: 71.5±4.7mΩ; type II:83.6±6.4mΩ) **(D). (F)** Type I cells and type II cells show no difference in membrane potential (type I: -67.8±0.9mV; type II: -68.1±1.2mV). Asterisks indicate a p-value less than 0.05.

Non-N-methyl-D-Aspartate-Receptor Mediated Excitatory Post-Synaptic Potentials

Non-NMDA receptor mediated EPSP trains were measured from layer V pyramidal neurons by blocking NMDA receptor activation with 50 µM APV. Representative traces recorded following layer V stimulation are shown for all frequencies (10-50Hz) in figure 20A. At 10Hz, non-NMDA EPSPs show two distinct amplitude profiles, which we define simply as facilitating (the second EPSP is larger than

the first EPSP; EPSP2>EPSP1) (fig. 20C, top; black trace) or depressing (the second and subsequent EPSPs are smaller than the first EPSP; EPSP2<EPSP1) (fig. 20C, bottom; teal trace). In 12 out of 20 layer V cells (6 type I, 6 type II), layer V-evoked non-NMDA EPSPs showed a depressing pattern in control solution. In the remaining 8 of 20 cells (3 type I, 5 type II), layer V-evoked non-NMDA EPSPs were facilitating. In 14 out of 16 cells (8 type I, 6 type II), layer I-evoked non-NMDA EPSPs were depressing, while only 2 of 16 cells (both type I cells) were facilitating. Notably, we did not see a significant difference between type I and type II cells (as identified by criteria listed in methods) regarding their short term synaptic dynamics (layer V evoked non-NMDA EPSPs [EPSP2/EPSP1; $p>0.05$; $n=20$]; layer I evoked non-NMDA EPSPs [EPSP2/EPSP1; $p>0.05$; $n=16$]).

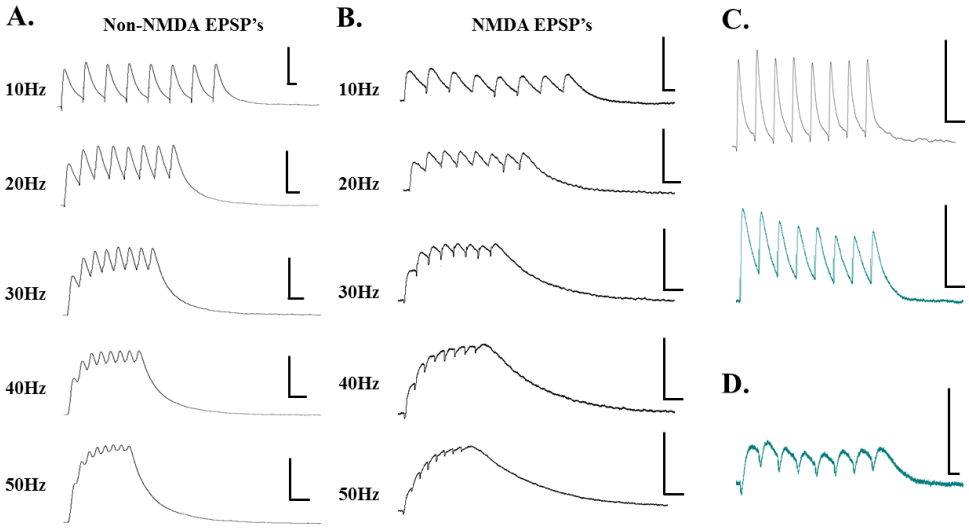

Figure 20: EPSP trains evoked by layer V stimulation. (A) Representative traces showing non-NMDAR-mediated EPSP trains evoked by layer V stimulation. Traces are shown for each stimulation frequency (10-50Hz from top to bottom). **(B)** Representative traces showing NMDAR-mediated EPSP trains evoked by layer V stimulation. Traces are shown for each stimulation frequency (10-50Hz from top to bottom). **(C)** non-NMDAR-mediated EPSP trains show two types of short-term dynamics, facilitating (EPSP2> EPSP1; black trace, top) and depressing (EPSP2<EPSP1; teal trace, bottom). **(D)**

NMDAR-mediated EPSP trains only displayed depressing (EPSP2<EPSP1; teal trace, bottom) short-term dynamics.

N-Methyl-D-Aspartate-Receptor Mediated Excitatory Post-Synaptic Potentials

NMDA receptor-mediated EPSP trains were measured from layer V pyramidal neurons by blocking non-NMDA receptors with 20μM DNQX. Representative traces for all frequencies (10-50Hz) recorded following layer V stimulation are shown in figure 20B. NMDA EPSPs showed only a depressing dynamic profile (EPSP2<EPSP1; figure 20D; teal trace). All NMDA EPSP responses measured in control solution showed depressing profiles, regardless of which layer was stimulated (layer V [n=11; 5 type I, 6 type II]; layer I [n=17; 8 type I, 9 type II]). Notably, we did not see a significant difference between type I and type II cells with regards to their short term synaptic dynamics (layer V evoked NMDA EPSPs [EPSP2/EPSP1; $p>0.05$; n=11]; layer I evoked NMDA EPSPs [EPSP2/EPSP1; $p>0.05$; n=17]).

Frequency Dependent Properties of Excitatory Post-Synaptic Potential Trains

We examined the frequency dependent short-term synaptic dynamics of both non-NMDAR and NMDAR-mediated EPSP's by stimulating at various frequencies between 10Hz and 50Hz. Non-NMDAR-mediated EPSP's evoked by layer V and layer I stimulation, display an EPSP2/EPSP1 ratio that is significantly less at 50Hz compared to 10Hz (fig. 21A&B, top). Further, non-NMDAR mediated EPSPs evoked with both layer V and layer I stimulation, the maximal amplitude reached throughout the train is higher, and the latency to peak was shorter, at 50Hz compared to 10Hz (fig. 21A&B, tables).

Thus, at higher frequencies, temporal summation of non-NMDAR EPSP's is more robust and occurs more readily.

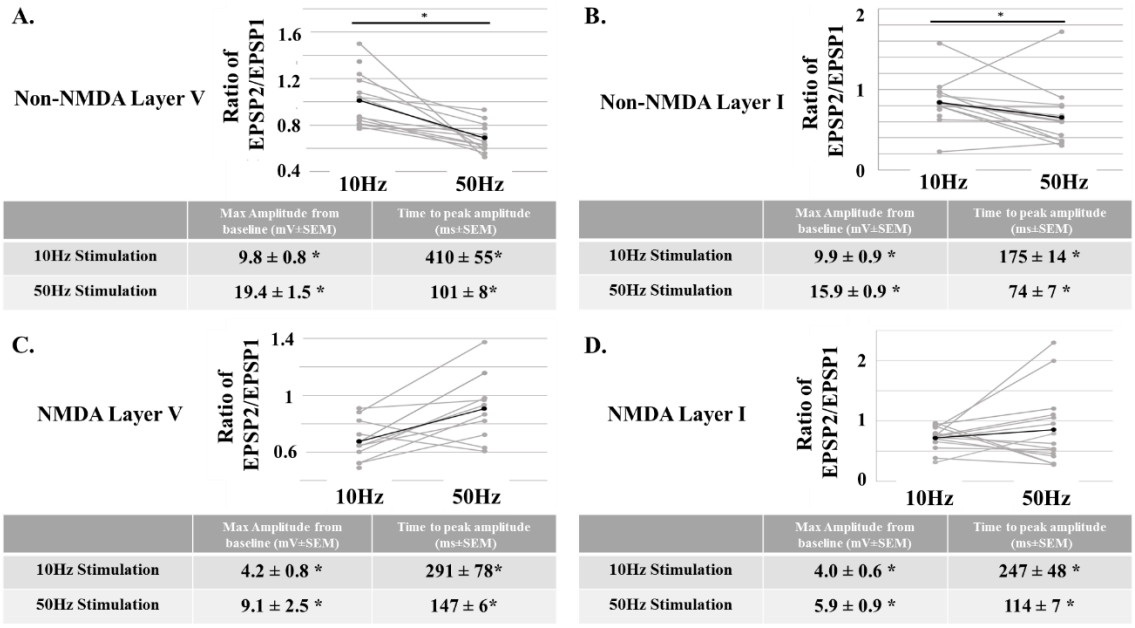

	Max Amplitude from baseline (mV±SEM)	Time to peak amplitude (ms±SEM)
10Hz Stimulation	9.8 ± 0.8 *	410 ± 55*
50Hz Stimulation	19.4 ± 1.5 *	101 ± 8*

	Max Amplitude from baseline (mV±SEM)	Time to peak amplitude (ms±SEM)
10Hz Stimulation	9.9 ± 0.9 *	175 ± 14 *
50Hz Stimulation	15.9 ± 0.9 *	74 ± 7 *

	Max Amplitude from baseline (mV±SEM)	Time to peak amplitude (ms±SEM)
10Hz Stimulation	4.2 ± 0.8 *	291 ± 78*
50Hz Stimulation	9.1 ± 2.5 *	147 ± 6*

	Max Amplitude from baseline (mV±SEM)	Time to peak amplitude (ms±SEM)
10Hz Stimulation	4.0 ± 0.6 *	247 ± 48 *
50Hz Stimulation	5.9 ± 0.9 *	114 ± 7 *

Figure 21: Frequency dependent properties of non-NMDA and NMDA EPSP's evoked by either layer V or layer I stimulation. With layer V **(A)**, but not layer I **(B)** stimulation, the ratio of EPSP2/EPSP1 is significantly less at 50Hz compared to 10Hz for non-NMDA EPSP's. Additional characteristics are tabled (bottom). With layer V **(A)**, but not layer I **(B)** stimulation, the ratio of EPSP2/EPSP1 is significantly greater at 50Hz compared to 10Hz for NMDA EPSP's. Additional characteristics are tabled (bottom). For each graph, gray lines represent each individual cell and black lines represent the average of all cells. Asterisks in tables and graphs depict a significant difference ($p<0.05$) between 10Hz and 50Hz.

Opposite of non-NMDAR-mediated EPSPS's, NMDAR-mediated EPSP's evoked by layer V and layer I stimulation, showed no difference in EPSP2/EPSP1 ratio between 10Hz and 50Hz. However, NMDAR-mediated EPSPs evoked by both layer V and layer I stimulation, the maximal amplitude reached throughout the train is higher, and the latency to peak is shorter, at 50Hz compared to 10Hz (fig. 21C&D, tables). Like non-NMDAR mediated EPSPs, these results also indicate that, regardless of layer stimulation, temporal summation of NMDAR-mediated EPSP's is more robust at higher frequencies.

Dopaminergic D1 Receptor Effects on Excitatory Post Synaptic Potential Trains

Layer V evoked non- N-methyl-D-Aspartate-receptor mediated excitatory post-synaptic potentials. The D1 agonist, SKF38393, increased the initial non-NMDA EPSP amplitude in both cell types similarly; therefore, data is presented as an average of the two cell types. Initial EPSP amplitude was increased from 7.0±0.8mV to 15.3±1.9mV at 10Hz ($p<0.05$; n=14). Representative non-NMDA EPSP trains recorded from layer V stimulation are shown in control solution and in the presence of the D1 agonist (fig. 22A, black and gray traces, respectively) for all frequencies. This increase in non-NMDA initial EPSP amplitude by D1R activation was blocked by co-application of the D1R antagonist, SCH23390 (at 10Hz: D1 antagonist: 12.7±1.1mV; D1 agonist: 12.8±1.7mV; $p>0.05$; n=7). Additionally, a five-minute activation of dopamine receptors may lead to changes that outlast the direct effects of downstream signaling events. Thus, we wanted to explore whether the effects of D1 receptor activation were reversible. Non-NMDA EPSP trains were measured at 10Hz in response to layer V stimulation in control solution, following a 5 minutes application of SKF38393 and a 5 minutes of agonist washout. The enhancement of EPSP amplitude observed in the presence of SKF38393 was completely reversed within 5 minutes of drug washout (at 10Hz: control: 11.8±2.6mV; D1 agonist: 15.3±3.7mV; wash: 10.8±0.8mV; n=6).

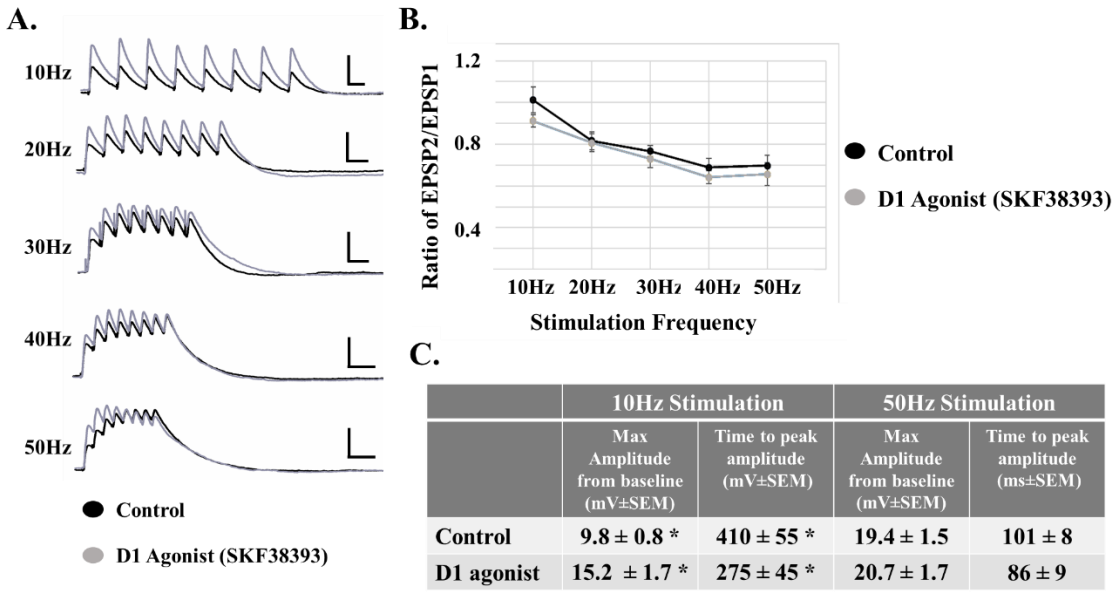

C.

	10Hz Stimulation		50Hz Stimulation	
	Max Amplitude from baseline (mV±SEM)	Time to peak amplitude (mV±SEM)	Max Amplitude from baseline (mV±SEM)	Time to peak amplitude (ms±SEM)
Control	9.8 ± 0.8 *	410 ± 55 *	19.4 ± 1.5	101 ± 8
D1 agonist	15.2 ± 1.7 *	275 ± 45 *	20.7 ± 1.7	86 ± 9

Figure 22: D1 receptor effects on non-NMDA EPSP's evoked by layer V stimulation. (A) D1 receptor activation with SKF38393 significantly increases the amplitude of non-NMDA EPSP's in all (both type I and type II) pyramidal neurons. Traces are shown for each stimulation frequency (10-50Hz from top to bottom; control: black traces; SKF38393: gray traces; scale bars: x=100ms; y=10mV). **(B)** The EPSP amplitude ratio of EPSP2/EPSP1 was unaffected by the D1 agonist at any frequency. **(C)** The effects of the D1 agonist on maximal amplitude and time to peak amplitude at 10Hz and 50Hz are tabled. Asterisks (*) indicate a significant difference between control and D1 receptor activation ($p<0.05$).

The effects of D1 receptor activation on non-NMDAR-mediated short-term synaptic dynamics were frequency dependent. SKF38393 application had no effect on the EPSP2/EPSP1 ratio at any frequency (fig. 22B). However, D1 receptor activation significantly increased the maximum amplitude reached during the train and shortened the latency to peak amplitude at 10Hz, but not at higher frequencies (data for 10Hz and 50Hz are tabled in fig. 22C; Asterisks indicate $p<0.05$; RM ANOVA). These effects of D1 receptor activation on maximum amplitude reached were blocked by co-application of the D1 antagonist (at 10Hz, maximum amplitude: D1 antagonist: 13.0±1.0; D1 agonist: 13.2±1.6). Additionally, these effects were reversed within 5 minutes of drug washout (at

10Hz: control: 12.5±1.4; D1 agonist 15.3±1.8; wash: 9.6±1.2). Further, the effects of D1 receptor activation on latency to peak amplitude were also blocked by co-application of the D1 antagonist (at 10Hz, maximum amplitude: D1 antagonist: 142.9±29.7; D1 agonist: 228.6±99.3) and were reversed within 5 minutes of drug washout (at 10Hz: control: 116.7±16.7; D1 agonist 100±0.0; wash: 100±0.0).

Layer V evoked N-methyl-D-Aspartate-receptor mediated excitatory post-synaptic potentials. The D1 agonist, SKF38393, increased the initial NMDA EPSP amplitude in both cell types similarly; therefore, data is presented as an average of the two cell types. Initial NMDA EPSP amplitude was increased from 4.0±0.9V to 5.0±1.0mV at 10Hz ($p<0.05$; n=20). Representative traces of NMDAR mediated EPSP trains recorded following layer V stimulation are shown in control solution and in the presence of the D1 agonist (fig. 23A, black and gray traces, respectively). This increase in NMDA initial EPSP amplitude was blocked by co-application of the D1R antagonist, SCH23390 (at 10Hz D1 antagonist: 4.5±0.8mV; D1 agonist: 4.3±0.8mV; $p>0.05$; n=7). Additionally, the enhancement of initial NMDA EPSP amplitude, observed in the presence of SKF38393, was completely reversed within 5 minutes of drug washout (at 10Hz, control: 4.5±1.2mV; D1 agonist: 6.6±1.7mV; wash: 4.2±1.5mV; n=7).

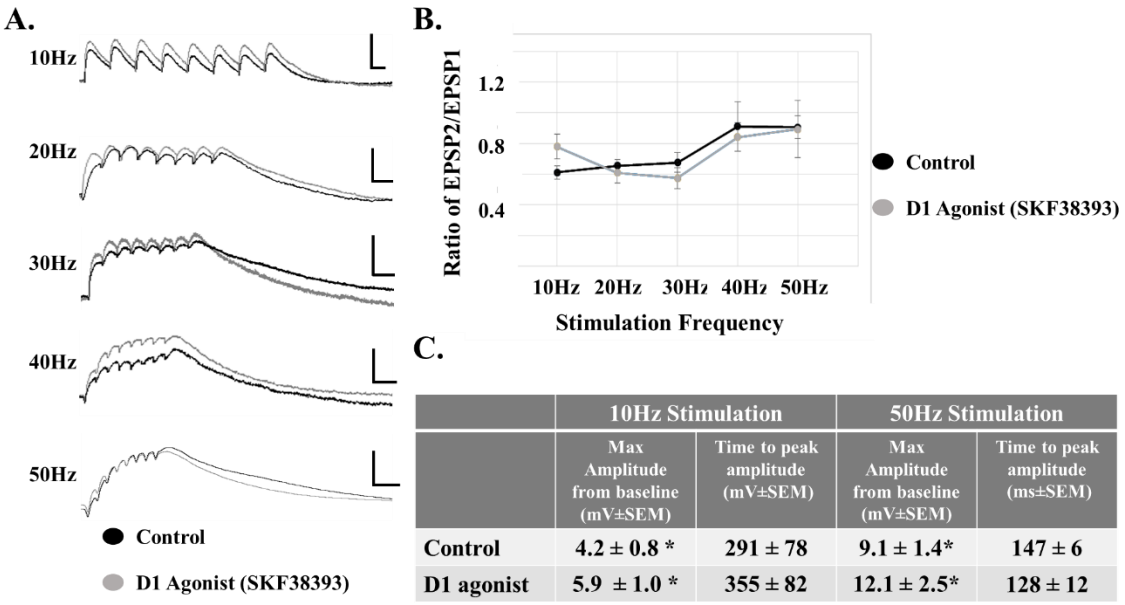

C.

	10Hz Stimulation		50Hz Stimulation	
	Max Amplitude from baseline (mV±SEM)	Time to peak amplitude (mV±SEM)	Max Amplitude from baseline (mV±SEM)	Time to peak amplitude (ms±SEM)
Control	4.2 ± 0.8 *	291 ± 78	9.1 ± 1.4*	147 ± 6
D1 agonist	5.9 ± 1.0 *	355 ± 82	12.1 ± 2.5*	128 ± 12

Figure 23: D1 receptor effects on NMDA EPSP's evoked by layer V stimulation. (A) D1 receptor activation with SKF38393 significantly increases the amplitude of NMDA EPSP's in all (both type I and type II) pyramidal cells. Traces are shown for each stimulation frequency (10-50Hz from top to bottom; control: black traces; SKF38393: gray traces; scale bars: x=100ms; y=5mV). **(B)** The EPSP amplitude ratio of EPSP2/EPSP1 was unaffected by the D1 agonist at any frequency. **(C)** The effects of the D1 agonist on maximum amplitude and time to peak amplitude at 10Hz and 50Hz are tabled. Asterisks (*) indicate a significant difference between control and D1 receptor activation ($p<0.05$).

In contrast with non-NMDA receptor mediated responses, the effects of D1 receptor activation on NMDAR-mediated short-term synaptic dynamics were not frequency dependent. SKF38393 application had no significant effect on the EPSP2/EPSP1 ratio at any frequency (fig. 23B). However, D1 receptor activation increased the maximum amplitude reached during the train at all frequencies, yet had no effect on time to peak (data for 10Hz and 50Hz tabled in fig. 23C; Asterisks indicate $p<0.05$; RM ANOVA; n=20). These effects of D1 receptor activation were blocked by co-application of the D1 antagonist (at 10Hz, maximum amplitude: D1 antagonist:

4.5±0.8; D1 agonist: 4.3±0.8; n=7). Additionally, these effects were reversed within 5 minutes of drug washout (at 10Hz: control: 4.6±1.2; D1 agonist 6.8±1.7; wash: 4.6±1.4; n=7).

Layer I evoked non-N-methyl-D-Aspartate-receptor mediated excitatory post-synaptic potentials. D1 receptor activation had no significant effects on non-NMDAR EPSP trains evoked by layer I stimulation in either cell type. Thus, data is presented as an overall average of the two cell types. The D1 agonist did not alter the initial EPSP amplitude (from 4.0±0.9V to 5.0±1.0mV at 10Hz [p>0.05; n=16] or the ratio of EPSP2/EPSP at any frequency (fig. 24A&B). Further, SKF38393 had no effect on maximum amplitude reached during the train or latency to peak amplitude at any frequency compared with controls (data shown for 10 and 50Hz; fig. 24C).

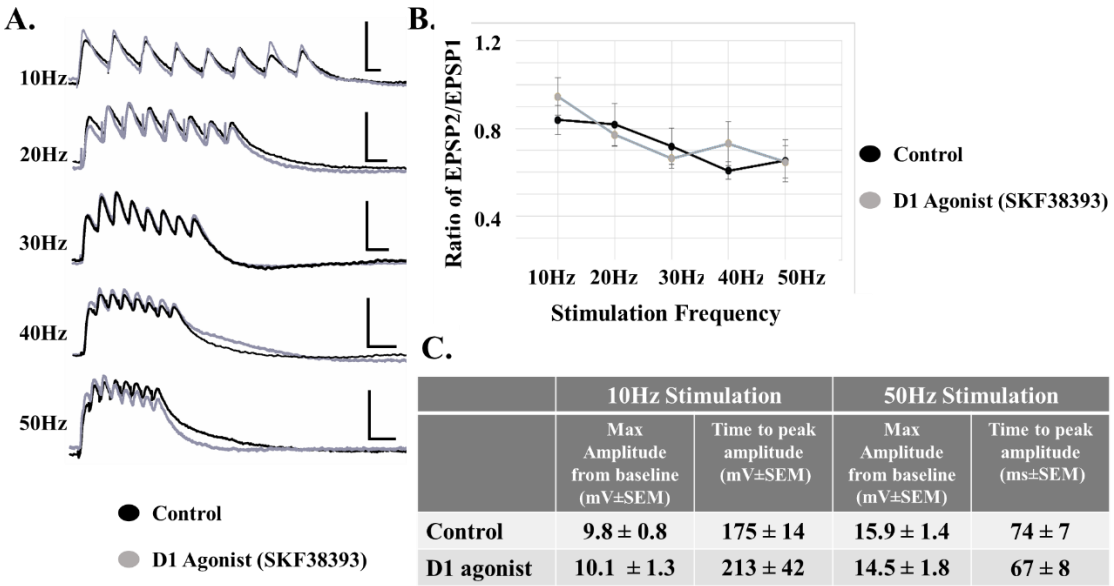

C.

	10Hz Stimulation		50Hz Stimulation	
	Max Amplitude from baseline (mV±SEM)	Time to peak amplitude (mV±SEM)	Max Amplitude from baseline (mV±SEM)	Time to peak amplitude (ms±SEM)
Control	9.8 ± 0.8	175 ± 14	15.9 ± 1.4	74 ± 7
D1 agonist	10.1 ± 1.3	213 ± 42	14.5 ± 1.8	67 ± 8

Figure 24: D1 receptor effects on non-NMDA EPSP's evoked by layer I stimulation. **(A)** D1 receptor activation with SKF38393 had no effect on the amplitude of non-NMDA EPSP's in either pyramidal cell type. Traces are shown for each stimulation frequency (10-50Hz from top to bottom; control: black traces; SKF38393: gray traces; scale bars: x=100ms; y=10mV). **(B)** The EPSP amplitude ratio of EPSP2/EPSP1 was unaffected by the D1 agonist at any frequency. **(C)** The effects of the D1 agonist on maximum amplitude and time to peak amplitude at 10Hz and 50Hz are tabled.

Layer I evoked N-methyl-D-Aspartate-receptor mediated excitatory post-synaptic potentials. The D1 agonist, SKF38393, decreased the initial EPSP amplitude in both cell types similarly; therefore data is presented as an average of the two cell types. Initial EPSP amplitude was decreased from 5.1±1.0mV to 1.5±0.3mV at 10Hz ($p<0.05$; n=8). Representative NMDA EPSP traces recorded from layer I stimulation are shown in control solution and in the presence of the D1 agonist for all frequencies (fig. 25A, black and gray traces, respectively). This decrease in initial EPSP amplitude was blocked by co-application of the D1R antagonist, SCH23390 (at 10Hz: D1 antagonist = 4.1±0.6mV; D1 agonist = 3.5±0.5mV; $p>0.05$; n=7). Additionally, the decrease in initial EPSP amplitude observed in the presence of SKF38393 was completely reversed within 5 minutes of drug washout (at 10Hz, control=3.5±0.2mV; D1 agonist=2.5±0.5mV; wash=3.7±1.0mV; $p>0.05$; RM ANOVA; n=4).

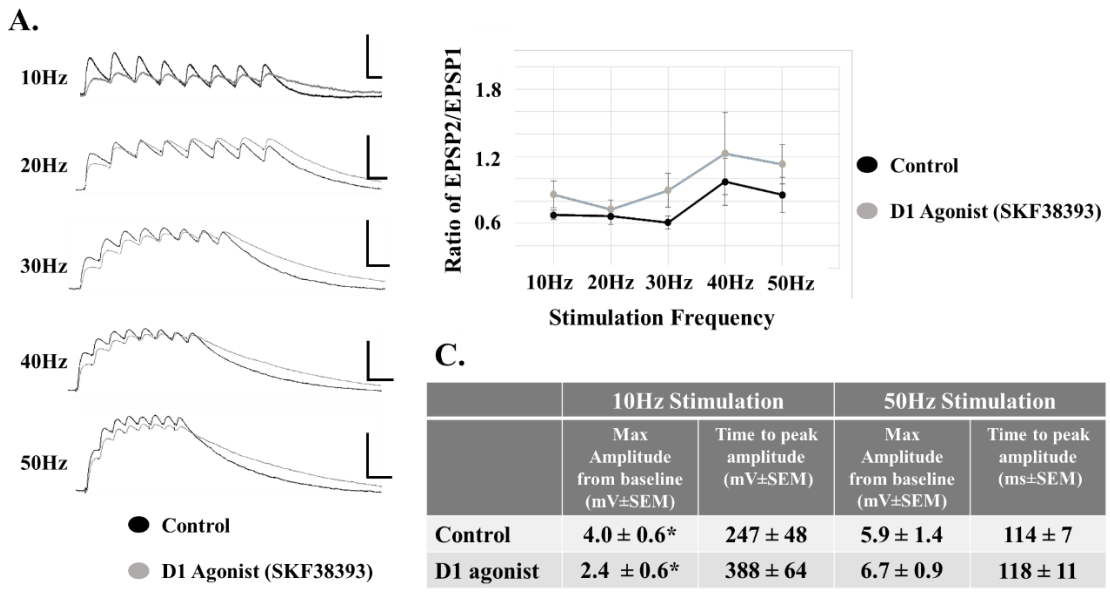

C.

	10Hz Stimulation		50Hz Stimulation	
	Max Amplitude from baseline (mV±SEM)	Time to peak amplitude (mV±SEM)	Max Amplitude from baseline (mV±SEM)	Time to peak amplitude (ms±SEM)
Control	4.0 ± 0.6*	247 ± 48	5.9 ± 1.4	114 ± 7
D1 agonist	2.4 ± 0.6*	388 ± 64	6.7 ± 0.9	118 ± 11

Figure 25: D1 receptor effects on NMDA EPSP's evoked by layer I stimulation. (A) D1 receptor activation with SKF38393 significantly decreased the amplitude of NMDA EPSP's in all (both type I and type II) pyramidal cells. Traces are shown for each stimulation frequency (10-50Hz from top to bottom; control: black traces; SKF38393: gray traces; scale bars: x=100ms; y=5mV). **(B)** The EPSP amplitude ratio of EPSP2/EPSP1, in either cell type, was unaffected by the D1 agonist at any frequency. **(C)** The effects of the D1 agonist on maximum amplitude and time to peak amplitude at 10Hz and 50Hz are tabled.

The effects of D1 receptor activation on NMDAR-mediated short-term synaptic dynamics were frequency dependent. SKF38393 application had no effect on the EPSP2/EPSP1 ratio at any frequency (fig. 25B). However, D1 receptor activation decreased the maximum train amplitude at 10Hz, but not at higher frequencies. Further, the D1 receptor agonist had no effect on latency to peak amplitude at any frequency (data for 10Hz and 50Hz are tabled in fig. 25C; Asterisks indicate $p<0.05$; RM ANOVA). These effects of D1 receptor activation were blocked by co-application of the D1 antagonist (at 10Hz, maximum amplitude: D1 antagonist: 4.1±0.6; D1 agonist: 3.5±0.5

n=7). Additionally, these effects were reversed within 5 minutes of drug washout (at 10Hz: control: 3.5±0.2; D1 agonist 2.5±0.5; wash: 5.6±0.9; n=4).

Discussion

Summary

In the present study, type I and type II layer V pyramidal neurons were distinguished based on their electrophysiological properties and the effects of D1 receptor activation on high frequency synaptic trains evoked by apical tuft (layer I) or basal dendritic (layer V) stimulation were characterized. The main results were as follows: (1) Non-NMDAR and NMDAR-mediated EPSP's differ in frequency dependent properties; non-NMDAR-mediated EPSPs are more depressing at high frequencies compared to low, whereas NMDAR-mediated EPSPs show similar depression at all frequencies. (2) With layer V stimulation, D1 receptor activation increased both the non-NMDAR and NMDAR-mediated initial EPSP amplitude in both type I and type II cells. The peak amplitude of the train was also enhanced for both non-NMDA and NMDAR-mediated EPSPs and the time to reach peak amplitude was decreased in non-NMDAR-mediated EPSP's with D1 receptor activation at low, but not high frequencies. (3) D1 receptor activation had no significant effect on layer I-evoked non-NMDAR mediated EPSP amplitude, peak train amplitude or time to peak at any frequency. (4) D1 receptor activation decreased the initial amplitude of layer I evoked NMDAR mediated EPSPs, but had no effect on peak train amplitude or time to peak.

Comparisons with Previous Studies

Several studies have used dual recordings to characterize short-term EPSP dynamics at connections between layer V pyramidal cell subtypes; both facilitating and

depressing patterns have been observed (20, 28, 108). For example, Lee et al. (20) found that interconnected type I pyramidal cells exhibit facilitating EPSPs, and interconnected type II cells show depressing EPSPs. In contrast, Morishima et al. (108) and Wang et al. (28) demonstrated that both type I and type II pyramidal cells can show facilitating and depressing EPSP patterns. In the present study, our stimulation protocol resulted in activation of a heterogeneous population of fibers, including other Layer V cells (both type I and II), axons from other cortical layers, and axons from other brain regions. Thus, our results are consistent with these studies utilizing dual recordings, in that one would expect a mixture of both facilitating and depressing EPSP dynamics at layer V synapses. While the dual recording studies focused on synapses targeting primarily basal dendrites in layer V, the emphasis in our study was to characterize the dynamics at layer V synapses as compared with the dynamics at layer I synapses. To our knowledge, the short-term dynamics of EPSPs evoked by layer I stimulation have not been characterized in the literature. However, Hempel et al. (109) reported a short-term decrease in amplitude of EPSC trains (i.e. depressing responses) recorded in layer V cells evoked by layer II/III stimulation.

The modulation of evoked EPSP short-term dynamics by dopamine receptor activation has been studied to some extent (76, 79, 98, 105, 106, 110-112). However, these studies of dopamine effects on the amplitude of low-frequency evoked EPSCs and EPSPs have often yielded diverse, and sometimes contradicting results. Consistent with our results, two studies have reported that dopamine produces short-term potentiation of EPSP amplitude in layer V pyramidal cells (105, 112). Additionally, D1 receptor activation has also been shown to increase EPSC amplitude (79, 110) and EPSP

amplitude (111) at layer V pyramidal synapses evoked by layer V stimulation. Seamans et al. (79) also reported that D1 receptor activation enhances both isolated NMDAR and non-NMDAR mediated EPSC components in layer V pyramidal cells of rat mPFC evoked by layer V stimulation, similar to our current findings.

Although many studies have shown similar results to our study, others have reported contradicting findings. For example, studies have shown that D1 receptor activation depressed EPSP amplitude in layer V pyramidal neurons evoked by layer V (106) and layer VI (98) stimulation. Furthermore, Law-Tho and colleagues (1994) have reported a similar effect on isolated EPSP components in rat mPFC layer V pyramidal cells evoked by layer VI stimulation. Lastly, others have reported D1 receptor activation to have no effect on layer III evoked EPSC amplitude in layer V pyramidal neurons (76). To our knowledge, the present study is the first to characterize the effects of D1 receptor activation on the frequency-dependent properties of isolated NMDA and non-NMDA EPSP components, evoked by layer I versus layer V evoked stimulation.

Implications for Prefrontal Cortical Function

The mPFC is highly interconnected with other neocortical and subcortical regions. This complex interconnectivity may play a role in long-range reverberant activity, initiating and maintaining the persistent activity required for many prefrontal executive functions. Additionally, it is suggested that both intrinsic and extrinsic factors are likely important for generating persistent neuronal activity within the prefrontal cortex and may be heavily reliant on dopaminergic modulation (80, 113, 114), and proper levels of dopamine are essential for PFC memory-related tasks. However, the mechanistic details underlying this phenomenon are incompletely understood. The current study

suggests that dopamine, through D1 receptor activation, has compartmentalized effects on non-NMDAR and NMDAR-mediated EPSP's on layer V pyramidal neurons. Our results suggest that D1 receptor activation increases the influence of local inputs from other layer V pyramids, while restricting the influence of layer I (tuft) inputs. It has also been suggested by others that D1 receptor facilitation of the NMDA EPSP component (as observed in our study) may favor recurrent connections between pyramidal neurons in close proximity (111). Additionally, our results suggest that D1 receptor activated increases the ability of a cell to summate in response to layer V stimulation (primarily recurrent connections between pyramidal cells) at low frequencies (i.e. 10Hz). This summation may enhance the ability of layer V cells to integrate information that contributes to persistent firing. Our results are also consistent with the hypothesis proposed by Yang and Seamans (115) that D1 receptor activation in layer V pyramidal cells suppresses synaptic input to the apical tufts in layer I while augmenting synaptic inputs to basal dendrites by altering intrinsic ion currents. We further hypothesize that dopamine, acting via D1 receptors, may play a role in strengthening selected local connections within layer V, enhancing output from a specific ensemble via NMDAR-dependent plasticity, while inhibiting plasticity at layer I synapses. One role of D1 receptor activation in modulating memory functions may thus be to facilitate choice selection by layer V output neurons, while inhibiting or stabilizing 'top-down' influences impinging on layer I.

Overall, our results suggest that one role of D1R activation in modulating memory functions may be to promote environmental/ongoing information impinging on the basal dendritic region, while inhibiting feedback information targeting the tufts. Our

demonstration of differential regulation of short term synaptic dynamics within different compartments of PFC layer V neurons by D1 receptor modulation may shed light onto the mechanisms by which dopamine may modulate mPFC function, and thus working memory tasks.

Conclusion

Our results are consistent with the hypothesis that dopamine, through activation of D1 receptors on layer V cells in mPFC, may play a role in inhibiting top-down (contextual) information while promoting local (bottom-up) influences and plasticity during memory-related tasks. Thus, information impinging onto the basal dendrites is integrated differently than information targeting the apical tufts of pyramidal cells. Additionally, in combination with our previous study (in press, Leyrer-Jackson 2017) characterizing the effects of D2 receptor activation on short-term, frequency-dependent synaptic dynamics, we hypothesize that dopamine, has differential effects on layer V pyramidal neurons dependent on D1 and D2 receptor activation. In contrast to D1 receptor activation, D2 receptor activation had no effect on local layer V activity, but may play a role in regulating the signal-to-noise ratio in the apical tufts by inhibiting low-frequency inputs and facilitating high frequency inputs. Taken together, these results suggest that with optimal dopamine levels, local influences (i.e. environmental / "bottom-up") and plasticity will be promoted within layer V of the mPFC, while "top-down" or contextual information impinging on layer I is stabilized.

Based on the results obtained within these studies, several hypotheses can be made regarding the psychiatric disorder, schizophrenia. Interestingly, patients with schizophrenia go through periods of dysregulated dopamine levels. During times of

insufficient activation (i.e. depressive states; hypodopaminergic activity), local connections between layer V cells may lose their ability to maintain recurrent connectivity. Additionally, without sufficient activation of D1 receptors, information impinging onto the apical tufts may not be properly suppressed, leading to excessive "top-down" / contextual signals; thus, insufficient suppression could lead to inappropriate contextual associations. Further, insufficient activation of D1 receptors may also result in blunted integration of basal dendritic inputs and recurrent connectivity.

In contrast, during times of hyperactive dopaminergic activity (i.e. during psychotic episodes / manic states), our results would suggest that layer V connectivity may be overly promoted and contextual information overly suppressed. This combination may lead to the promotion of inappropriate environmental information, giving rise to hallucinations and perseveration often observed in the disorder.

It has been proposed that cognitive symptoms may be due in part to insufficient dopamine release in the prefrontal cortex (64, 116, 117). Based on our results and those of others, it is conceivable that insufficient activation of dopaminergic receptors in schizophrenic patients could lead to an inability to maintain recurrent activity between layer V output cells, and/or an excessive influence of top-down signals. The former would contribute to poor performance on working memory tasks, while the latter could contribute to false attributions regarding contextual information and the disorganized thought patterns commonly observed in the disorder.

Overall, the results presented here lend insight into normal dopaminergic function within the prefrontal cortex. These results further the understanding of how dopamine may contribute to normal executive functioning and working memory capabilities. These

studies also provide an important step to linking cellular level phenomena with normal PFC function and dopaminergic effects on working memory. Finally, these findings lend insight into how dysregulation of the dopamine system may give rise to symptoms often observed in patients with psychiatric disorders, like schizophrenia.

CHAPTER V

OPTOGENETIC ACTIVATION OF COMMISSURAL MEDIAL PREFRONTAL CORTICAL EXCITATORY SYNAPTIC INPUTS TARGETING BOTH SUBTYPES OF LAYER V PYRAMIDAL NEURONS

Contribution of Authors and Co-Authors

Manuscript in Chapter V

Author: Jonna M. Jackson

Contributions: Conceived the study topic. Developed and implemented the study design. Generated and analyzed data. Wrote first draft of the manuscript.

Co-Author: Dr. Mark P. Thomas

Contributions: Helped conceive the study design. Provided feedback and data interpretation and edited manuscript.

Abstract

In humans, prefrontal cortical (PFC) areas are known to support goal-directed behaviors, mediating a variety of functions that render behavior more flexible in the face of changing environmental demands. In mice, these functions are mediated by homologous regions in the medial prefrontal cortex (mPFC). Layer V pyramidal cells of the mPFC can be subcategorized into two subpopulations, which are defined as type I and type II based on their projection patterns, and known to be the major cortical output cells. While it is well established that the mPFC receives inputs from several different brain areas (the amygdala, the thalamus, the hippocampus and the contralateral mPFC via commissural fibers) it remains relatively unknown how information coming from these inputs is integrated by layer V pyramidal cell subtypes. This study characterizes the excitatory synaptic responses of commissural mPFC inputs onto type I and type II layer V pyramidal cells. To study isolated inputs, an optogenetic approach, using genetically encoded light-sensitive proteins (Channelrhodopsin-2) to manipulate neuronal activity, was utilized. Fluorescent green retrobeads were injected into the pontine of the brainstem and the contralateral mPFC, which accurately labeled type I and type II pyramidal neurons, respectively. Additionally, the depolarizing opsin, Channelrhodopsin-2, was injected into the contralateral mPFC, to label commissural fibers originating from that region. Using electrophysiological techniques, whole-cell current clamp recordings were performed on type I and type II pyramidal cells labeled with green retrobeads. During recording from pyramidal cells, a blue LED was used to optogenetically activate inputs from the contralateral mPFC synapsing onto layer V cells. Additionally, the effects of dopaminergic D1 receptor activation on synaptic responses were also characterized.

These experiments may enhance the understanding of how the mPFC integrates convergent synaptic inputs from the commissural mPFC that in-turn may contribute to working memory functions.

Introduction

In humans, prefrontal cortical (PFC) areas are known to support goal-directed behaviors, rendering behavior more flexible during changing environmental demands. It has been hypothesized that the function of medial regions of the PFC is to learn associations between context, events, and corresponding emotional responses, ie. action-outcome associations (6). These functions are mediated by homologous regions in the medial prefrontal cortex (mPFC), in mice (7, 8).

Normal prefrontal cortical function is critically dependent on dopaminergic input from the ventral tegmental area of the midbrain (37). Dopamine, acting on D1-like and D2-like receptors in the PFC, has been implicated in a wide variety of prefrontal functions, including updating working memory representations (61) and contextual representations (62), as well as rewarding appetitive behaviors (63). Expression of dopamine receptor subtypes shows cellular localization within the mPFC, with D1 receptors being substantially greater than D2 receptors on pyramidal neurons (68, 69). Studies within the mPFC have revealed that dopamine, acting through D1-type receptors, regulates cognition in a dose dependent manner. That is, insufficient activation of D1 receptors leads to distractibility, while excessive activation leads to perseveration; an optimal level of D1 receptor activation is thus necessary for proper working memory function (72-74). Despite many studies addressing the effects of dopaminergic D1-type receptor activation on synaptic responses in the PFC, it remains unclear how dopamine's

actions at D1-type receptors leads to these dose-dependent effects on PFC functions. To fully understand how dopamine, acting via D1 receptor activation, modulates these functions requires characterization of the effects of D1 receptor activation on glutamatergic synaptic responses targeting cortical pyramidal neurons.

The mPFC integrates synaptic inputs from several brain regions (47), including the mediodorsal thalamus (48-50), the basolateral amygdala (48, 51), the hippocampus (47, 48), and the contralateral mPFC (19, 20, 48). However, how layer V pyramidal cells integrate these various inputs remains poorly understood. Within the mPFC, layer I has been shown to be targeted by afferents from contralateral mPFC, the ventral hippocampus, and the basolateral amygdala, which show preference for the innermost part of layer I (50), spanning throughout layer I (48), and deep layer I (53), respectively. Of these inputs, it is well known that afferents from the commissural mPFC largely innervate layers I through VI of the contralateral hemisphere. Interestingly, it has been shown that commissural fibers show strongest density rates for layer V of the contralateral mPFC (32). Although it is known that the mPFC is innervated by many brain regions, it is unknown how type I (pontine projecting) and type II (commissural projecting) layer V pyramidal cells differentially process information from each of these afferents. Thus, characterization of the specific afferents targeting the mPFC and synapsing onto layer V pyramidal cells is warranted. In the current study, we focus on commissural-specific inputs impinging onto both subtypes of layer V pyramidal neurons.

It has been proposed (39) that, in layer V neocortical pyramidal neurons, feed-back (top-down or contextual) information is received via apical tuft synapses (in layer I), while feed-forward (bottom-up or environmental) information is delivered to synapses on

the apical trunk (via layer IV or III cells). Additionally, local processing occurs between layer V neurons via synapses on the basal dendrites located predominantly in layer V. Thus, it is likely that this information, arriving from different afferents, is coordinated by rhythms impinging on layer V pyramidal neurons (40-42). In this study, we aimed to dissect out this circuitry, isolating the effects of commissural mPFC inputs onto both subtypes of layer V pyramidal cells. In this study, we aimed to characterize excitatory postsynaptic potential (EPSP) dynamics in type I and type II cells, evoked by commissural fiber activation at variable high frequency stimulation (simulating rhythmic activity in the alpha through low gamma ranges). Here, we explored the hypothesis that type I and type II cells differentially integrate information from the commissural mPFC in a frequency-dependent manor. Additionally, we entertained the idea that this integration may be altered by dopaminergic modulation, through D1 receptor activation, which may play a role in persistent activity observed in prefrontal cortical networks during memory-related tasks.

Materials and Methods

Dual Injection Stereotaxic Surgeries

Stereotaxic surgeries were conducted following an UNC Institutional Animal Care and Use Committee approved procedure and in accordance with NIH guidelines. Young (4-6 week old) mice, of both sex, were anesthetized with a combination of isoflurane and oxygen. Once under full anesthesia, the mouse was transferred to a stereotaxic frame (Stoelting 51500U, Ultra-Precise, Wood Dale, IL, USA), and a nose cone was placed for continuous administration of anesthesia during the surgery. Regardless of injection paradigm, two burr holes were made in the skull to inject

retrobeads and an adeno-associated virus (AAV) encased channelrhodopsin-2 (ChR-2) tagged with mCherry (AAV9.CAG.hChR2[H134R]-mCherry.WPRE.SV40; Penn Vector Core, Philadelphia, PA). For one set of experiments, type I cell and commissural fibers were labeled, where the AAV-ChR2-mCherry containing vector and 1X green retrobeads (Lumafluor, Naples, FL) were injected at the coordinates, ML: +0.35mm, DV: -2.3 to -1.3mm and +1.8mm and ML: -1.1, DV: -5.2mm and RC: -3.5mm from bregma, respectively. For experiments labeling type II cells and commissural fibers with green retrobeads and AAV-ChR2-mCherry were injected at the coordinates of ML: +0.35mm, DV: -2.3 to -1.3mm and +1.8mm. A schematic representations of injections labeling type I or type II cells with retrobeads and commissural fibers with ChR2 are shown in figure 26A and figure 27A, respectively. Coordinates for both experiments were determined based on previous literature (20, 21) as well as the Paxinos Brain Atlas. Lumafluor 1X green retrobeads and the channelrhodopsin-2 containing vector (AAV9.CAG.hChR2[H134R]-mCherry.WPRE.SV40) were injected with a 1µL neuros syringe (Hamilton Company, Reno, NV, USA) at the coordinates above at volumes of 600-900nL, each. Following injection, the incision site was sutured with 4-6 stitches (Roboz RS-7985-12 needles; Roboz SUT-15-2 sutures). Mice were then subcutaneously injected with Rimadyl (Carprofen; Pfizer Pharmaceuticals, Brooklyn, NY, USA). Mice were housed for 3-10 weeks post-injection before tissue slices were made.

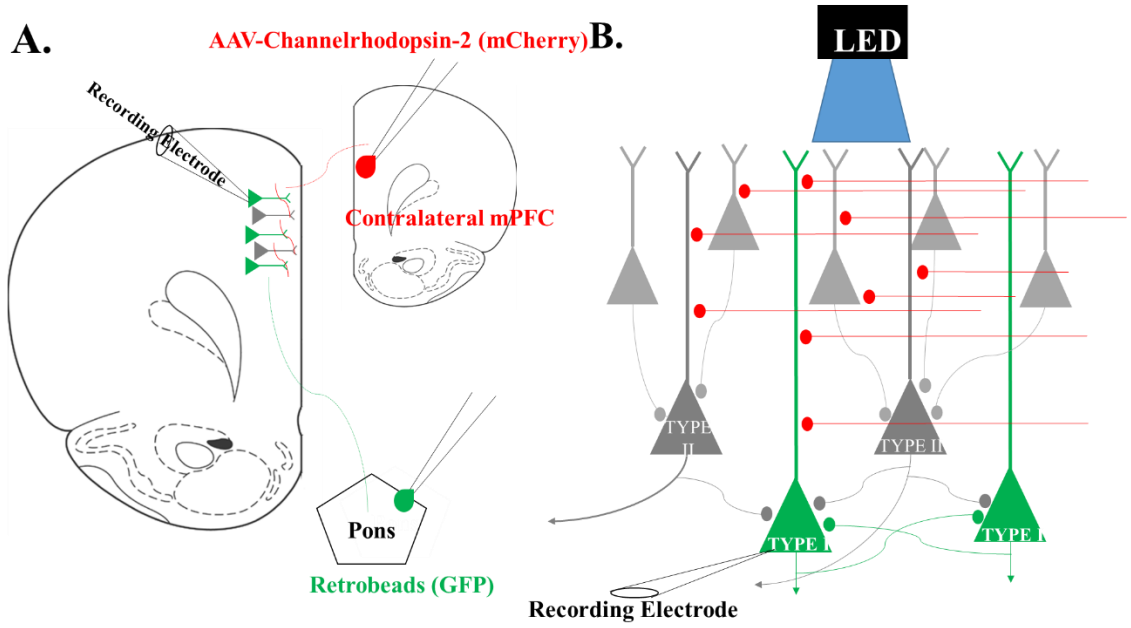

Figure 26: Schematic representation of stereotaxic injections and experimental protocol for type I cells. (A) Type I layer V pyramidal cells were labeled with green retrobeads injected into the pontine of the brainstem, while an AAV-encased channelrhodopsin-2 vector, tagged with mCherry was injected into the contralateral mPFC to label commissural fibers. **(B)** Recordings were made from the soma of type I layer V pyramidal cells (green cells), and fibers labeled with channelrhodopsin-2 (tagged with mCherry [red]), impinging onto type I cells, were activated using a blue LED to elicit EPSPs within type I cells.

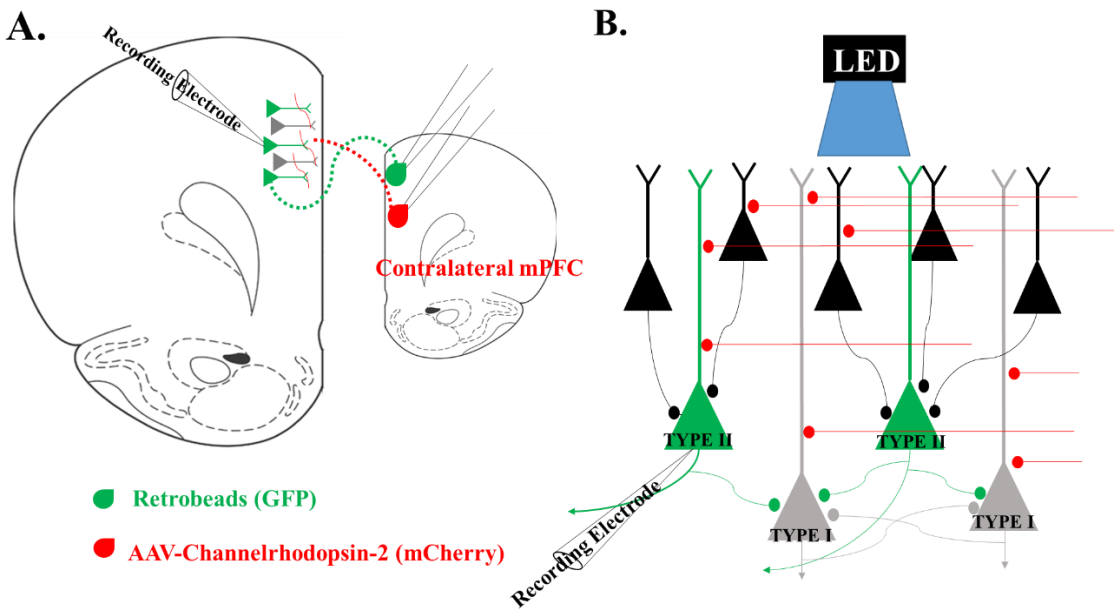

Figure 27: Schematic representation of stereotaxic injections and experimental protocol for type II cells. (A) Green retrobeads and an AAV-encased channelrhodopsin-2 vector, tagged with mCherry were injected into the contralateral mPFC to label type II cells and commissural fibers, respectively. **(B)** Recordings were made from the soma of type II layer V pyramidal cells (green cells), and fibers labeled with channelrhodopsin-2 (tagged with mCherry [red]), impinging onto type II cells, were activated using a blue LED to elicit EPSPs within type II cells.

Tissue Preparation

Tissue slices were prepared from 7-16 week old dual-injected mice (C57 BL/6 strain, UNC breeding colony). Animals were anesthetized with carbon dioxide and rapidly decapitated following procedures outlined in a UNC Institutional Animal Care and Use Committee approved protocol in accordance with NIH guidelines. Brains were rapidly removed and immersed in ice-cold carbogen (95% O_2 / 5% CO_2) saturated sucrose-enriched artificial cerebrospinal fluid (cutting aCSF) containing (in mmol/L): sucrose, 206; $NaHCO_3$, 25; dextrose, 10; KCl, 3.3; NaH_2PO_4, 1.23; $CaCl_2$, 1.0; $MgCl_2$, 4.0, osmolarity adjusted to 295±5 mOsm and pH adjusted to 7.40±0.03. The brains were then transferred to the cutting chamber of a vibrating tissue slicer (OTS500, Electron

Microscopy Sciences, Hatfield, PA) and coronal slices of the prefrontal cortex (PFC) were prepared in ice-cold cutting aCSF. Slices were cut 300µm thick and were taken from approximately 200µm to 1400µm caudal to the frontal pole. Slices were then placed in a holding chamber filled with recording aCSF solution containing (in mmol/L): NaCl, 120; $NaHCO_3$, 25; KCl, 3.3; NaH_2PO_4, 1.23; $CaCl_2$, 0.9; $MgCl_2$, 2.0; dextrose, 10, osmolarity adjusted to 295±5 mOsm and pH adjusted to 7.40±0.03. The holding chamber aCSF was continuously bubbled with carbogen and incubated at 34°C for 45 minutes and then allowed to cool to room temperature before slice recording. Prior to experiments, slices were transferred to a recording chamber where they were perfused continuously at a flow rate of 1-2 mls/min with filtered, carbogen-saturated recording aCSF solution. Throughout recordings, the recording chamber was held at 32±1°C with a temperature controller equipped with a chamber heater and an in-line heater (TC-344B, Warner Instruments, Hamden CT).

Electrophysiology

Retrobead labelled, type I and type II, layer V pyramidal neurons of the infralimbic, prelimbic and anterior cingulate cortices were visually identified using infrared DIC microscopy at 400x magnification with an Olympus BX51WI microscope (Tokyo, Japan). Fluorescence was visualized using light emitted from an X-Cite LED (Excelitas, Waltham, MA, USA). Whole cell current clamp recordings were made from the soma of fluorescently labeled layer V pyramidal neurons after establishing a Giga-ohm seal (resistance range: 1-10 Gohm). Only cells that exhibited a thin (i.e. action potential half-width of less than 2ms), overshooting action potential, as well as continuous spiking throughout a depolarizing current injection were used in this study.

Access resistance (R_A) was compensated throughout experiments, and cells were excluded from analysis if uncompensated R_A exceeded 20MΩ. Liquid junction potentials (estimated at approximately -6mV for K^+ gluconate internal solution) were not compensated in adjusting Vm for synaptic recordings. Amplifier bridge balance was utilized and monitored throughout current injections. Recording pipettes (4-6MΩ tip resistance), produced from thin-wall glass capillary tubes (1.5µm OD, 1.12µm ID, World Precision Instruments, Sarasota, FL), were filled with an intracellular solution containing (in mM): potassium gluconate, 135; KCl, 10; EGTA, 1.0; HEPES, 10; MgATP, 2; TrisGTP, 0.38, osmolarity adjusted to 285±5 mOsm and pH adjusted to 7.30±0.01.

In addition to retrograde labeling, type I and type II layer V pyramidal cells were also identified based on their electrophysiological properties. Type I cells were identified based on the presence of a prominent "sag" in response to a 150 pA hyperpolarizing current (minimal 12% depolarization from peak of hyperpolarization, indicating the strong presence of the hyperpolarization activated cation current), and by initial firing of doublets (which was only observed in type I cells); both of these criteria have been used in previous studies (19-21, 86). Type II cells were identified based on their lack of a prominent "sag", and constant spiking patterns. For all analyses, type I and type II cells were categorized and compared between experimental groups. The responses were digitized at 10kHz and saved on disk using a Digidata 1322A interface (Axon instruments) and pCLAMP version 8.1 software (Clampex program, Axon Instruments). Data were analyzed off-line in Clampfit (Axon Instruments). Values are presented as mean ± SEM (standard error of the mean), and student's t-tests were used for comparison between groups.

Experimental Protocols

While recording from type I or type II layer V pyramidal cells (labeled with fluorescent retrobeads), a blue LED was used to activate commissural fibers expressing channelrhodopsin-2 (ChR2). A schematic representation is shown in figure 26B and figure 27B for type I and type II cell experiments, respectively. The presence of green retrobead labeled type I and type II cells could be observed surrounded by ChR2 labeled commissural fibers containing an mCherry tag. A "light intensity / evoked response" curve was established, where the light intensity was adjusted to evoke an EPSP amplitude midrange between threshold and maximum (i.e. saturated EPSP amplitude; ranging between 4-12mV). These evoked amplitudes were chosen to avoid cell spiking during the pulse trains, where summation was often observed at higher train frequencies. EPSPs were evoked at 1Hz (to measure EPSP rise time and decay time) and with 8-pulse stimulus trains at 5Hz, 10Hz, 20Hz, 30Hz, 40Hz and 50Hz, with a 10 second intertrain interval. This protocol was repeated 5 times and the 5 responses were averaged. For all experiments, cells were manually held at -75mV throughout the duration of experiment. Responses evoked in control aCSF, immediately following a 5-minute application of the D1 agonist, SKF38393 (10μM), and immediately following a 5-minute applicationof the D1 antagoinst, SCH23390 (10μM).

Drugs

The dopamine D1/D5 receptor agonist, SKF38393, the dopamine D1/D5 antagonist, SCH23390, and the $GABA_a$ receptor antagonist, gabazine, were purchased from Tocris Biosciences (Bristol, UK). The sodium channel blocker, tetrodotoxin (TTX), was purchased from Ascent Scientific (now Abcam; Cambridge, MA). SKF38393,

SCH23390, gabazine and tetrodotoxin were all diluted into stock aliquots of 10mmol/L. Drugs were stored at -80ºC and were diluted to working concentrations of 10µmol/L. Any drugs not used within 3 days of thawing were discarded.

Results

General Characteristics of Evoked Excitatory Post Synaptic Potentials

Type I and type II cells (figure 28 and figure 29, respectively) were identified with green retrobeads, and channelrhodopsin-2 expressing fibers were verified by mCherry expression. The size of the EPSP's elicited could be manipulated based on the light intensity. Thus, when light intensity was maximal, EPSP size was maximal (figure 30). Also, fibers containing channelrhodopsin-2 had kinetics fast enough to be activated at frequencies ranging from 1Hz to 80Hz (stimulation frequencies between 5Hz and 80Hz are shown in figure 31).

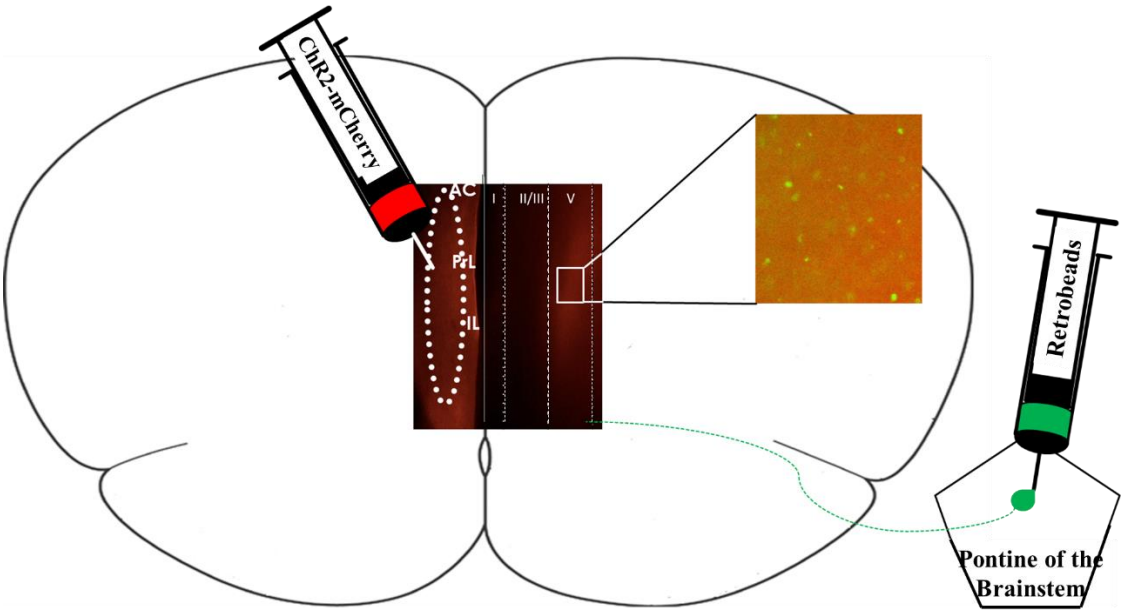

Figure 28: Type I cells and channelrhodopsin-2 expressing commissural fibers. AAV-encased channelrhodopsin-2 tagged with mCherry was injected into layer V of the

medial prefrontal cortex. As fibers began expression channelrhodopsin-2, fibers could be visualized with presence of mCherry. After 3-4 weeks, mcherry expressing fibers could be visualized on the contralateral side of the PFC, primarily located within layer V. Upon zoomed magnification, retrobead labelled type I cells could be visualized within the contralateral mPFC, surrounded by fibers containing channelrhodopsin-2 tagged with mCherry.

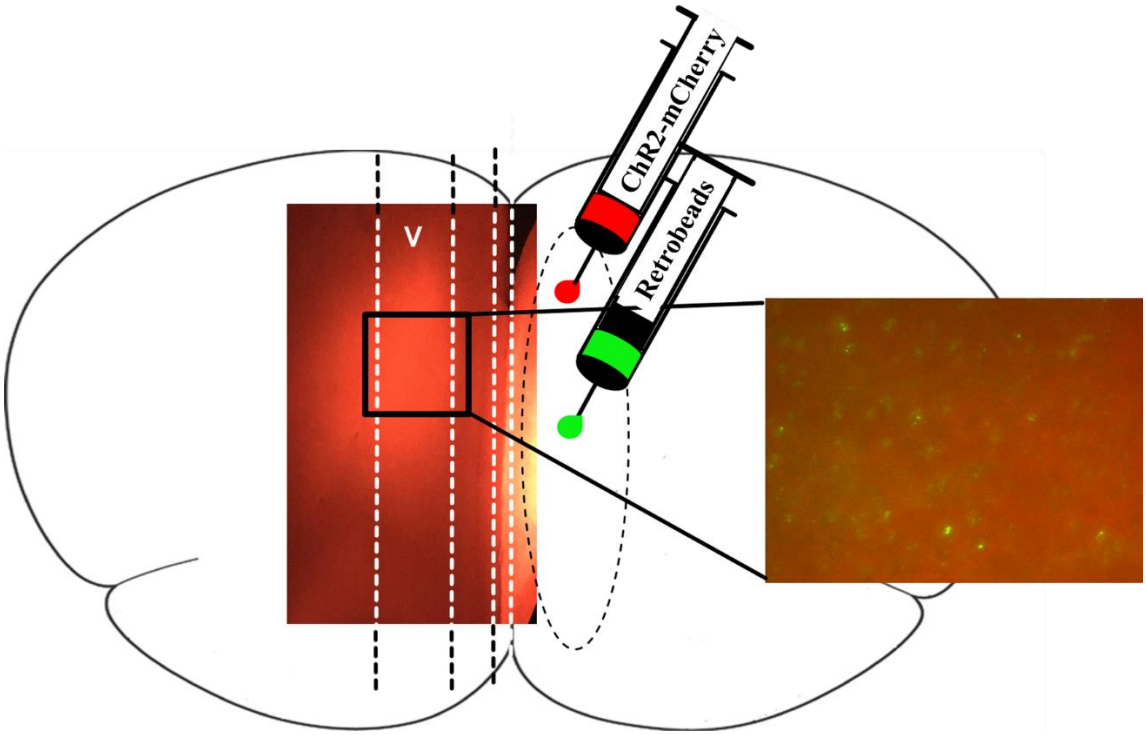

Figure 29: Type II cells and channelrhodopsin-2 expressing commissural fibers. AAV-encased channelrhodopsin-2 tagged with mCherry was injected into layer V of the medial prefrontal cortex. As fibers began expression channelrhodopsin-2, fibers could be visualized with presence of mCherry. After 7-10 weeks, mCherry expressing fibers could be visualized on the contralateral side of the PFC, located within layer I-VI, but accented within layer V. With zoomed magnification, retrobead labelled type II cells could be visualized within the contralateral mPFC, surrounded by fibers containing channelrhodopsin-2 tagged with mCherry.

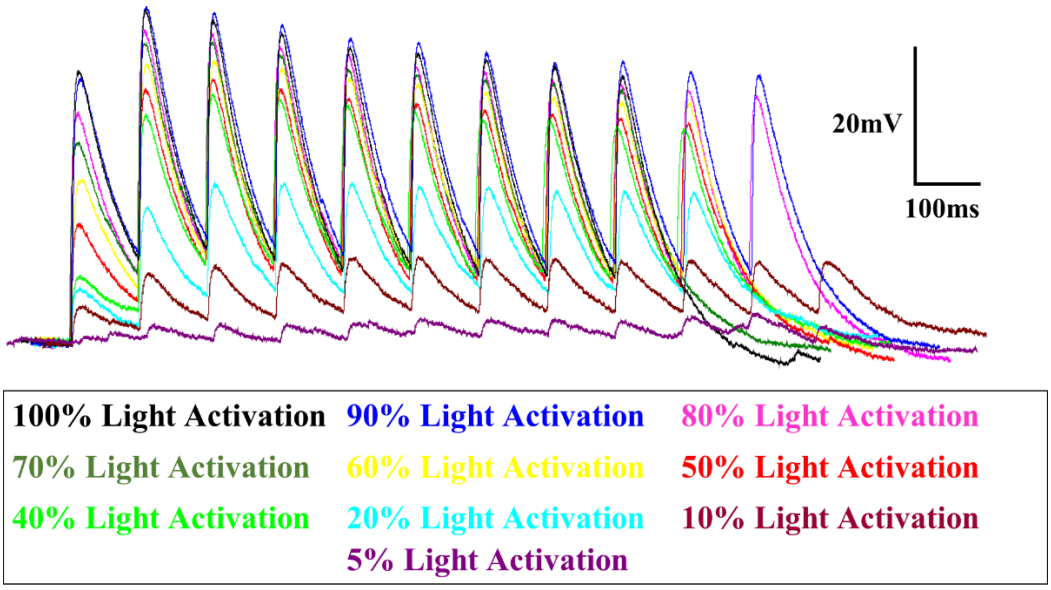

Figure 30: Intensity of light stimulation determines the size of the elicited EPSP's. EPSP's elicited with maximal light activation was largest in amplitude (black trace), and EPSP size decreased in response to decreasing light intensity (scale bar: x=20mV; y=100ms).

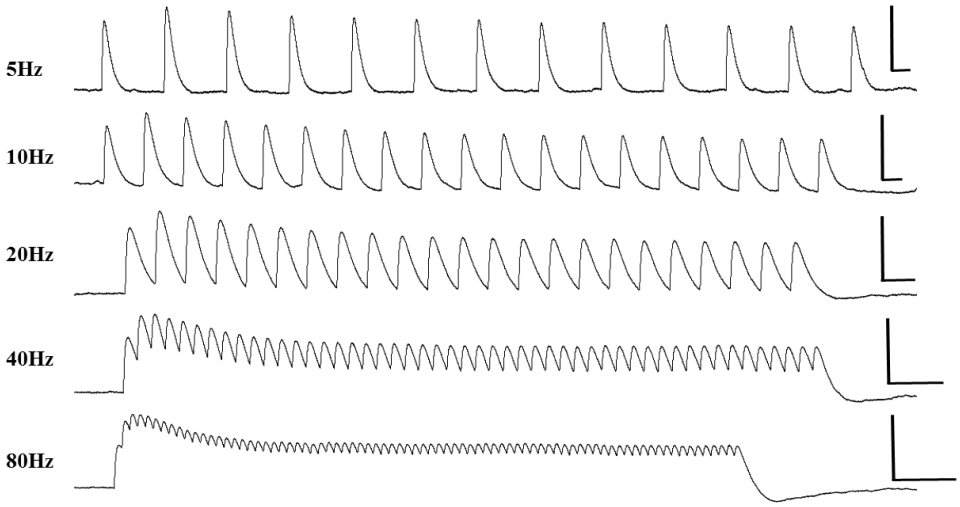

Figure 31: Channelrhodopsin-2 can be effectively activated at various frequencies. Representative traces are shown from top to bottom for varying frequencies (5Hz-80Hz). Although frequencies of less than 5Hz were also used within the study, only 5-80Hz are shown here. Due to its kinetics, channelrhodopsin-2 could be activated at all frequencies observed in this study, with entire EPSPs within the inter-pulse ratio. (scale bar: x=10mV; y=100ms).

Evoked Excitatory Post Synaptic Potential Responses Were Due to Pre-synaptic Action Potential Evoked Neurotransmitter Release

First, we aimed to determine that EPSPs were not evoked due to electrical artifact resulting from the LED. When the LED shutter was closed, EPSP's could not be elicited upon LED activation. However, when the shutter was re-opened, EPSPs were successfully evoked upon every flash of light (figure 32A). Second, to ensure that the EPSPs were due to pre-synaptic action potential evoked neurotransmitter release, tetrodotoxin (TTX; 20μM) was used to block sodium channels, and therefore action potentials evoked in pre-synaptic axons. The blockade of action potentials inhibits neurotransmitter release from the pre-synaptic terminals and in turn, post-synaptic responses. When the tissue was bathed in TTX, EPSP's were diminished (figure 32B), indicating that the optogenetically elicited EPSPs were due to pre-synaptic neurotransmitter release.

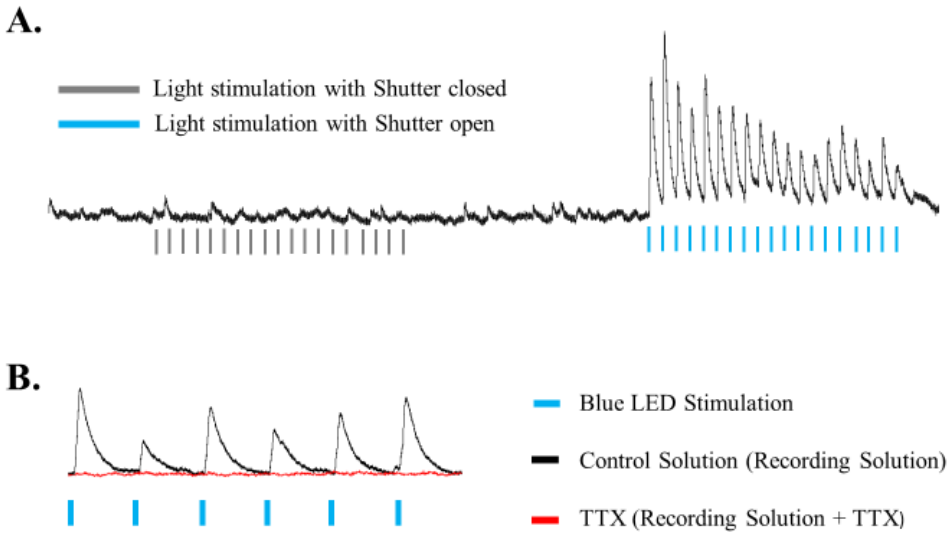

Figure 32: Elicited EPSPs were due to pre-synaptic action potential-evoked neurotransmitter release. (A) Representative trace depicting that EPSPs were not elicited due to electrical artifact. With the LED shutter closed (i.e. blue light was unable to reach the tissue; gray lines indicate blue light flashes, while the shutter was closed) EPSPs were not elicited upon LED activation with the shutter closed. When the shutter was open (i.e. blue light could now penetrate the tissue), EPSP's were successfully elicited at every light flash (blue lines depict each stimulation point). **(B)** In the presence of TTX (red trace), EPSPs elicited by blue light (blue dashes) were blocked compared to control (black trace).

Characteristics of Excitatory Post Synaptic Potentials Evoked by Commissural Afferents in Type I and Type II Pyramidal Cells

Representative EPSP traces for a type I and type II cell, evoked at 1Hz, are shown in figure 33A (top and bottom, respectively). EPSP's elicited in type I cells by activation of commissural inputs show an average rise time of 15.3±1.7ms and decay time of 101.3±10.1ms. Additionally, at 1Hz, these EPSP's displayed an average amplitude of 7.7±1.4mV. EPSP's elicited in type II cells by activation of commissural inputs show an

average rise time of 17.7±3.9ms and decay time of 198.8±51.9ms. Additionally, at 1Hz, these EPSP's displayed an average amplitude of 11.2±3.7mV. EPSP morphology was not significantly different between type I and type II cells (rise time: $p=0.6$; decay time: $p=0.2$).

In type I cells, a large after hyperpolarization was observed after high frequency stimulation trains, which was absent following low frequency trains (figure 33B, top). This after hyperpolarization was absent in type II cells, regardless of the frequency train (figure 33B, bottom). Most interestingly, when commissural inputs onto type I pyramidal cells were optogenetically activated, facilitation (EPSP2>EPSP1) was observed in all cells (figure 34B). However, when commissural inputs onto type II cells were optogenetically activated, depression (EPSP2<EPSP1) was observed in all cells (figure 34C). Type I and type II pyramidal cells showed an average EPSP2/EPSP1 ratio of 1.9±0.5 and 0.6±0.1, respectively, which was significantly different ($p=0.02$).

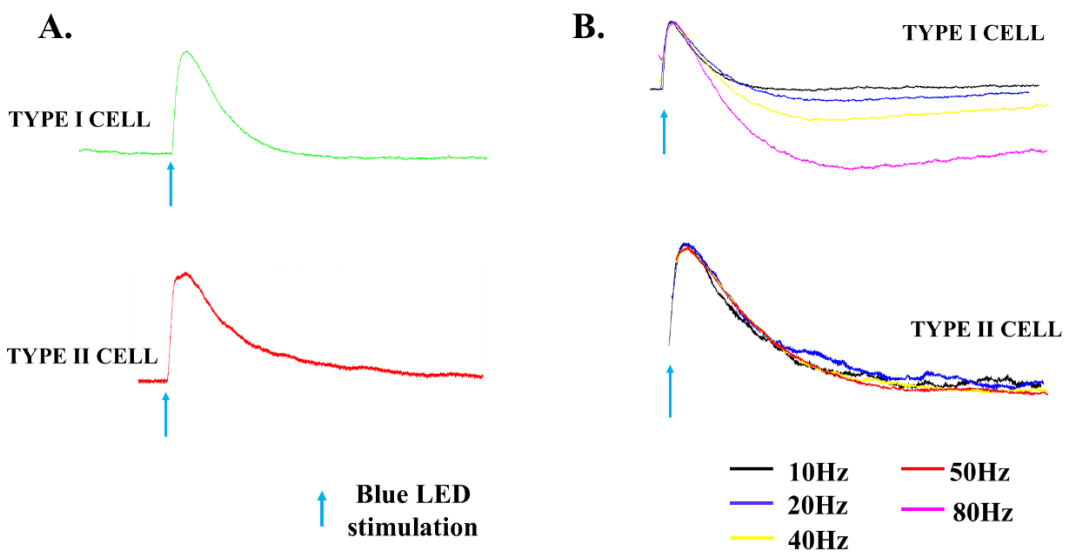

Figure 33: Characteristics of EPSPs in type I and type II cells, elicited by optogenetic activation of commissural fibers. (A) Representative trace depicts a single EPSP induced by a 1ms light pulse (blue arrow) in both type I (top) and type II (bottom). **(B)** Representative traces, at varying frequencies display an increase in after-hyperpolarization amplitude with faster frequencies in type I cells (top), an effect that was absent in type II cells (bottom).

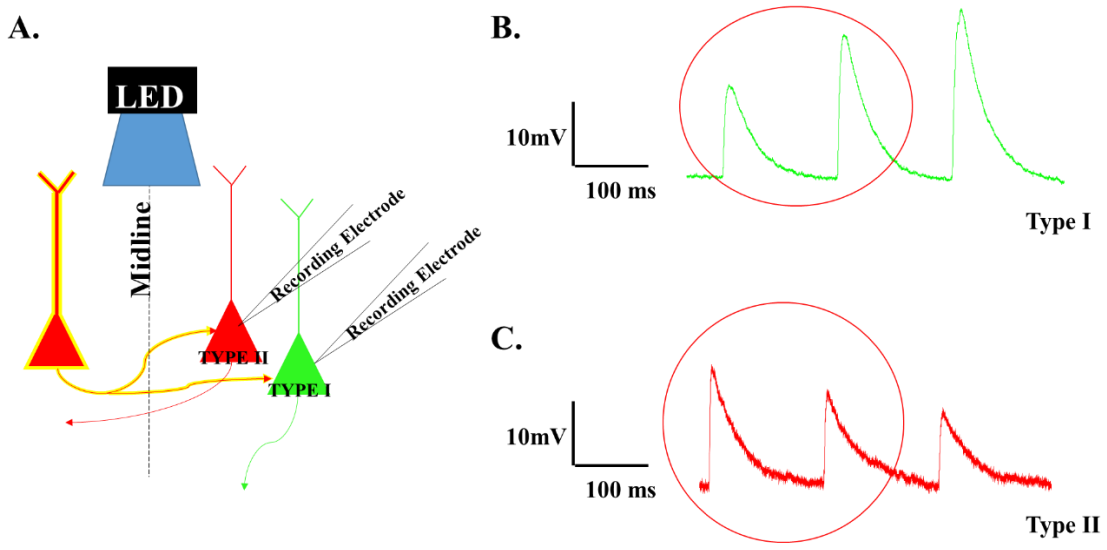

Figure 34: Type I and type II cells display facilitating and depressing dynamics when elicited by optogenetic activation of commissural fibers, respectively. (A) Schematic representation of recordings and optogenetic stimulation. **(B)** Representative trace of EPSPs elicited by commissural inputs onto a type I pyramidal cell, which depict EPSP facilitation (EPSP2>EPSP1), a characteristic observed in all type I cells. **(C)** Representative trace of EPSPs elicited by commissural inputs onto a type II pyramidal cell, which depict EPSP depression (EPSP2<EPSP1), a characteristic observed in all type II cells. (scale bar: x=10mV; y=100ms).

Effects of D1 Receptor Activation on Excitatory Post Synaptic Potentials Evoked in Type I Cells

D1 receptor activation with SKF38393 had three effects on EPSPs evoked in type I cells. First, D1 receptor activation significantly increased the amplitude of EPSPs (7.7±1.4mV in control; 11.1±2.3mV in SKF38393; figure 35A; p=0.01; n=9). This effect was partially blocked by a 5-minute application of the D1 antagonist SCH23390 (9.6±3.6mV). Second, more than half of the cells recorded from (5/9) showed enhanced facilitation in the presence of the D1 agonist (i.e. the EPSP2/EPSP1 ratio was greater in the presence of the D1 agonist). A representative trace demonstrating enhanced facilitation is shown in figure 35B. Third, D1 receptor activation had no effect on the rise

time of EPSPs (15.3±1.6ms in control vs 14.9±2.1ms in SKF38393; p=0.9), yet showed a trend to increase the decay time of the EPSP (101.3±10.1ms in control vs 119.2±15.9ms in SKF38393; p=0.1; figure 35C).

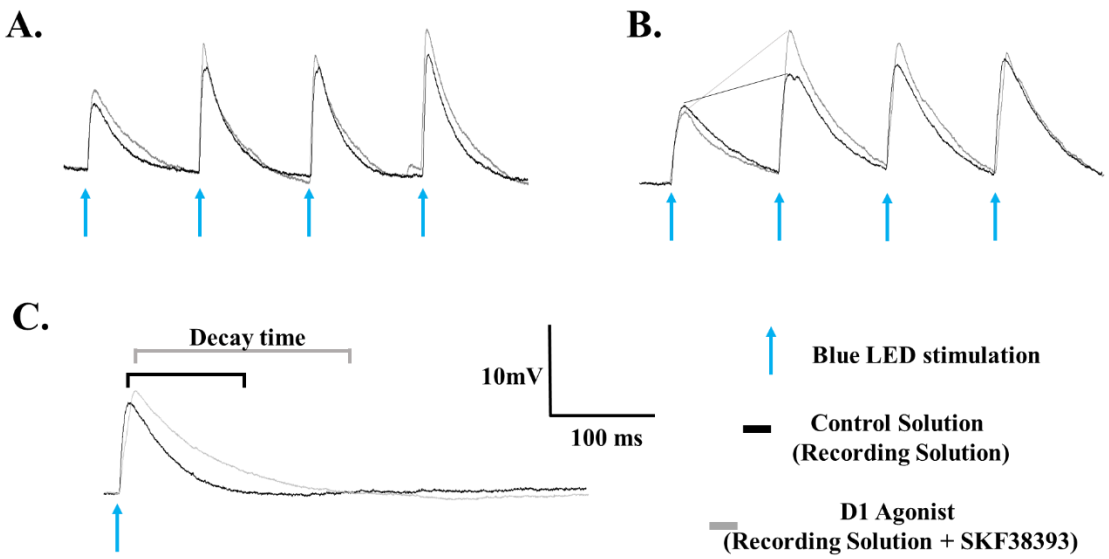

Figure 35: Dopaminergic D1 receptor activation on type I EPSP's elicited by commissural fiber activation. (A) EPSP amplitude was increased in presence of the D1 receptor agonist (gray trace), compared to control (black trace). **(B)** A representative trace displaying an enhancement in EPSP2/EPSP1 ratio with D1 receptor activation (gray trace), compared to control. Black and gray lines connecting EPSP1 to EPSP2 show the relative change in EPSP facilitation. **(C)** A representative trace showing the change in decay time elicited by D1 receptor activation. Control trace is shown in black, and D1 receptor activation is shown in gray. (For A-C, scale bar: x=10mV; y=100ms).

Effects of D1 Receptor Activation on Excitatory Post Synaptic Potentials Evoked in Type II Cells

D1 receptor activation with SKF38393, had two effects on EPSPs evoked in type II cells. First, D1 receptor activation trended to increase the amplitude of EPSPs (11.2±3.7mV in control; 15.7±4.3mV in SKF38393; figure 36A; p=0.2; n=3). This effect was blocked in the presence of the D1 antagonist SCH23390 (10.7±3.6mV). Second, D1 receptor activation had no effect on the rise time of EPSPs (17.7±3.9ms in control vs

20.4±10.9ms in SKF38393; p=0.7) yet showed a trend to increase the decay time of the EPSP (198.8±51.9ms in control vs 328.6±97.3ms in SKF38393; p=0.06; figure 36B). In contrast to type I cells, D1 receptor activation had no effect on the ratio of EPSP2/EPSP1 in type II cells (p=0.7).

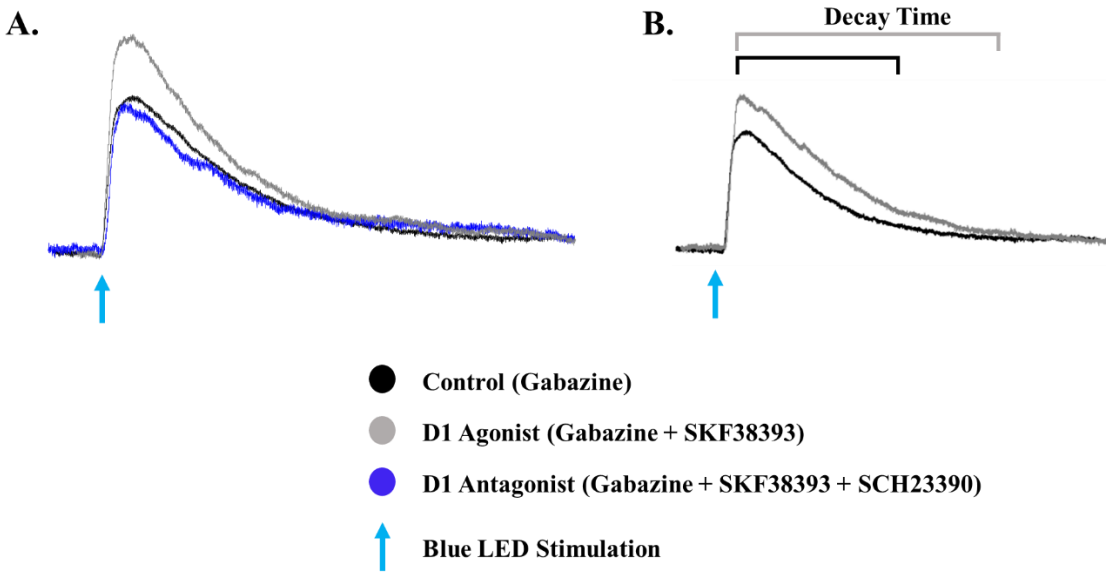

Figure 36: Dopaminergic D1 receptor activation on type II EPSP's elicited by commissural fiber activation. (A) EPSP amplitude was increased in presence of the D1 receptor agonist (gray trace), compared to control (black trace), an effect that was blocked in the presence of the D1 antagonist (SCH23390). **(B)** A representative trace showing the change in decay time elicited by D1 receptor activation. Control trace is shown in black, and D1 receptor activation is shown in gray.

D1 Receptor Activation Elicited Bursting in a Subset of Type I Cells

In a subset of type I layer V pyramidal cells (3/9), application of SKF38393 elicited bursting behavior. Bursting occurred at all train frequencies from 10-50Hz (10Hz is shown in figure 37). Interestingly, the D1 antagonist prevented bursting, but did not completely restore EPSP responses to control within 5 minutes of application. Although

SCH23390 prevented bursting and returned the EPSP amplitude to control, EPSPs remained prolonged (i.e. the EPSP time course was longer than observed in control solution; figure 37C). This suggests that D1 receptor activation may enhance bursting capabilities in a subset of type I cells.

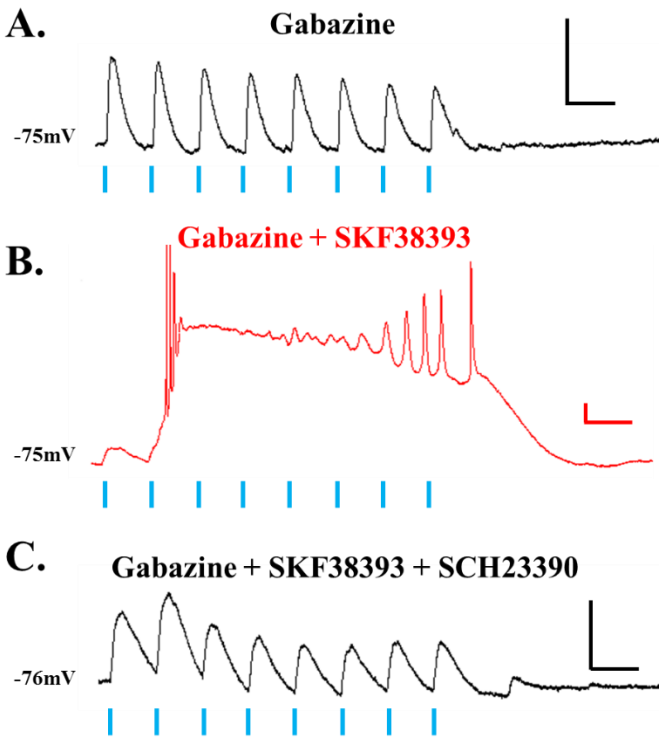

Figure 37: D1 receptor activation elicits bursting in a subset of type I pyramidal cells. (A) In control solution (gabazine containing), a train of 8 EPSPs were elicited in type I cells by optogenetic activation of commissural fibers at 10Hz. **(B)** Upon D1 receptor activation with bath applied SKF38393, the cell elicits a bursting pattern with the same stimulation protocol and light intensity. **(C)** In the presence of the D1 receptor antagonist SCH23390, this bursting behavior is blocked, however the timing of EPSP's remained prolonged compared to control. Scale bars: x=100ms, y=10mV. Blue lines indicate 1ms blue LED light pulses.

Discussion

Summary

In the present study, type I and type II layer V pyramidal neurons were distinguished based on their projection patterns and electrophysiological properties. The main results were as follows: (1) channelrhodopsin-2 can be expressed in commissural mPFC fibers and can be activated using a blue LED. (2) Channelrhodopsin-2 expressing fibers can be activated to elicit EPSPs in type I and type II pyramidal cells at a wide range of frequencies, and these EPSPs were due to pre-synaptic action potential evoked transmitter release. (3) Commissural inputs onto type I and type II cells display facilitation and depression patterns of EPSPs, respectively. (4) D1 receptor activation increased the amplitude, enhanced facilitation and altered the decay times of commissural evoked EPSPs in type I cells. (5) D1 receptor activation increased the amplitude and prolonged EPSP decay time of commissural evoked EPSPs in type II cells. (6) D1 receptor activation can elicit burst firing in a subset of type I layer V pyramidal cells.

Comparisons with Previous Studies

Some studies have suggested that commissural activation onto type I and type II pyramidal cells results in different EPSP characteristics. As reported by Dembrow and colleagues (2015), we also observed that optogenetic activation of commissural fibers onto type I and type II cells elicits a longer decay time in type II cells compared to type I cells. Additionally, like Dembrow et al. (2015) we also report that the rise times of commissural evoked EPSPs elicited in type I and type II cells are non-significantly different. Further, we report a large hyperpolarization after EPSP trains evoked at high frequencies in type I but not type II cells.

Also consistent with other studies (20), we report that type I and type II cells exhibit facilitating and depressing responses, respectively, when excited by repetitive commissural fiber stimulation. In addition to reports of differences in local connectivity (20, 28, 108, 118), Wang and colleagues (2006) suggest that some layer V pyramidal cells display only facilitating EPSP patterns, while others only display a depressing pattern. However, this study did not distinguish between layer V pyramidal subtypes. Interestingly, with paired dual recordings, Morishima and colleagues (2011) report that type II inputs onto type I cells can display a either facilitating and depressing responses. However, using opotogenetic activation, Lee et al. (2014) reported that commissural activation of type I and type II cells results in facilitating and depressing paired-pulse responses, respectively. Our results support the hypothesis that layer V pyramidal cell subtypes integrate synaptic inputs differently, consistent with previous studies that use a similar optogenetic protocol (e.g. Lee et al. 2014).

Implications for Prefrontal Function

To our knowledge this study is the first to characterize the effects of D1 receptor activation on optogenetically activated commissural inputs targeting type I and type II cells. However, it is known that type I cells are the only subtype of layer V cells that can fire persistently in response to neuromodulators (19), whereas type II cells primarily function as temporal integrators (32, 108). Our results suggest that D1 receptor activation could promote persistent firing in type I cells by increasing commissural-evoked EPSP amplitude, promoting facilitation, and promote synaptic integration by widening the timing window of EPSPs. Because this study is the first to identify the effects of dopamine on commissural inputs targeting layer V pyramidal cells, it is difficult to

compare these results to other studies. However, one study suggests that moderate D1 receptor activation can promote persistent firing in deep prefrontal cortical neurons by producing prolonged depolarization in response to a train of inputs (119), supporting the hypothesis that D1 receptor activation may promote persistent firing in type I cells.

Furthermore, our results suggest that D1 receptor activation may promote temporal integration of commissural inputs by enhancing EPSP amplitude and widening the timing window of EPSPs. Because these cells cannot be induced to fire persistently in the presence of neuromodulators (19), we hypothesize that D1 receptor activation may have a differential effect on commissural EPSP integration impinging onto type II cells.

Lastly, we report that dopaminergic D1 receptor activation can lead to burst firing in a subset of type I layer V pyramidal cells. We hypothesize that D1 receptor activation may uncover the subset of type I layer V pyramidal cells, identified previously as "intrinsic bursting" or IB cells (120).

Conclusion

As discussed above, the mPFC is highly interconnected with other neocortical areas, including the contralateral mPFC. The data presented here suggest that D1 receptor activation may promote persistent firing and temporal integration in type I and type II cells, respectively. Dopamine can play an important role in reverberant and persistent neuronal activity within the mPFC (113), and it is known that proper levels of dopamine are essential for memory-related tasks. However, it remains unclear where dopamine acts to modulate such functions. Thus, our data suggests that normal activation of D1 receptors may aid in working-memory related tasks by enhancing persistent activity of type I cells and enhancing temporal integration of type II cells. Based on our results and

those of others, it is conceivable that insufficient activation of D1 receptors in schizophrenic patients (i.e. during a depressive state) may lead to distractibility due to an inability to maintain recurrent activity between layer V output cells. In contrast, during hyperdopaminergic states (i.e. during psychotic episodes) excessive activation of D1 receptors may lead to perseveration due to inappropriate layer V cell firing. Also, the former would contribute to poor performance on working memory tasks, while the latter could contribute to false attributions regarding contextual information and the disorganized thought patterns commonly observed in the disorder.

CHAPTER VI

CONCLUSIONS

In summary, the data presented here provide evidence that layer V pyramidal cells of the prefrontal cortex differentially integrate information based on their projection patterns and intrinsic properties. Additionally, these data support the idea that type I and type II cells integrate information in a compartmentalized manner. Thus, information impinging onto the basal dendrites is integrated differently than information targeting the apical tufts of pyramidal cells. These studies also reveal that dopamine, acting through D1 and D2 receptors, can differentially modulate layer V pyramidal subtypes, in a compartment-dependent fashion. Furthermore, the results suggest that dopamine modulates specific afferents targeting layer V pyramidal cells of the mPFC.

In the studies conducted, I provide evidence for compartmentalized dopaminergic effects on type I and type II cells. Overall, these data suggest that D1 receptor activation promotes local connectivity (primarily layer V to layer V connections) in the basal dendrites, while simultaneously inhibiting synaptic plasticity within the apical tufts through the suppression of NMDAR-mediated responses (discussed in chapter IV). Additionally, D2 receptor activation had no significant effect on local layer V synapses, but may play a role in regulating the signal-to-noise ratio in the apical tufts, by inhibiting low-frequency inputs and facilitating high frequency inputs, assuming that afferents firing at high frequencies are carrying more pertinent information (discussed in chapter

III). Taken together, these results suggest that with optimal dopamine levels, local influences (i.e. environmental / "bottom-up") and plasticity will be promoted within layer V of the mPFC, while "top-down" or contextual information impinging on layer I is stabilized.

Interestingly, patients with schizophrenia go through periods of dysregulated dopamine levels. During depressive states of the disorder, the patient often has depleted levels of dopamine (i.e. hypodopaminergic activity), which would lead to insufficient activation of D1 receptors. Our data suggests that insufficient activation would cause local connections between layer V cells to lose their ability to maintain recurrent connectivity. Additionally, without sufficient activation of D1 receptors, information impinging onto the apical tufts may not be properly suppressed, leading to excessive "top-down" / contextual signals. Therefore, insufficient suppression could lead to inappropriate contextual associations and blunted integration of basal dendritic inputs.

In contrast, during psychotic episodes and manic states of the disorder, patients often have elevated levels of dopamine (i.e. hyperactive dopaminergic activity). These results would suggest that layer V connectivity may be overly promoted and contextual, information impinging on the apical dendrites, overly suppressed. This combination may lead to the promotion of inappropriate environmental information, giving rise to hallucinations and perseveration often observed in the disorder.

It has been proposed that insufficient dopamine release in the prefrontal cortex may in part give rise to cognitive dysfunction observed in schizophrenia (64, 116, 117). Based on our results and those of others, it is conceivable that insufficient activation of dopaminergic receptors in schizophrenic patients could lead to an inability to maintain

recurrent activity between layer V output cells, and/or an excessive influence of top-down signals. The former would contribute to poor performance on working memory tasks, while the latter could contribute to false attributions regarding contextual information and the disorganized thought patterns commonly observed in the disorder.

The data presented in chapter V, demonstrate that dopamine differentially modulates afferents targeting mPFC layer V pyramidal cells. I found that D1 receptor modulation may enhance the ability of type I and type II cells to integrate information from commissural afferents. Therefore, I hypothesize that the effects of D1 receptor activation on commissural synaptic responses facilitate persistent firing in type I cells and facilitate temporal integration by type II cells.

Regarding schizophrenia, hyperdopaminergic activity and overstimulation of dopaminergic receptors, type I cells and type II cells would integrate information inappropriately, thus again promoting hallucinations and perseveration as discussed above. In contrast, insufficient D1 receptor activity would prevent the ability of type I and type II cells to integrate information, leading to disruptions in working memory capabilities, a symptom which is also commonly observed within the disorder.

Overall, the results presented in this dissertation lend insight into normal dopaminergic function within the prefrontal cortex. These results further the understanding of how dopamine may contribute to normal executive functioning and working memory capabilities. These studies provide an important step in linking cellular level phenomena with normal PFC function and dopaminergic effects on working memory. Further, these findings may lend insight into how dysregulation of the dopamine system may give rise to symptoms often observed in patients with psychiatric disorders like schizophrenia.

Future Directions

In the last specific aim of my dissertation work, I have characterized the effects of dopaminergic D1 receptor activation on commissural inputs targeting both type I and type II layer V pyramidal cells. However, to fully understand the integration properties of layer V pyramidal cells, it is essential to characterize how layer V pyramidal cells integrate all inputs targeting the mPFC. Layer V cells are known to integrate information from the hippocampus, amygdala and thalamus. Thus, it would prove beneficial to characterize how layer V pyramidal cells integrate these additional inputs. Using an optogenetic approach, like the one conducted in chapter V, the properties of excitatory inputs from hippocampus, amygdala and thalamus onto layer V pyramidal cells could be determined. These studies would lend insight into how layer V pyramidal cells integrate information necessary for working memory function. Additionally, because dopamine plays an essential role in normal prefrontal function, it would greatly advance the current knowledge of prefrontal function to determine the effects of dopamine on these various connections.

Furthermore, studies presented here suggest that dopamine, through D1 receptor activation, may unmask a subtype of type I pyramidal cells previously characterized as intrinsic bursting cells. Because this phenomenon has not yet been described in other studies, I believe further characterization of this layer V subtype would prove beneficial. The unmasking of intrinsic bursting cells through D1 receptor activation may promote coincidence detection in this subset of cells. It would be of interest to determine whether this subset of type I cells characterized in these experiments show similar electrophysiological characteristics as those previously described as intrinsic bursting

cells (121). These studies would address whether this subpopulation of type I cells is the same subset characterized in other studies, or whether this is an additional type I subtype. Additionally, identifying the gene expression differences between the bursting and non-bursting cells, using single cell mRNA sequencing would ultimately distinguish the two subtypes. These experiments would assess whether bursting and non-bursting subtypes display genetic differences that could account for bursting in response to D1 receptor activation.

Although the current studies suggest that D1 receptor activation elicits bursting in response to activation of commissural in type I cells, it would be of further interest to determine whether this subtype displays bursting in response to other optogenetically activated inputs, such as the hippocampus, amygdala and thalamus. These experiments would provide insight into whether D1 receptor activation unmasks bursting in this subtype through its effects on specific inputs.

Overall, the additional studies outlined here would identify whether type I cells could be further subcategorized based on intrinsic properties and dopaminergic effects. Additionally, these studies may lend further insight into how different layer V pyramidal cell subtypes contribute to working memory functions through integration of relevant information from distinct sources. In order to understand overarching cognitive functioning, it is pertinent to understand the different cell types and their contributions within the prefrontal cortex.

REFERENCES

1. Moskowitz GB (2012) The Representation and Regulation of Goals. *Goal-Directed Behavior*, ed Elliot HAaAJ (Psychology Press Taylor & Francis Group, New York, London).

2. Deci EL & Ryan RM (1991) A motivational approach to self: Integration in personality. *Nebraska symposium on motivation*, ed Dienstbier IR (University of Nebraska Press, Lincoln), Vol 38, pp 237-288.

3. Kruglanski A, *et al.* (2002) A theory of goal systems. *Advances in experimental social psychology*, ed Zanna MP (Academic Press, San Diego, CA), Vol 34, pp 331-378.

4. Diekhof EK & Gruber O (2010) When desire collides with reason: functional interactions between anteroventral prefrontal cortex and nucleus accumbens underlie the human ability to resist impulsive desires. *J Neurosci* 30(4):1488-1493.

5. Denckla MB (1994) Measurement of executive function. *Frames of reference for the assessment of learning disabilities: New views on measurement issues*, ed Lyon GR (Paul H. Brooks, Baltimore, MD), pp 117-142.

6. Euston DR, Gruber AJ, & McNaughton BL (2012) The role of medial prefrontal cortex in memory and decision making. *Neuron* 76(6):1057-1070.

7. Heidbreder CA & Groenewegen HJ (2003) The medial prefrontal cortex in the rat: evidence for a dorso-ventral distinction based upon functional and anatomical characteristics. *Neurosci Biobehav Rev* 27(6):555-579.

8. Seamans JK, Lapish CC, & Durstewitz D (2008) Comparing the prefrontal cortex of rats and primates: insights from electrophysiology. *Neurotox Res* 14(2-3):249-262.

9. Lewis DA & Gonzalez-Burgos G (2006) Pathophysiologically based treatment interventions in schizophrenia. *Nat Med* 12(9):1016-1022.

10. Bicks LK, Koike H, Akbarian S, & Morishita H (2015) Prefrontal Cortex and Social Cognition in Mouse and Man. *Front Psychol* 6:1805.

11. Morgan MA & LeDoux JE (1995) Differential contribution of dorsal and ventral medial prefrontal cortex to the acquisition and extinction of conditioned fear in rats. *Behav Neurosci* 109(4):681-688.

12. Quirk GJ, *et al.* (2010) Erasing fear memories with extinction training. *J Neurosci* 30(45):14993-14997.

13. Arnsten AF, Raskind MA, Taylor FB, & Connor DF (2015) The Effects of Stress Exposure on Prefrontal Cortex: Translating Basic Research into Successful Treatments for Post-Traumatic Stress Disorder. *Neurobiol Stress* 1:89-99.

14. Milad MR & Quirk GJ (2002) Neurons in medial prefrontal cortex signal memory for fear extinction. *Nature* 420(6911):70-74.

15. Peters J, Dieppa-Perea LM, Melendez LM, & Quirk GJ (2010) Induction of fear extinction with hippocampal-infralimbic BDNF. *Science* 328(5983):1288-1290.

16. Davis M (1992) The role of the amygdala in fear and anxiety. *Annu Rev Neurosci* 15:353-375.

17. Rudy JW & O'Reilly RC (2001) Conjunctive representations, the hippocampus, and contextual fear conditioning. *Cogn Affect Behav Neurosci* 1(1):66-82.

18. Mountcastle VB (1997) The columnar organization of the neocortex. *Brain* 120 (Pt 4):701-722.

19. Dembrow NC, Chitwood RA, & Johnston D (2010) Projection-specific neuromodulation of medial prefrontal cortex neurons. *J Neurosci* 30(50):16922-16937.

20. Lee AT, *et al.* (2014) Pyramidal neurons in prefrontal cortex receive subtype-specific forms of excitation and inhibition. *Neuron* 81(1):61-68.

21. Gee S, *et al.* (2012) Synaptic activity unmasks dopamine D2 receptor modulation of a specific class of layer V pyramidal neurons in prefrontal cortex. *J Neurosci* 32(14):4959-4971.

22. Defelipe J, Markram H, & Rockland KS (2012) The neocortical column. *Front Neuroanat* 6:22.

23. Hubel DH & Wiesel TN (1974) Sequence regularity and geometry of orientation columns in the monkey striate cortex. *J Comp Neurol* 158(3):267-293.

24. Markram H (2008) Fixing the location and dimensions of functional neocortical columns. *HFSP J* 2(3):132-135.

25. Thomson AM & Morris OT (2002) Selectivity in the inter-laminar connections made by neocortical neurones. *J Neurocytol* 31(3-5):239-246.

26. Deuchars J, West DC, & Thomson AM (1994) Relationships between morphology and physiology of pyramid-pyramid single axon connections in rat neocortex in vitro. *J Physiol* 478 Pt 3:423-435.

27. Markram H, Lübke J, Frotscher M, Roth A, & Sakmann B (1997) Physiology and anatomy of synaptic connections between thick tufted pyramidal neurones in the developing rat neocortex. *J Physiol* 500 (Pt 2):409-440.

28. Wang Y, *et al.* (2006) Heterogeneity in the pyramidal network of the medial prefrontal cortex. *Nat Neurosci* 9(4):534-542.

29. Reiner A, Jiao Y, Del Mar N, Laverghetta AV, & Lei WL (2003) Differential morphology of pyramidal tract-type and intratelencephalically projecting-type corticostriatal neurons and their intrastriatal terminals in rats. *J Comp Neurol* 457(4):420-440.

30. Morishima M, Morita K, Kubota Y, & Kawaguchi Y (2011) Highly differentiated projection-specific cortical subnetworks. *J Neurosci* 31(28):10380-10391.

31. Sherman SM & Guillery RW (1998) On the actions that one nerve cell can have on another: distinguishing "drivers" from "modulators". *Proc Natl Acad Sci U S A* 95(12):7121-7126.

32. Dembrow NC, Zemelman BV, & Johnston D (2015) Temporal dynamics of L5 dendrites in medial prefrontal cortex regulate integration versus coincidence detection of afferent inputs. *J Neurosci* 35(11):4501-4514.

33. Goldman-Rakic PS, Funahashi S, & Bruce CJ (1990) Neocortical memory circuits. *Cold Spring Harb Symp Quant Biol* 55:1025-1038.

34. Wang XJ (2001) Synaptic reverberation underlying mnemonic persistent activity. *Trends Neurosci* 24(8):455-463.

35. Durstewitz D, Seamans JK, & Sejnowski TJ (2000) Dopamine-mediated stabilization of delay-period activity in a network model of prefrontal cortex. *J Neurophysiol* 83(3):1733-1750.

36. Jensen O & Tesche CD (2002) Frontal theta activity in humans increases with memory load in a working memory task. *Eur J Neurosci* 15(8):1395-1399.

37. Goldman-Rakic PS (1995) Cellular basis of working memory. *Neuron* 14(3):477-485.

38. von Stein A & Sarnthein J (2000) Different frequencies for different scales of cortical integration: from local gamma to long range alpha/theta synchronization. *Int J Psychophysiol* 38(3):301-313.

39. Larkum ME, Nevian T, Sandler M, Polsky A, & Schiller J (2009) Synaptic integration in tuft dendrites of layer 5 pyramidal neurons: a new unifying principle. *Science* 325(5941):756-760.

40. Klausberger T & Somogyi P (2008) Neuronal diversity and temporal dynamics: the unity of hippocampal circuit operations. *Science* 321(5885):53-57.

41. Lasztóczi B & Klausberger T (2014) Layer-specific GABAergic control of distinct gamma oscillations in the CA1 hippocampus. *Neuron* 81(5):1126-1139.

42. Belluscio MA, Mizuseki K, Schmidt R, Kempter R, & Buzsáki G (2012) Cross-frequency phase-phase coupling between θ and γ oscillations in the hippocampus. *J Neurosci* 32(2):423-435.

43. Larkum M (2013) A cellular mechanism for cortical associations: an organizing principle for the cerebral cortex. *Trends Neurosci* 36(3):141-151.

44. Thomas M & Erickson J (2011) Effects of dopamine on electrical resonance properties of mouse layer 5 pyramidal neurons. *Society for Neuroscience*, (Society for Neuroscience).

45. van Aerde KI, *et al.* (2009) Flexible spike timing of layer 5 neurons during dynamic beta oscillation shifts in rat prefrontal cortex. *J Physiol* 587(Pt 21):5177-5196.

46. Schnitzler A & Gross J (2005) Normal and pathological oscillatory communication in the brain. *Nat Rev Neurosci* 6(4):285-296.

47. Hoover WB & Vertes RP (2007) Anatomical analysis of afferent projections to the medial prefrontal cortex in the rat. *Brain Struct Funct* 212(2):149-179.

48. Little JP & Carter AG (2012) Subcellular synaptic connectivity of layer 2 pyramidal neurons in the medial prefrontal cortex. *J Neurosci* 32(37):12808-12819.

49. Condé F, Audinat E, Maire-Lepoivre E, & F C (1990) *Afferent connections of the medial frontal cortex of the rat. A study using retrograde transport of fluorescent dyes. I. Thalamic afferents*. *Brain Research Bulletin* 24:341-354.

50. Cruikshank SJ, *et al.* (2012) Thalamic control of layer 1 circuits in prefrontal cortex. *J Neurosci* 32(49):17813-17823.

51. Orozco-Cabal L, *et al.* (2006) A novel rat medial prefrontal cortical slice preparation to investigate synaptic transmission from amygdala to layer V prelimbic pyramidal neurons. *J Neurosci Methods* 151(2):148-158.

52. Vertes RP, Hoover WB, Do Valle AC, Sherman A, & Rodriguez JJ (2006) Efferent projections of reuniens and rhomboid nuclei of the thalamus in the rat. *J Comp Neurol* 499(5):768-796.

53. Bacon SJ, Headlam AJ, Gabbott PL, & Smith AD (1996) Amygdala input to medial prefrontal cortex (mPFC) in the rat: a light and electron microscope study. *Brain Res* 720(1-2):211-219.

54. Riga D, *et al.* (2014) Optogenetic dissection of medial prefrontal cortex circuitry. *Front Syst Neurosci* 8:230.

55. Nagel G, *et al.* (2003) Channelrhodopsin-2, a directly light-gated cation-selective membrane channel. *Proc Natl Acad Sci U S A* 100(24):13940-13945.

56. Mattis J, *et al.* (2012) Principles for applying optogenetic tools derived from direct comparative analysis of microbial opsins. *Nat Methods* 9(2):159-172.

57. Gonzalez-Burgos G & Lewis DA (2008) GABA neurons and the mechanisms of network oscillations: implications for understanding cortical dysfunction in schizophrenia. *Schizophr Bull* 34(5):944-961.

58. Malinow R & Malenka RC (2002) AMPA receptor trafficking and synaptic plasticity. *Annu Rev Neurosci* 25:103-126.

59. Herron CE, Lester RA, Coan EJ, & Collingridge GL (1986) Frequency-dependent involvement of NMDA receptors in the hippocampus: a novel synaptic mechanism. *Nature* 322(6076):265-268.

60. Malenka RC & Nicoll RA (1993) NMDA-receptor-dependent synaptic plasticity: multiple forms and mechanisms. *Trends Neurosci* 16(12):521-527.

61. Sawaguchi T & Goldman-Rakic PS (1991) D1 dopamine receptors in prefrontal cortex: involvement in working memory. *Science* 251(4996):947-950.

62. D'Ardenne K, *et al.* (2012) Role of prefrontal cortex and the midbrain dopamine system in working memory updating. *Proc Natl Acad Sci U S A* 109(49):19900-19909.

63. Arias-Carrión O & Pöppel E (2007) Dopamine, learning, and reward-seeking behavior. *Acta Neurobiol Exp (Wars)* 67(4):481-488.

64. Goto Y, Otani S, & Grace AA (2007) The Yin and Yang of dopamine release: a new perspective. *Neuropharmacology* 53(5):583-587.

65. Abi-Dargham A (2014) Schizophrenia: overview and dopamine dysfunction. *J Clin Psychiatry* 75(11):e31.

66. Surmeier JDB, JoseHemmings, H.C. Jr.Greengard, Paul (1995) Modulation of calcium currents by a D_1 dopaminergic protein kinase/phosphatase cascade in rat neostriatal neurons. *Neuron* 14(2):385-397.

67. Obadiah J, *et al.* (1999) Adenylyl cyclase interaction with the D2 dopamine receptor family; differential coupling to Gi, Gz, and Gs. *Cell Mol Neurobiol* 19(5):653-664.

68. Gaspar P, Bloch B, & Le Moine C (1995) D1 and D2 receptor gene expression in the rat frontal cortex: cellular localization in different classes of efferent neurons. *Eur J Neurosci* 7(5):1050-1063.

69. Floresco SB (2013) Prefrontal dopamine and behavioral flexibility: shifting from an "inverted-U" toward a family of functions. *Front Neurosci* 7:62.

70. Sesack SR, Snyder CL, & Lewis DA (1995) Axon terminals immunolabeled for dopamine or tyrosine hydroxylase synapse on GABA-immunoreactive dendrites in rat and monkey cortex. *J Comp Neurol* 363(2):264-280.

71. Wedzony K, Czepiel K, & Fijał K (2001) Immunohistochemical evidence for localization of NMDAR1 receptor subunit on dopaminergic neurons of the rat substantia nigra, pars compacta. *Pol J Pharmacol* 53(6):675-679.

72. Arnsten AF (1997) Catecholamine regulation of the prefrontal cortex. *J Psychopharmacol* 11(2):151-162.

73. Zahrt J, Taylor JR, Mathew RG, & Arnsten AF (1997) Supranormal stimulation of D1 dopamine receptors in the rodent prefrontal cortex impairs spatial working memory performance. *J Neurosci* 17(21):8528-8535.

74. Williams GV & Castner SA (2006) Under the curve: critical issues for elucidating D1 receptor function in working memory. *Neuroscience* 139(1):263-276.

75. Ito HT & Schuman EM (2007) Frequency-dependent gating of synaptic transmission and plasticity by dopamine. *Front Neural Circuits* 1:1.

76. Young CE & Yang CR (2005) Dopamine D1-like receptor modulates layer- and frequency-specific short-term synaptic plasticity in rat prefrontal cortical neurons. *Eur J Neurosci* 21(12):3310-3320.

77. Rosenkranz JA & Johnston D (2006) Dopaminergic regulation of neuronal excitability through modulation of Ih in layer V entorhinal cortex. *J Neurosci* 26(12):3229-3244.

78. Gorelova NA & Yang CR (2000) Dopamine D1/D5 receptor activation modulates a persistent sodium current in rat prefrontal cortical neurons in vitro. *J Neurophysiol* 84(1):75-87.

79. Seamans JK, Durstewitz D, Christie BR, Stevens CF, & Sejnowski TJ (2001) Dopamine D1/D5 receptor modulation of excitatory synaptic inputs to layer V prefrontal cortex neurons. *Proc Natl Acad Sci U S A* 98(1):301-306.

80. Wang J & O'Donnell P (2001) D1 Dopamine Receptors Potentiate NMDA-mediated Excitability Increase in Layer V Prefrontal Cortical Pyramidal Neurons. *Cerebral Cortex* 11(5):10.

81. Seeman P (2010) Dopamine D2 receptors as treatment targets in schizophrenia. *Clin Schizophr Relat Psychoses* 4(1):56-73.

82. Allison DB & Casey DE (2001) Antipsychotic-induced weight gain: a review of the literature. *J Clin Psychiatry* 62 Suppl 7:22-31.

83. Divac N, Prostran M, Jakovcevski I, & Cerovac N (2014) Second-generation antipsychotics and extrapyramidal adverse effects. *Biomed Res Int* 2014:656370.

84. Molnár Z & Cheung AF (2006) Towards the classification of subpopulations of layer V pyramidal projection neurons. *Neurosci Res* 55(2):105-115.

85. Leyrer-Jackson JM & Thomas MP (2016) Differential effects of dopaminergic D2 receptor activation on synaptic responses in a subset of layer V mouse medial prefrontal pyramidal neurons. *Society for Neuroscience*.

86. Spindle MS & Thomas MP (2014) Activation of 5-HT2A receptors by TCB-2 induces recurrent oscillatory burst discharge in layer 5 pyramidal neurons of the mPFC in vitro. *Physiol Rep* 2(5).

87. Chuhma N, Choi WY, Mingote S, & Rayport S (2009) Dopamine neuron glutamate cotransmission: frequency-dependent modulation in the mesoventromedial projection. *Neuroscience* 164(3):1068-1083.

88. Castro-Alamancos MA (2002) Properties of primary sensory (lemniscal) synapses in the ventrobasal thalamus and the relay of high-frequency sensory inputs. *J Neurophysiol* 87(2):946-953.

89. Castro-Alamancos MA (2002) Different temporal processing of sensory inputs in the rat thalamus during quiescent and information processing states in vivo. *J Physiol* 539(Pt 2):567-578.

90. Davies CH & Collingridge GL (1996) Regulation of EPSPs by the synaptic activation of GABAB autoreceptors in rat hippocampus. *J Physiol* 496 (Pt 2):451-470.

91. Arnsten AF, Cai JX, Steere JC, & Goldman-Rakic PS (1995) Dopamine D2 receptor mechanisms contribute to age-related cognitive decline: the effects of quinpirole on memory and motor performance in monkeys. *J Neurosci* 15(5 Pt 1):3429-3439.

92. Druzin MY, Kurzina NP, Malinina EP, & Kozlov AP (2000) The effects of local application of D2 selective dopaminergic drugs into the medial prefrontal cortex of rats in a delayed spatial choice task. *Behav Brain Res* 109(1):99-111.

93. Tseng KY & O'Donnell P (2007) D2 dopamine receptors recruit a GABA component for their attenuation of excitatory synaptic transmission in the adult rat prefrontal cortex. *Synapse* 61(10):843-850.

94. Trantham-Davidson H, Neely LC, Lavin A, & Seamans JK (2004) Mechanisms underlying differential D1 versus D2 dopamine receptor regulation of inhibition in prefrontal cortex. *J Neurosci* 24(47):10652-10659.

95. Seamans JK, Gorelova N, Durstewitz D, & Yang CR (2001) Bidirectional dopamine modulation of GABAergic inhibition in prefrontal cortical pyramidal neurons. *J Neurosci* 21(10):3628-3638.

96. Kotecha SA, *et al.* (2002) A D2 class dopamine receptor transactivates a receptor tyrosine kinase to inhibit NMDA receptor transmission. *Neuron* 35(6):1111-1122.

97. Cepeda C & Levine MS (1998) Dopamine and N-methyl-D-aspartate receptor interactions in the neostriatum. *Dev Neurosci* 20(1):1-18.

98. Law-Tho D, Hirsch JC, & Crepel F (1994) Dopamine modulation of synaptic transmission in rat prefrontal cortex: an in vitro electrophysiological study. *Neuroscience Research* 21(2):9.

99. Zheng P, Zhang XX, Bunney BS, & Shi WX (1999) Opposite modulation of cortical N-methyl-D-aspartate receptor-mediated responses by low and high concentrations of dopamine. *Neuroscience* 91(2):527-535.

100. Benoit-Marand M & O'Donnell P (2008) D2 dopamine modulation of corticoaccumbens synaptic responses changes during adolescence. *Eur J Neurosci* 27(6):1364-1372.

101. Grace AA (2000) Gating of information flow within the limbic system and the pathophysiology of schizophrenia. *Brain Res Brain Res Rev* 31(2-3):330-341.

102. Kline DD, Takacs KN, Ficker E, & Kunze DL (2002) Dopamine modulates synaptic transmission in the nucleus of the solitary tract. *J Neurophysiol* 88(5):2736-2744.

103. Otani S, Blond O, Desce JM, & Crépel F (1998) Dopamine facilitates long-term depression of glutamatergic transmission in rat prefrontal cortex. *Neuroscience* 85(3):669-676.

104. Rocchetti J, *et al.* (2015) Presynaptic D2 dopamine receptors control long-term depression expression and memory processes in the temporal hippocampus. *Biol Psychiatry* 77(6):513-525.

105. Matsuda Y, Marzo A, & Otani S (2006) The presence of background dopamine signal converts long-term synaptic depression to potentiation in rat prefrontal cortex. *J Neurosci* 26(18):4803-4810.

106. Gao WJ, Krimer LS, & Goldman-Rakic PS (2001) Presynaptic regulation of recurrent excitation by D1 receptors in prefrontal circuits. *Proc Natl Acad Sci U S A* 98(1):295-300.

107. Leyrer-Jackson JM & Thomas MP (2014) Layer dependent effects of dopaminergic D1R activation on frequency dependent excitatory synaptic responses in mouse medial prefrontal cortex. in *Society for Neuroscience* (San Diego, California).

108. Morishima M, Morita K, Kubota Y, & Kawaguchi Y (2011) Highly differentiated Projection-Specific Cortical Subnetworks. *Journal of Neuroscience* 31(28):11.

109. Hempel CM, Hartman KH, Wang XJ, Turrigiano GG, & Nelson SB (2000) Multiple forms of short-term plasticity at excitatory synapses in rat medial prefrontal cortex. *J Neurophysiol* 83(5):3031-3041.

110. Yang SN (2000) Sustained enhancement of AMPA receptor- and NMDA receptor-mediated currents induced by dopamine D1/D5 receptor activation in the hippocampus: an essential role of postsynaptic Ca2+. *Hippocampus* 10(1):57-63.

111. Rotaru DC, Lewis DA, & Gonzalez-Burgos G (2007) Dopamine D1 receptor activation regulates sodium channel-dependent EPSP amplification in rat prefrontal cortex pyramidal neurons. *J Physiol* 581(Pt 3):981-1000.

112. Xu TX & Yao WD (2010) D1 and D2 dopamine receptors in separate circuits cooperate to drive associative long-term potentiation in the prefrontal cortex. *Proc Natl Acad Sci U S A* 107(37):16366-16371.

113. Scheler G & Fellous JM (2001) Dopamine modulation of prefrontal delay activity-reverberatory activity and sharpness of tuning curves. *Neurocomputing* 38-40:7.

114. Durstewitz D & Seamans JK (2002) The computational role of dopamine D1 receptors in working memory. *Neural Netw* 15(4-6):561-572.

115. Yang CR & Seamans JK (1996) Dopamine D1 receptor actions in Layers V-VI Rat Prefrontal Cortex Neurons *In Vitro:* Modulation of Dendritic-Somatic Signal Integration. *Journal of Neuroscience* 16(5):13.

116. Andreasen NC, *et al.* (1992) Hypofrontality in neuroleptic-naive patients and in patients with chronic schizophrenia. Assessment with xenon 133 single-photon emission computed tomography and the Tower of London. *Arch Gen Psychiatry* 49(12):943-958.

117. Yang CR & Chen L (2005) Targeting prefrontal cortical dopamine D1 and N-methyl-D-aspartate receptor interactions in schizophrenia treatment. *Neuroscientist* 11(5):452-470.

118. Brown SP & Hestrin S (2009) Intracortical circuits of pyramidal neurons reflect their long-range axonal targets. *Nature* 457(7233):1133-1136.

119. Kroener S, Chandler LJ, Phillips PE, & Seamans JK (2009) Dopamine modulates persistent synaptic activity and enhances the signal-to-noise ratio in the prefrontal cortex. *PLoS One* 4(8):e6507.

120. Yang CR, Seamans JK, & Gorelova N (1996) Electrophysiological and morphological properties of layers V-VI principal pyramidal cells in rat prefrontal cortex in vitro. *J Neurosci* 16(5):1904-1921.

121. Chagnac-Amitai Y, Luhmann HJ, & Prince DA (1990) Burst generating and regular spiking layer 5 pyramidal neurons of rat neocortex have different morphological features. *J Comp Neurol* 296(4):598-613.

APPENDIX A

BRAIN TISSUE HARVEST FOR AN IN VITRO MOUSE MODEL OF SCHIZOPHRENIA: INSTITUTIONAL ANIMAL CARE AND USE COMMITTEE MEMORANDUM APPROVAL

Protocol Approval: 1304C-MT-M-16 (MPT)

UNIVERSITY of NORTHERN COLORADO

IACUC Memorandum

To: Mark Thomas

From: Laura Martin, Director of Compliance and Operations

CC: IACUC Files

Date: 6/26/2015

Re: IACUC Protocol Approval 1304C-MT-M-16

The UNC IACUC has completed a final review of your protocol "Brain Tissue Harvest for an In Vitro Mouse Model of Schizophrenia".

The committee's review was based on the requirements of the Government Principles, the Public Health Policy, the USDA Animal Welfare Act and Regulations, and the Guide for the Care and Use of Laboratory Animals, as well as university policies and procedures related to the care and use of live vertebrate animals at the University of Northern Colorado.

Based on the review, the IACUC has determined that all review criteria have been adequately addressed. The PI/PD is approved to perform the experiments or procedures as described in the identified protocol as submitted to the Committee. **This protocol has been assigned the following number 1304C-MT-M-16.**

APPENDIX B

STEREOTAXIC INJECTION FOR FIBER TRACKING IN MOUSE BRAIN: INSTITUTIONAL ANIMAL CARE AND USE COMMITTEE MEMORANDUM APPROVAL

Protocol Approval: 1406BC-MT-M-17 (MPT)

UNIVERSITY of NORTHERN COLORADO

IACUC Memorandum

To: Mark Thomas

From: Laura Martin, Director of Compliance and Operations

CC: IACUC Files

Date: 9/4/2014

Re: IACUC Protocol Approval 1406BC-MT-M-17

The UNC IACUC has completed a final review of your protocol "Stereotaxic Injection for Fiber Tracking in Mouse Brain".

The committee's review was based on the requirements of the Government Principles, the Public Health Policy, the USDA Animal Welfare Act and Regulations, and the Guide for the Care and Use of Laboratory Animals, as well as university policies and procedures related to the care and use of live vertebrate animals at the University of Northern Colorado.

Based on the review, the IACUC has determined that all review criteria have been adequately addressed. The PI/PD is approved to perform the experiments or procedures as described in the identified protocol as submitted to the Committee. **This protocol has been assigned the following number 1406BC-MT-M-17.**

The next annual review will be due before **September 4, 2015**.

APPENDIX C

STEREOTAXIC INEJCTION FOR FIBER TRACKING AND OPTOGENETICS IN MOUSE BRAIN: INSTITUTIONAL ANIMAL CARE AND USE COMMITTEE MEMORANDUM APPROVAL

Protocol Approval: 1606D-MT-M-19 (MPT)

UNIVERSITY OF NORTHERN COLORADO

IACUC Memorandum

To: Mark Thomas

From: Laura Martin, Director of Compliance and Operations

CC: IACUC Files

Date: 08/02/2016

Re: IACUC Protocol 1606D-MT-M-19 Approval

The UNC IACUC has completed a final review of your protocol "Stereotaxic injection for fiber tracking & optogenetics in mouse brain". The protocol review was based on the requirements of Government Principles for the Utilization and Care of Vertebrate Animals Used in Testing, Research, and Training; the Public Health Policy on Humane Care and Use of Laboratory Animals; and the USDA Animal Welfare Act and Regulations. Based on the review, the IACUC has determined that all review criteria have been adequately addressed. The PI/PD is approved to perform the experiments or procedures as described in the identified protocol as submitted to the Committee. This protocol has been assigned the following number 1606D-MT-M-19.

The next annual review will be due before August 2, 2017.

Sincerely,

Laura Martin, Director of Compliance and Operations